NASA CR-54221
UACRL C910096-13

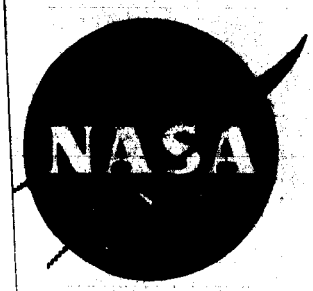

INVESTIGATION OF NONEQUILIBRIUM FLOW EFFECTS IN HIGH EXPANSION RATIO NOZZLES

by

V.J. SARLI, W.G. BURWELL, and T.F. ZUPNIK

prepared for

NATIONAL AERONAUTICS AND SPACE ADMINISTRATION

CONTRACT NAS 3-2572

United Aircraft Research Laboratories

UNITED AIRCRAFT CORPORATION

EAST HARTFORD, CONNECTICUT

#46

NASA CR-54221
UACRL C910096-13

[redacted]

INVESTIGATION OF NONEQUILIBRIUM FLOW EFFECTS IN HIGH EXPANSION RATIO NOZZLES

by

V. J. Sarli, W. G. Burwell and T. F. Zupnik

prepared for

NATIONAL AERONAUTICS AND SPACE ADMINISTRATION

December 3, 1964

CONTRACT NAS3-2572

Technical Management
NASA Lewis Research Center
Cleveland, Ohio
Advanced Rocket Technology Branch
P. N. Herr

RESEARCH LABORATORIES
United Aircraft Corporation
East Hartford, Connecticut

C910096-13

INVESTIGATION OF NONEQUILIBRIUM FLOW EFFECTS IN HIGH EXPANSION RATIO NOZZLES

Final Report Contract NAS 3-2572

TABLE OF CONTENTS

TABLE OF CONTENTS
(Cont.)

ABSTRACT

Investigation of Nonequilibrium Flow Effects in

High Expansion Ratio Nozzles

by

V. J. Sarli, W. G. Burwell and T. F. Zupnik

The Research Laboratories of United Aircraft Corporation under NASA Contract NAS 3-2572 have performed analytical studies to investigate chemical nonequilibrium flow effects in high expansion ratio liquid propellant rocket nozzles. These studies have included analyses (a) to determine the sensitivity of calculated nonequilibrium performance to variations in the chemical kinetic rate constants used in the calculations (b) to establish the limits of applicability of the Bray sudden-freezing criterion for predicting chemical nonequilibrium performance (c) to determine the effect of variations in nozzle contour on nonequilibrium performance and (d) to determine the effect of nozzle scale (i.e., thrust level) on nonequilibrium performance. The propellant systems selected for use in these studies were H_2-O_2 and N_2O_4-50% N_2H_4/50% UDMH. Also as part of this contract, the one-dimensional finite-kinetics machine program developed as part of Contract NASw-366 was modified to facilitate its use on the NASA Lewis Research Center IBM 7094 computer.

The results of the studies performed under this contract indicate that the nonequilibrium performance of both selected propellant systems is particularly sensitive to the kinetic recombination rate for the three-body water recombination reaction, $H + OH + M \rightleftharpoons H_2O + M$. Because of this sensitivity, the single-reaction Bray sudden-freezing criterion is adequate for predicting the nonequilibrium performance of these two propellant systems. However, the calculated sensitivity results also indicate that a modification of the single-reaction Bray criterion may be necessary in other propellant systems to account for energy contributions from several concurrent chemical reactions taking place during nozzle expansion.

Additional results obtained from these studies indicate that increasing the nozzle scale (thrust level) can increase the nonequilibrium specific impulse. The relative magnitude of the performance increase is dependent however upon the rocket chamber pressure level. The effects of variations in nozzle contour on performance are not significant for the propellants and operating conditions selected.

FOREWORD

This work was performed by United Aircraft Corporation Research Laboratories for the National Aeronautics and Space Administration under Contract NAS3-2572 initiated September 4, 1963.

Included among those who cooperated in performance of the work under Contract NAS3-2572 were Dr. V. J. Sarli, Program Manager; Mr. A. W. Blackman, Chief, Rocket and Air-Breathing Propulsion Section; and Dr. W. G. Burwell, Supervisor, Kinetics and Heat Transfer Group of the UACRL and Dr. E. N. Nilson, Chief, Scientific Staff and Mr. T. F. Zupnik, Scientific Staff of Pratt & Whitney Aircraft Division of UAC.

This work was conducted under program management of Mr. H. Burlage, Jr., Chief, Liquid Propulsion Systems, NASA Headquarters, Washington, D. C. and the Project Manager was Mr. P. N. Herr, NASA Lewis Research Center, Cleveland, Ohio.

This document is unclassified in its entirety.

CONCLUSIONS

1. The chemical nonequilibrium performance of the H_2-O_2 and N_2O_4-50% N_2H_4/50% UDMH propellant systems is sensitive to the specific kinetic rate constants for the water recombination reaction, $H + OH + M \rightleftharpoons H_2O + M$. Variations in this rate constant as small as plus or minus a factor of 10 about the standard value can result in the nozzle performance changing from that for near-frozen flow to that for near-equilibrium flow.

2. The chemical nonequilibrium performance of the H_2-O_2 and N_2O_4-50% N_2H_4/50% UDMH propellant systems could become sensitive to the rates of the hydrogen recombination reaction, $H + H + M \rightleftharpoons H_2 + M$ if the kinetic rate data considered standard for hydrogen recombination were significantly lower than the true rates or if the standard kinetic rate data for the water-recombination reaction were significantly higher than the true rates.

3. The single-reaction Bray sudden-freezing criterion can be used to predict performance results for H_2-O_2 and N_2O_4-50% N_2H_4/50% UDMH which are in agreement with results based on exact one-dimensional numerical solutions for the nonequilibrium nozzle expansion. The sudden-freezing approximation also predicts within acceptable limits (a) species concentration except for atoms and radicals present in very small amounts and (b) all thermodynamic variables except the static temperature. Typically, the difference between the temperature predicted by the approximate procedure and that predicted by the exact procedure can be as much as 10% of the temperature difference between the frozen and equilibrium expansion values. When applied to the above propellant combinations, the single dominating reaction to be considered is the water recombination, $H + OH + M \rightleftharpoons H_2O + M$.

4. The single-reaction Bray sudden-freezing criterion may not be sufficiently general to predict the performance for arbitrary propellant systems. Use may be required of the exact one-dimension machine computation program and/or a modified sudden-freezing analysis which permits accounting for energy contributions from more than a single recombination reaction.

5. Caution should be exercised in interpreting the results of any sudden-freezing calculation if the freezing point is located in the near vicinity of the nozzle throat. To illustrate, for the N_2O_4-50% N_2H_4/50% UDMH propellant system, a shift in the freezing area ratio from 1.1 subsonic to 1.1 supersonic results in about a 30 percent decrease in the nonequilibrium impulse loss (almost 8 sec). The freezing area ratio may not be certain within the above limits due to the approximate nature of the sudden-freezing analysis.

6. Design and contouring of nozzles for use with the H_2-O_2 propellant system should not be affected by chemical kinetic considerations. The cost and difficulty in establishing a nozzle configuration based on chemical nonequilibrium expansion is not warranted due to the lack of sensitivity of the physical contour to inclusion of finite kinetics in the design procedure. However, having once established a design for this propellant system, the performance of the design should be evaluated using a procedure which incorporates chemical kinetics. The specific impulse performance of propellant systems may be sensitive to nozzle scale or thrust level depending upon the combustion chamber pressure level. The effect of nozzle scale on nonequilibrium performance can readily be calculated for the H_2-O_2 system by employing the sudden-freezing analysis.

7. Combustion chamber inefficiencies do not have significant effect on calculated nozzle performance within the framework of the inefficiency model employed in this study.

8. Vibrational nonequilibrium within the N_2 molecules does not degrade significantly the rocket nozzle performance of the N_2O_4-50% N_2H_4/50% UDMH propellant system.

C910096-13

INVESTIGATION OF NONEQUILIBRIUM FLOW EFFECTS IN HIGH EXPANSION RATIO NOZZLES

V. J. Sarli, W. G. Burwell and T. F. Zupnik

United Aircraft Corporation

SUMMARY

12839 12839

Investigations are described in this report concerning nonequilibrium flow effects in high expansion ratio nozzles. These investigations have been directed primarily toward determining the role that reaction kinetics, contour geometry, and nozzle scale play in influencing rocket nozzle performance. In addition, studies have been carried out to establish the applicability of the Bray sudden-freezing criterion for predicting nonequilibrium nozzle performance.

The results of the studies conducted indicate that the nonequilibrium performance for the selected propellant systems, H_2-O_2 and N_2O_4-50% N_2H_4/50% UDMH, is particularly sensitive to the kinetic recombination rate for the three-body water recombination reaction, $H + OH + M \rightleftharpoons H_2O + M$. Because of this sensitivity, the single-reaction Bray sudden-freezing criterion is adequate for predicting the nonequilibrium performance of these two propellant systems.

Additional results obtained from these studies indicate that increasing the nozzle scale (thrust level) can reduce the nonequilibrium specific impulse loss associated with the above propellants. The relative magnitude of the performance change is dependent, however, upon the rocket chamber pressure level. The effects of variations in nozzle contour on performance are not significant for the propellants and operating conditions selected.

Author

INTRODUCTION

The theoretical maximum performance of high energy liquid rocket propellant systems is seldom realized in practice because of departures from equilibrium flow during the exhaust nozzle expansion process. Under contract, NASw-366, which was completed in September of 1963, the United Aircraft Corporation Research Laboratories in cooperation with Pratt and

Whitney Aircraft Division and the United Technology Center of UAC conducted an analytical and experimental investigation of nonequilibrium exhaust nozzle flows (Ref. 1). The results of this program were primarily (1) an estimation of the relative importance with respect to selected propellant combinations of nozzle performance losses resulting from several nonequilibrium flow processes such as chemical recombination, vibrational relaxation, condensation, and two-phase flow, (2) development of machine computational programs to treat nonequilibrium gas-dynamic flows of reacting gas mixtures in both one-dimensional and two-dimensional or axisymmetric exhaust nozzles, and (3) verification of the two-dimensional computational procedures by means of an experiment in which the recombination of NO_2 to N_2O_4 was studied. Although the previous work under contract NASw-366 revealed considerable information concerning particular nonequilibrium effects in exhaust nozzles, additional studies were necessary to facilitate the prediction and optimization of rocket nozzle performance. These additional studies have been performed as follow-on investigations to the above mentioned developments under NASA contract NAS 3-2572.

The specific objectives of this work are defined under five Task headings. The objective of Task I, entitled "Sensitivity Studies," was to determine the sensitivity of overall performance to variations in reaction rates. The objective of Task II, entitled "Evaluation of Bray Criterion," was to determine limits of applicability of the simplified Bray Criterion for estimating nonequilibrium nozzle performance. Task III, entitled "Effect of Nozzle Contour on Performance," had as its objective determination of the effect of convergent nozzle contour and off-design divergent contours on overall performance. The objective of Task IV entitled "Nozzle Scaling," was to investigate nozzle scaling criteria, and the objective of Task V, entitled "Computer Program," was (1) to convert the one-dimensional kinetic flow nozzle performance computer program developed under contract NASw-366 to Fortran IV, and (2) to modify the procedure in the program to permit starting at near equilibrium conditions. A further objective of Task V was the preparation of a manual and flow charts describing in detail the one-dimensional kinetic flow program. This program manual has been published as a NASA Contractor's Topical Report entitled, "Investigation of Nonequilibrium Flow Effects in High Expansion Ratio Nozzles, Computer Flow Manual," NASA CR-54042. This report is available from NASA, Office of Scientific and Technical Information and the machine program may be obtained by contacting the IBM Program Distribution Center.

TECHNICAL DISCUSSION

Task I - Sensitivity Studies

The accuracy of predicted performance for rocket propulsion systems in which chemical recombination processes may be reaction rate limited is directly dependent on the ability to specify correctly the reaction mechanism for the recombination process and to determine accurately the reaction rates of the elemental steps which comprise this mechanism. The mechanism that is employed is usually a compromise between the many reactions that can be written and the few reactions which are considered to be controlling. For some systems, the recombination reactions can be so strongly dependent on one or two elemental steps that the elimination of all other reactions does not affect the resulting calculated nozzle performance.

The one-dimensional finite-kinetics computational program developed under Contract NASw-366 and reported under separate cover as a NASA Topical Report (Ref. 2) provides the necessary flexibility in the choice of the number and rates of the elemental reactions for the study of the relative importance of the various elemental steps. Analyses to indicate the sensitivity of the calculated nonequilibrium performance to changes (or errors) in the reaction kinetic data are therefore feasible using this program, and Task I was undertaken to calculate for the H_2-O_2 and N_2O_4-50% N_2H_4/50% UDMH propellants the effects of variations in the major reaction rates on rocket nozzle performance.

Reaction Mechanism Utilized in Sensitivity Studies

The important elemental recombination reactions and reaction rate constants for H_2-O_2 and N_2O_4-50% N_2H_4/50% UDMH propellant systems which have been utilized for this study are listed in Table 1. The reaction mechanisms for the two propellants have the hydrogen-oxygen reactions in common while the reactions involving nitrogen and carbon in Table 1 are applicable only to the N_2O_4-50% N_2H_4/50% UDMH propellant. With the exception of the shuffle reaction involving the recombination of CO, the reaction mechanisms for the recombination of the combustion products of the two propellants are therefore similar. It is noted that combination of the elemental reactions

$$H_2 + OH \rightleftharpoons H_2O + H \qquad (1)$$

$$CO + OH \rightleftharpoons CO_2 + H \qquad (2)$$

yields the well known water-gas reaction,

$$CO + H_2O \rightleftharpoons CO_2 + H_2 \qquad (3)$$

The reaction rate constants for hydrogen-oxygen reactions and nitrogen-oxygen reactions are the same as those reported in previous studies by this Contractor (Refs. 1, 3 and 4). The elemental water-gas reaction (2) and its specific reaction rate constant have been reported in Refs. 5, 6, and 7.

Effect of Reaction Rate Perturbations on Performance

The similarity in the reaction mechanism for H_2-O_2 and N_2O_4-50% N_2H_4/50% UDMH propellants suggests that the relative importance of the elemental reaction steps can be evaluated using the finite kinetic machine program with only one of these propellants. The N_2O_4-50% N_2H_4/50% UDHM propellant system was selected because it includes the water-gas reaction as well as the H_2-O_2 recombination reaction.

The sensitivity of the performance to reaction rates for the N_2O_4-50% N_2H_4/50% UDMH system was determined by perturbing the reaction rates of the elemental reactions which should be controlling in the over-all mechanism. These reactions are

$$H + H + M \rightleftharpoons H_2 + M \qquad \Delta H_R^{298K} = -104.2 \qquad (4)$$

$$CO + OH \rightleftharpoons CO_2 + H \qquad \Delta H_R^{298K} = -24.86 \qquad (5)$$

$$H + OH + M \rightleftharpoons H_2O + M \qquad \Delta H_R^{298K} = -119.2 \qquad (6)$$

For each reaction, three reaction rates were used and calculations were made for two oxidizer-fuel ratios. The three rates used included the best determination of the reaction rate ("standard" rates listed in Table I) and perturbations of $10^{\pm 1.5}$ on the standard rates. The conditions for which the calculations were performed were O/F = 1.75 and 2.25 and combustion chamber pressure equal to 60 psia, in a 150 lb thrust nozzle. The nozzle geometry is that of Configuration 1 in Table II.

The effect of changes in reaction rates on the nonequilibrium performance should be accentuated at the low pressure and thrust levels because of increased dissociation and short nozzle residence times. If all possible combinations of this system were calculated, it would have taken 8 individual runs for each O/F ratio. However, since only the relative importance of the reaction rates is of interest investigation of all

possible combinations of rates was not necessary. It was assumed that the vacuum specific impulse was effectively a linear function of the reaction rate, that is:

$$I_{sp} = a + bx + cy + dz$$

where x, y and z are the changes in the reaction rates for reactions (4), (5) and (6) respectively, and b, c, and d are constants to be determined. The constant, a, is equal to the vacuum specific impulse obtained using the standard kinetic data. The method of Latin Squares was utilized to select combinations of the reactions whose rates were perturbed. This method is primarily designed to display gross effects and its application to evaluate reaction rate effects implicitly involves the assumption of roughly linear dependence of I_{sp} upon the reaction rates.

Figures 1 and 2 show the performance variations for the N_2O_4-50% N_2H_4/50% UDMH propellant system of O/F ratios of 2.25 and 1.75, respectively, which resulted from the use of reaction rates that were perturbed by factors of $10^{1.5}$. Displayed on each graph (Figs. 1 and 2) are summaries of the variations studied, along with the equilibrium, frozen and standard kinetic flow performance results. In the display "H" indicates that the standard forward rate was multiplied by $10^{1.5}$ and the letter "L" indicates that the standard forward rate was multiplied by $10^{-1.5}$. For each grouping the sequence of letters coincides with the sequence of reactions, (4), (5) and (6) listed previously. The resulting coefficients b, c, and d defined previously are listed below and indicate the relative effect of the reactions on performance. The values of b, c, and d for each of the O/F ratios studied are:

$$O/F = 1.75;\ b = 0.0617;\ c = -0.0332;\ d = 0.296$$

$$O/F = 2.25;\ b = 0.0780;\ c = -0.00470;\ d = 0.407$$

For both O/F ratios, the effect of the water recombination reaction (6) is the most important (i.e., d is larger than b or c). For the same change in all the rates, the water recombination reaction (6) affects the specific impulse approximately five times as much as the hydrogen recombination reaction (4) and about nine times as much as the carbon recombination reaction (5).

It is also apparent from the numerical values of coefficients that increase in the rates of the hydrogen and water recombination reactions increase the specific impulse; whereas, an increase in the rate of carbon recombination reaction decreases the specific impulse (i.e., c is negative). The fact that an increase in the rate of the carbon recombination reaction reduces

the performance of the nozzle implies that the highly energetic three-body water formation reaction tends to freeze earlier during the expansion as a result of increased depletion rate of OH radicals. The net result is a decrease in energy conversion because the carbon recombination reaction is much less energetic than the water recombination reaction due to the formation of a hydrogen atom for each hydroxyl radical that recombines by this route, e.g., see equations (4), (5), (6).

It should be noted from Figs. 1 and 2 that the difference in vacuum specific impulse caused by adjusting the reaction rates over the specified range is approximately five percent while the difference between equilibrium and frozen specific impulse is approximately eight percent.

In addition to the results presented above, certain preliminary calculations were performed in which the standard forward reaction rates for reactions (4), (5) and (6) were varied by three orders of magnitude. These results are summarized in Table 3. Although the specific impulse in Table 3 appears to be sensitive to the rate of water recombination reaction, the deviations from equilibrium impulse were so slight in these subsonic kinetic flow calculations that the results were considered inconclusive. Additional sensitivity calculations were performed based on the composite-reaction sudden-freezing analysis described in a subsequent section (Task II) of this report. A summary of these calculations for the H_2-O_2 propellant system is given in Fig. 3. The results plotted in Fig. 3 show the effect on performance of variations in the specific reaction rates of the H_2-O_2 three-body recombination reactions for the conditions specified on the graph.

As was previously observed from exact kinetic results, the results shown in Fig. 3 indicate that the three-body water recombination reaction is rate controlling for the H_2-O_2 system at the conditions specified. However, the results of Fig. 3 also show that an order of magnitude increase in the hydrogen atom recombination rate constant results in this reaction assuming the controlling role (i.e., the atom recombination reaction will freeze farther downstream than the three-body water formation reaction) although large increases in this rate constant are required to change the performance significantly.

It should further be noted from Fig. 3 that a relatively small increase in the water formation constant (e.g., about one order of magnitude) is sufficient to produce near-equilibrium performance, and a reduction of the same amount results in near-frozen flow. A reduction in the hydrogen atom recombination rate constant, however, has practically no effect on performance.

While the sensitivity study results discussed above for the H_2-O_2 and N_2O_4 - Aerozine 50 propellants clearly indicate that a single recombination reaction dominates in determining the nonequilibrium performance of the system, it is equally clear that more than one reaction could be performance controlling in other propellant systems or in the propellant systems studied if the kinetic rate constants employed are in error. As was observed in Fig. 3, depending on as small a change (or error) in rate constants as a factor of 10, the dominant reaction can be switched from that involving H + OH recombination to that involving H + H recombination. A factor of 5 increase in the hydrogen recombination reaction would probably result in this reaction becoming competitive with the water recombination reaction. It may therefore be concluded that simplified sudden-freezing techniques such as that of Bray (discussed in Task II) should be modified in order to account the kinetic contributions from more than one reaction.

Effect of Combustion Inefficiency on Performance

As part of the studies to evaluate the effect of variations in reaction rate constants on performacne, several calculations were carried out assuming that incomplete combustion had occurred prior to entrance into the nozzle and initiation of the expansion. The combustion inefficiency with which this study is concerned involves only that type resulting from incomplete chemical reactions such as occurs in short combustion chambers (resulting in short residence times) in contrast to the inefficiencies arising from non-uniform mixtures or stratification of fuel and oxidizers.

Sensitivity studies were carried out for a fuel-rich mixture of N_2O_4 and 50% N_2H_4/50% UDMH having an assumed combustion efficiency of 90% (the temperature rise in the combustion chamber is 90 percent of the maximum temperature rise). Because of the complete lack of reaction kinetics data for initiation of N_2O_4-50% N_2H_4/50% UDMH reaction, it was not possible to attain the 90% temperature rise by kinetic flow calculations via the ignition delay and rapid temperature rise route in the combustion chamber. Instead, the 90% temperature rise condition for an O/F = 1.75 was simulated by mixing the equilibrium combustion products of a fuel-rich stream (O/F = 1.25) and a fuel-lean stream (O/F = 4.00) at constant pressure so that the resulting overall O/F ratio is 1.75 (fuel-rich and near the optimum O/F for P_c = 60 psia). The mixed stream was a nonequilibrium stream with regard to chemical composition since the O/F ratios of the contributing streams were such that the corresponding adiabatic, equilibrium temperature rise was 90 percent of that for a homogeneous stream having an O/F of 1.75. The actual mixing of the two streams to establish the starting conditions for the kinetic flow expansion was considered to take place after each of the streams was expanded separately to a predetermined pressure ratio which

corresponded to a practical contraction ratio. This was done in order to avoid the essentially infinite time that would have been required to perform the kinetic integration starting from an infinite reservoir (the combustion chamber). The conditions and composition after mixing the streams at constant pressure were calculated assuming a one-dimensional mixing process by solving the mass, energy, momentum, and state equations. The conditions of the contributing streams and fully mixed nonequilibrium stream are listed in Table 4.

The 90 percent combustion efficiency calculations were carried out using both the standard rate constants (Table 1) and the HHH combination of rate constants (i.e., the rate constants for each of reactions (4), (5) and (6) were increased by a factor of $10^{+1.5}$ from the standard values listed in Table 1). The vacuum specific impulse obtained using the standard rate constants was 320 sec at an exit area ratio of 40:1. This compares to 321 sec obtained for the 100 percent combustion efficiency calculation using the standard rates. The impulse for the HHH combination of rates at the same area ratio was 328 sec for both the 100 percent and 90 percent combustion efficiency conditions. The results indicate that the previously observed effects of reaction rate pertubations on performance are not altered by this type of combustion inefficiency. Also, it is apparent that the combustion inefficiency of the type considered does not have significant effect on the overall nozzle system performance.

It was noticed for these studies that during the early part of the expansion after uniform mixing, the temperature gradient in the nozzle was positive indicating that the reaction proceeded towards equilibrium. Based on these studies, it can be concluded that (1) the kinetics of homogeneous mixtures are sufficiently rapid in the converging section of the nozzle to compensate for a combustion inefficiency represented by the assumed model (i.e., too short a combustion chamber), and (2) the simulation of inefficiency by the above model is not representative of a true combustion inefficiency.

Further combustion inefficiency calculations are desirable for a propellant system such as H_2-O_2 whose mechanism can be defined for the combustion chamber. For such a system, mixing of the streams as described above could be eliminated and entrance to the nozzle could be executed analytically after a temperature rise corresponding to 90 percent of the maximum rise was achieved. However, it would still be necessary to assume uniform mixing and therefore the temperature rise in the early part of the expansion probably would still be positive as above and the continuing reactions would tend toward equilibrium. A major disadvantage to use of this procedure lies in the fact that a high initial temperature of pure fuel and oxidizer greater than 1500 ^{o}R must be specified in

order to initiate ignition within a reasonable ignition delay period. These starting conditions will, therefore, be unrealistic for rocket motors. Also, for comparison, the combustion inefficiency calculations for the H_2-O_2 fuel system would have to be performed by mixing two equilibrium streams of different O/F ratios to simulate 90 percent combustion efficiency as in the N_2O_4-50% N_2H_4/50% UDMH calculations reported above.

Combustion efficiency calculations have been performed utilizing the mixing concept for the H_2-O_2 propellant at low pressures and low initial temperatures. These calculations were required to specify the throat conditions for the axisymmetric nonequilibrium nozzle investigations of Task III. The performance calculations have been extended beyond the throat in a one-dimensional supersonic contour in order to evaluate the effect of combustion efficiency for the H_2-O_2 system as was done for the N_2O_4-50% N_2H_4/50% UDMH. Figure 4 shows the effect of combustion inefficiency on vacuum specific impulse for the H_2-O_2 propellant system, O/F = 5, as a result of mixing two equilibrium streams to simulate 90% combustion efficiency for a combustion chamber pressure of 60 psia. The properties of the equilibrium streams (O/F = 3.82 and 20.34) and mixed stream (O/F = 5) are presented in Table 5. The difference in performance between 90% combustion efficiency and 100% combustion efficiency results is less than 3 seconds. The similarities between these results for H_2-O_2 and the performance for N_2O_4-50% N_2H_4/50% UDMH are not surprising since both propellants are controlled by the same recombination mechanism.

Task II - Evaluation of Bray Criterion

In a rocket nozzle the elementary reactions between the dissociated species of a combustion process seldom proceed at a rate which is sufficeint to maintain true chemical equilibrium throughout the nozzle expansion. The greatest degree of reaction occurs in the early portion of an expansion nozzle, where the reactant concentrations and densities are high and the residence times are long due to moderate flow velocities relative to those in the downstream portion of the nozzle. Important reactions involving the largest energies require that at least two and often three bodies come together "simultaneously" to effect recombination. The "forward" rates or recombination rates of these reactions are, therefore, proportional to the cube (three-body reactions) of the reactive mixture density, suggesting that significant departure from equilibrium values may easily occur as the expansion proceeds and that very little of the heat of dissociation (recombination) will then be converted into kinetic energy. It is expected, therefore, that nonequilibrium chemical losses are accentuated when the combustion pressures are low and reduced when the combustion pressures are high.

Several approaches have been taken to predict chemical nonequilibrium nozzle performance ranging from simple, crude calculations to complex models which treat multireaction systems in one- and two-dimensional flow fields. For example, the first simplified calculations, carried out by Penner, (Ref. 8), allowed for flows to be classified as "near-equilibrium" or "near-frozen" throughout the expansion by application of a relaxation time criterion. The idea that the transition from equilibrium to frozen flow occurs within a small region in the nozzle was originally discussed by Bray (Ref. 9), who constructed a solution based on the assumption that the kinetic region for the single reaction system in one-dimensional expansion nozzle terminated at a point. The nozzle flow and composition up to the point ("the sudden-freezing-point") could be considered in equilibrium while the flow downstream of that point could be considered constant in composition. Discussions and applications of the Bray criterion to nozzle performance for a number of propellant systems and nozzle conditions have been given in previous work by this Contractor and reported in the final report for the NASA Contract NASw-366 (Ref. 1).

The utility of the Bray analysis has been verified by investigators for expansions in which one reaction, viz, atom recombination, takes place (Refs. 10, 11, and 12). However, no general expansion and verification of the sudden-freezing-point analysis has been made for multireaction systems. For such a chemically complex system, recourse has been made to numerical solutions of the gas-dynamic, chemical-kinetic and state equations for the reacting gas mixture (Refs. 1-3, 5, 13, 14). The employment of exact

solutions is not always justified, however, since experimental kinetic rate data for most reactions are not available, and reliance on statistical methods for calculating the rate data is precluded by the lack of detailed knowledge about the forces of interaction and manner of deactivation which prevail during atomic recombination. The deficiencies of kinetic data combined with the high cost of an exact machine solution make approximate computational procedures (such as the sudden-freezing criterion of Bray) look attractive if these procedures can be validated for multireaction flow systems such as are encountered in rocket nozzles.

An evaluation of the general applicability of the Bray criterion for estimating rocket nozzle performance and modification of the simple Bray criterion for multireaction systems were therefore the primary objectives of this task.

Description of Bray Sudden-Freezing Criterion

The Bray criterion is an approximate procedure for predicting the point in a reacting nozzle flow where a reaction has departed significantly from equilibrium. This is accomplished by determining the point at which the forward rate of reaction becomes of the same order as the rate required to maintain equilibrium. This concept is clarified by considering a nozzle expansion in which an arbitrary three-body recombination reaction takes place,

$$2J + M \underset{k_b}{\overset{k_f}{\rightleftharpoons}} J_2 + M \tag{7}$$

where the change of J_2 concentration with time and constant density is found from phenomenological chemical kinetics (Ref. 15),

$$\left(\frac{\partial [J_2]}{\partial t}\right)_\rho = k_f [J_2] [M] \left\{ \frac{[J]^2}{[J_2]} - \frac{[J]_{eq}^2}{[J_2]_{eq}} \right\} \equiv a \left\{ y - y_{eq} \right\} \tag{8}$$

In Eq. (8) the bracket, [ ], indicates the actual instantaneous concentration of the indicated species, k_f denotes the forward rate constant, and the sub-script "eq." denotes the instantaneous equilibrium values. For near-equilibrium flow, it is clear that $y - y_{eq} << y_{eq}$, so that

$$\left(\frac{\partial [J_2]}{\partial t}\right)_\rho << a\, y_{eq} \tag{9}$$

while for near-frozen flow $y_{eq} << y$, so that

$$\left(\frac{\partial [J_2]}{\partial t}\right)_\rho \simeq a\, y_{eq} >> a y_{eq} \tag{10}$$

Therefore, from Eqs. (9) and (10) it can be deduced that an approximate criterion for the freezing point of the reaction can be defined according to

$$\left(\frac{\partial [J_2]}{\partial t}\right)_\rho \simeq a\, y_{eq} \equiv (r_f)_{eq} \qquad (11)$$

as previously stated, where the forward reaction rate expression, r_f, is evaluated with very little loss in accuracy using equilibrium quantities up to the freezing point.

The Bray criterion has been used successfully to analyze flows in which only one reaction is energetically and kinetically important. In Refs. 10 and 11, this approach was applied to the nonequilibrium nozzle flow of air, assuming that oxygen atom recombination is the only important reaction. Wegener (Ref. 12) studied nozzle recombination of nitrogen dioxide in a nitrogen bath, in which an excellent correlation between the experimentally observed departure point from equilibrium and the Bray freezing point was found. However, this method of solution considering only a single reaction may be valid only for a relatively few complex chemical systems.

For the expansion of products of combustion in a nozzle, several reactions must be considered if an effective point of chemical freezing is to be found. This was clearly demonstrated in Fig. 3 and discussed in Task I - Sensitivity Studies. Extension of Bray's one-reaction criterion to multireaction non-equilibrium nozzle flows is not necessarily straightforward, unless one reaction out of the many taking place has tied up most of the energy in the combustion process, or unless all energetic reactions tend to leave equilibrium at nearly the same location in the nozzle. When this is not the case, the simple freezing criterion can at best bracket the actual nozzle flow parameters (by assuming that the fastest and slowest of the many reactions control).

Modified Bray Criterion For Multireaction Systems

The concept of a composite freezing point is based on the assumption that an important rate-controlling species exists whose net rate of formation or depletion becomes very small as the reactions in which it participates become very slow, and that once this species has frozen at some point in the nozzle (which will be referred to as the "composite reaction freezing point"), all remaining species can no longer react. The problem of finding a composite reaction freezing point reduces to determining the kinetically, and thermodynamically, important species and reactions which must be studied. The importance of many of the existing species can be evaluated on the basis of (1) their relative equilibrium composition values, a mole fraction of 0.005 being a practical lower limit, (2) the energy release of the chemical reactions in which they participate, and (3) their role in effecting the chain-breaking steps in the overall reaction mechanism.

The reaction rate that is necessary to keep an important species in equilibrium can easily be found knowing the equilibrium composition history as calculated using the conservation equations, state relations, and the pertinent Guldberg-Waage laws of mass action (Refs. 16 and 17). The required time rate of change of the concentration for component i due to reaction only, i.e., excluding expansion effects, is

$$\left(\frac{\partial [M_i]}{\partial t} \right)_{\rho, eq} = \left[\rho V \frac{d(X_i/\bar{W})}{dx} \right]_{eq} \qquad (12)$$

where $[M_i] = \rho X_i / \bar{W}$, X_i is the mole fraction of species i, and $\bar{W}$ is the mean molecular weight, $\sum_{i=1}^{n} X_i W_i$. While equilibrium machine solutions employ the local flow area to minimum flow area ratio (i.e., A/A_{min}) as an independent variable, the axial distance, x , is a more convenient variable since

$$\left(\frac{\partial [M_i]}{\partial t} \right)_{\rho, eq} = \left[\rho V \frac{d(X_i/\bar{W})}{d(A/A_{MIN})} \right]_{eq} \frac{d(A/A_{MIN})}{dx} \qquad (13)$$

becomes indeterminate at the minimum area (i.e., at $A = A_{min}$). Evaluation of Eq. (12) can proceed once the equilibrium properties and a nozzle geometry have been specified. Use of the equilibrium values for computing the required gradients will be accurate up to the point where the first important reaction freezes; but since the species under consideration will usually appear in this reaction, this does not represent a severe limitation on the method when one reaction is controlling or all reactions freeze at the same location in the nozzle.

In complete analogy with the simple one-reaction Bray criterion, it is necessary when treating a multireaction system to compare the required reaction rate, Eq. (12), with the total forward rate of reaction written in terms of all reactions that make substantial contributions to the overall rate of production or depletion of species. The forward reaction rate equation for the net rate of production of species M_i is

$$\left(\frac{\partial [M_i]}{\partial t} \right)_{\rho} = \sum_{j=1}^{N} (\alpha''_{ij} - \alpha'_{ij}) \left\{ k_{f_j} \prod_{k=1}^{n} [M_k]^{\alpha'_{kj}} \right\} \qquad (14)$$

where N is the total number of reactions, n the total number of species, k_{f_j} the forward rate constant for the j^{th} reaction, and α'_{ij} and α''_{ij} the stoichiometric coefficients of the i^{th} species in the j^{th} reaction for the reactants and products, respectively, when the j^{th} reaction taking place in the exothermic direction is written as (Ref. 15)

$$\sum_{i=1}^{n} \alpha'_{ij} M_i \underset{k_{b_j}}{\overset{k_{f_j}}{\rightleftharpoons}} \sum_{i=1}^{n} \alpha''_{ij} M_i \qquad (15)$$

When a single rate-controlling reaction exists, for example, the oxygen recombination reaction in the expansion of air up to 6000 K, Eq. (14) takes the simple form

$$\left(\frac{\partial [M_i]}{\partial t}\right)_\rho = (\alpha''_{ij} - \alpha'_{ij})\, k_{f_j} \prod_{k=1}^{n} [M_k]^{\alpha'_{kj}} \qquad j = j_o \qquad (16)$$

where M_i refers to the species in the j^{th} reaction which, in addition to being thermodynamically important, has a large variation in composition through the nozzle to ensure accurate differentiation of the composition with respect to axial distance in Eq. (12). An effective freezing point for a multireaction nozzle flow can then be defined from Eqs. (12) and (14) as

$$\left(\frac{\partial [M_i]}{\partial t}\right)_\rho = \left[\rho V \frac{d(X_i/\bar{W})}{dX}\right]_{eq} = \sum_{j=1}^{n} (\alpha''_{ij} - \alpha'_{ij}) \left\{ k_{f_j} \prod_{k=1}^{n} [M_k]^{\alpha'_{kj}} \right\} \qquad (17)$$

In the situation described above where one dominant reaction exists, the right-hand side of Eq. (17) is replaced by Eq. (16) so that this freezing criterion reduces essentially to the simple Bray criterion. In any event, it is clear that there can be as many freezing points as radicals or atoms to which Eq. (17) is applied, but these points usually remain in close proximity to one another in practice, depending on the choice of reactions employed in the forward reaction rate equation.

The most successful results from this composite reaction effective freezing point analysis are achieved when only three-body reactions are considered in evaluating the right side of Eq. (17), since bimolecular reactions in which one or more new radicals are formed for every radical consumed add very little energy to the flow after the three-body reactions have frozen. Graphical solutions to Eq. (17) are easily carried out for arbitrary flow systems, once the important reactions and species have been ascertained, by performing graphical differentiation of the equilibrium concentration profiles as a function of axial distance for a preselected nozzle geometry, $X = X(A/A_{MIN})$ Then for a given set of forward rate constants and with all the equilibrium properties known as a function of area ratio, the left side of Eq. (17) can be plotted against the right side over the range of area ratios. The point of crossing indicates where significant freezing has occurred.

Typical results showing the variation of the right and left hand sides of Eq. (17) are plotted in Fig. 5. These results are for the expansion of H_2-O_2 products of combustion from 60 psia and an O/F ratio of 8 using nozzle configuration 1 of Table 2 and several reaction combinations. Based on the depletion of the hydrogen atom, freezing of the atom recombination reaction

$$H + H + M \rightleftharpoons H_2 + M \qquad (18)$$

is seen to occur first, while the three-body water formation reaction

$$H + OH + M \rightleftharpoons H_2O + M \qquad (19)$$

freezes farther downstream. Considering a composite reaction rate for the consumption of hydrogen atoms, found by adding the kinetic rates resulting from the reactions (18) and (19), the freezing point is seen to move slightly farther downstream in the nozzle.

Comparison of Sudden-Freezing and Exact Kinetic Performance Results

Performance Results from simple Bray Freezing Analysis

The specific impulse of H_2-O_2, and N_2O_4-50% UDMH/50% N_2H_4 for a range of O/F ratios, and combustion pressures are presented in Figs. 6-13. In each case, the assumed controlling reaction, the freezing point location, and the resulting Bray performance I_{sp} vs A/A_{min} are indexed. In addition to the Bray performance curves, the results of shifting equilibrium, frozen and full kinetic flow are shown on each of the graphs. The reaction mechanisms and rate constants for the H_2-O_2 and N_2O_4-50% N_2H_4/50% UDMH system applicable to the analysis are given in Table 1 (nitrogen and carbon reactions are deleted for H_2-O_2 system). From these figures it is seen that the selection of the three-body water recombination reaction (19) as rate controlling leads to satisfactory agreement with the exact kinetic flow solutions. Also it is evident from Figs. 6-13 that agreement in predicted performance is unsatisfactory for any other arbitrarily assumed controlling reaction. Depending on the particular reaction selected, the performance level which can be attained spans a large fraction of the range bounded by frozen composition expansion and equilibrium composition expansion. The performance is somewhat more sensitive to the choice of controlling reaction for the N_2O_4-50% N_2H_4/50% UDMH system (Figs. 10-13) than for the H_2-O_2 system. It is obvious from these figures that arbitrary choice of the single controlling reaction can be complicated by lack of knowledge concerning the important reactions and species to be considered. This is particularly true for propellant systems for which the mechanism and rates are not as well known as those for H_2-O_2 and the water-gas reaction.

When the combustion products of a typical rocket-propellant system are expanded through a nozzle, several chemical reactions must take place in order to maintain chemical equilibrium. In general, more than one of these reactions may involve a significant fraction of the total energy change throughout the nozzle. If sufficient information is available for a detailed analysis of the chemistry, it is usually found that a major portion of the chemical energy release in the flow is controlled by one or

two elementary reactions. When there is only one controlling reaction, or when the controlling reactions are dependent or have nearly the same freezing point, it is possible to apply the Bray sudden-freezing method directly. When the freezing points of the controlling reactions are widely separated and the controlling reactions are independent, the Bray sudden-freezing method may be used to establish the limits of performance attainable.

The significant generalities that can be deduced from Figs. 6-13 are that the hydrogen recombination reaction, $H + H + M \rightleftharpoons H_2 + M$, freezes first in the expansion and the two-body reactions such as

$$H_2 + OH \rightleftharpoons H_2O + H$$

$$CO + OH \rightleftharpoons CO_2 + H$$

freeze well downstream of the throat region. From the studies performed it appears that as long as OH radicals are present in the gas mixture, OH recombination will occur well into the divergent section by two-body reactions. However, atomic hydrogen is correspondingly formed and can be consumed only by the hydrogen recombination reaction and water recombination reaction, $H + OH + M \rightleftharpoons H_2O + M$. Bacause the hydrogen recombination reaction freezes first, the amount of energy that can ultimately be recovered from hydrogen atom reactions is very strongly dependent on the freezing point of the three-body H_2O recombination reaction. This was shown to be the case in the sensitivity studies and therefore it is not surprising that the Bray analysis does indicate that better performance agreement relative to the full kinetic solution is obtained when the water recombination reaction is assumed controlling.

Performance Results from Composite Reaction Freezing Point Analysis

A simplification in selecting the rate controlling reaction and potentially better agreement with exact analysis are obtained by utilizing the composite-reaction freezing point of the hydrogen recombination reaction and the water recombination reaction since both reactions compete for hydrogen atoms through part of the expansion. The results utilizing the composite-reaction freezing point are included in Figs. 6-13. It should be noted from these figures however, that for the propellants and conditions of this report, the inclusion of both the three-body reactions for predicting a composite-reaction freezing point gives the same results as were obtained by considering the depletion of hydrogen atoms by means of the water recombination reaction (19) alone. These results are also in good agreement with the exact kinetic performance predicted by the one-dimensional program. Again this is not surprising since it was shown in the sensitivity studies that large variations in hydrogen atom recombination

rate constant, relative to the water formation rate constant, were required to influence performance.

It should be noted that, for other propellant systems, (e.g., hydrocarbons in combination with fluorine and oxygen), where two or three reactions are of equal significance the dominating role cannot be readily assigned to a single reaction and slight variations in the specific reaction rate may shift the dominant role from one reaction to another.

The individual three-body reactions are not expected to freeze at exactly the same location in the nozzle, so a single reaction will consume atoms and/or radicals and release energy in the flow after the other reactions have, for all practical purposes, ceased. The single-rate controlling reaction is automatically included in the composite-reaction sudden freezing analysis. The advantage and utility of this freezing analysis is in part a consequence of this fact, since attempts to guess the rate-controlling reaction in multireaction nozzle flow systems are rarely successful for all conditions of combustion pressures and O/F ratios.

Bimolecular Reactions

The indications are that (1) the hydroxyl radicals continue to scavenge the hydrogen atoms releasing energy long after the atom-atom recombination has ceased, and (2) that the bimolecular reactions forming hydrogen atoms

$$H_2 + OH \rightleftharpoons H_2O + H$$

and

$$CO + OH \rightleftharpoons CO_2 + H$$

which freeze far downstream, must not be considered in the composite-reaction sudden-freezing point analysis. The inclusion of bimolecular reactions would lead to near-equilibrium flow in every instance as a result of grossly misrepresenting the location of the composite-reaction freezing point. Therefore, the amount of energy added to the flow is a far more important consideration in assessing the importance of reactions for performance calculations than is the rate at which any single species is consumed or formed in all the reactions in which this species might participate. It is noted from Figs. 6-13 that the performance predicted by utilizing the composite-reaction freezing technique and the three-body recombination reactions generally is in agreement with or slightly lower than the exact kinetic flow calculations. The lower results are due to elimination of the energy contributions of the two-body reactions and the abrupt changeover from a shifting equilibrium

gas model to an invariant composition model at the freezing point. The real gas model (kinetic flow), of course, is one of continuing reaction throughout the expansion.

Third-Body Efficiency

A note about the third-body concentrations [M] used in Eq. (7) is in order. These were taken to be $\rho / \overline{W}$, $X_M = 1$, in conjunction with an average forward rate constant which favored molecular third bodies (Refs. 4 and 18), since these far outnumber the atoms and radicals present under the conditions considered. This simplified approach is tantamount to neglecting the different efficiencies of the various third-bodies for promoting recombination, but since the magnitude and temperature dependence of chemical kinetic data are not accurately known in most cases, no great loss in accuracy is incurred.

Sensitivity of Performance to Freezing Point

The basic role which the composite reaction serves is to predict an effective freezing area ratio, beyond which all reactions cease. To illustrate the interesting way in which this is related to overall nozzle performance, Figs. 14 and 15 have been prepared for the N_2O_4-50% N_2H_4/50% UDMH, and H_2-O_2 systems at different chamber pressures and stoichiometries, and show the variation of specific impulse between frozen and equilibrium limits as a function of the freezing area ratio. The dependence of the "nonequilibrium impulse parameter" on chamber pressure is seen to be very weak, even between the extreme pressure limits presented. However, this parameter is critically dependent on O/F ratio as a consequence of the greater amount of expansion required to recover an equivalent percentage of the heat of combustion with increasing flame temperatures.

The very large slopes of all these curves in the throat region suggest that if means are available for preventing chemical freezing near the nozzle throat (e.g., by catalyzing a rate-controlling reaction or by changing the particular nozzle contour in this region), significant improvements in performance can be realized when the values of frozen and equilibrium impulse are appreciably different. The recovery of energy as the freezing point location shifts from a slightly subsonic to a slightly supersonic area ratio can shift the performance from near frozen to near equilibrium. This marked dependency of performance on the freezing point location in the throat region suggests that caution be employed in the interpretation of results of the approximate sudden-freezing calculation. This is

evident because no sudden cessation of all chemical reactions occurs and the freezing criterion used may thus be ineffective for some propellant systems in predicting the point beyond which appreciable chemical energy addition to the flow stops. The suggestion is that exact calculations should be performed for those cases where sudden freezing occurs at or near the nozzle throat (e.g., between area ratio 1.1 subsonic and 1.1 supersonic).

Comparison of Exhaust Nozzle Performance Data Calculated by Approximate and Exact Procedures

It is of interest to compare other gas-dynamic and thermodynamic variables obtained by the approximate and exact analysis. Heretofore, the only comparison of exact and simple Bray solutions was carried out by Lordi (Ref. 19) for the restricted case of pure oxygen and hydrogen nozzle flows, in which the only variable compared was the degree of dissociation of the pure diatomic gas. In Figs. 16-19 selected parameters are presented for the N_2O_4-50% N_2H_4/50% UDMH system at 60 psia and an O/F ratio of 2.25. Equilibrium profiles are included to show the sensitivity of the particular parameter to nonequilibrium effects. The depressed values of temperature (Fig. 16) relative to the full kinetic solution are a result of omitting the entropy production and heat release caused by chemical reaction beyond the effective freezing point. The large difference between the frozen and equilibrium pressures indicates that results of the approximate analysis agree quite well with the results of the full kinetic solution (Fig. 17). The concentrations from the approximate analysis, however, do not agree with the results of the full kinetic solution as well as desired for all species included in Figs. 18 and 19. In particular the hydrogen atom and hydroxyl radical concentrations (Fig. 18) which are extremely important intermediate species in the recombination mechanisms vary by as much as 2.5 to 8 times the concentrations calculated for the full kinetic solution at area ratios, $A/A_{min} = 50$. This may not be important as far as specific impulse is concerned because the concentrations are extremely low at the cited area ratio. These results illustrate that although the overall performance (I_{sp}) reported previously (Figs. 4-11) for the same conditions agreed within one percent for composite-reaction freezing point analysis and exact kinetic calculations, important individual properties are not in as good agreement. This points out the potential difficulties and errors associated with attempting to extract kinetic results from overall performance data.

Vibrational Relaxation

The energy stored in the excited states of a system is redistributed during the thermodynamic relaxation processes at some finite rate until the population of the energy levels is at equilibrium for the environmental temperature and pressure. If equilibrium of the excited levels is not attained at each of the pressure and temperature conditions established during nozzle expansion, the specific heat or sensible enthalpy of the gases is not correctly defined by the equilibrium temperature condition. The loss in sensible enthalpy, as a result of energy stored in excited states, cannot be converted into directed kinetic energy and rocket thrust.

A technique similar to the Bray freezing criterion for chemical recombination was assumed satisfactory to establish the region in a nozzle expansion when nonequilibrium vibrational relaxation is significant with respect to nozzle performance. An outline of the freezing point analysis for vibrational relaxation appears in Ref. 20 and 21 and was discussed by this Contractor in the Final Report for Contract NASw-366 (Ref. 1).

The vibrational relaxation freezing point is very sensitive to pressure level and diluent gas composition. The pressure effect is to be expected since the number of collisions that a given molecule undergoes is directly proportional to the density of the gases and consequently the relaxation times are reduced proportionately. The composition effect is most pronounced when water is present even in small amounts. Water reduces the N_2 relaxation times by as much as three orders of magnitude. Nozzle size also has an effect on the location of the vibrational freezing point. Large nozzles result in increased residence time and thus are favorable to the reduction of vibrational nonequilibrium losses. In view of these facts, the maximum effect of nonequilibrium vibrational losses should occur at low combustion pressure in small expansion nozzles when the vibrational relaxation time of nitrogen is a maximum (presence of water is neglected).

The present studies utilizing a fuel rich N_2O_4-50% N_2H_4/50% UDMH mixture at a low combustion pressure of 60 psia (nozzle configuration 1 of Table 2) indicate that N_2 molecules freeze vibrationally at the nozzle throat when these N_2 molecules see only other N_2 molecules. Freezing of the N_2 molecules occurs downstream of the throat region in the presence of H_2O molecules. The conditions (combustion pressure = 60 psia, O/F = 1.75) selected for the present vibrational relaxation studies were the same as those utilized for the one-dimensional kinetic flow calculations, and the vibrational relaxation times for N_2 were obtained from Ref. 22.

Performance calculations based on one-dimensional kinetic flow analysis and uncoupled vibrational relaxation indicate that losses in performance in excess of those already reported for kinetic flow were less than 1% (i.e., less than 3 seconds at $A/A_{min} = 50$). The performance (vacuum specific impulse) is therefore approximately the same as that reported for the full kinetic flow without vibrational relaxation given in Figs. 6-13. The performance calculations with uncoupled vibrational relaxation involved the full multireaction kinetic flow calculations to the N_2-vibrational mode freezing point. At this point the specific heat of diatomic nitrogen was fixed at a value of 6.96 BTU/lb-mole x ^{o}R which corresponds to the specific heat for nitrogen with no vibrational excitation (rotational and translational modes are fully excited). The energy which was stored in the vibrational mode at the freezing point was considered to be retained by the nitrogen throughout the remainder of the expansion. The full kinetic-flow calculation was continued to the nozzle exit.

On the basis of the calculations performed, it can be concluded that vibrational effects of diatomic nitrogen in the combustion products of N_2O_4-50% UDMH/50% N_2H_4 propellant are negligible in rocket performance calculations even for low combustion pressures (60 psia).

Task III - Effect of Nozzle Contours on Performance

In order to understand and to perfect techniques for predicting the performance of exhaust nozzles with reactive gas flows and/or for designing optimum nozzles with reactive gas flows, it is necessary to establish the effect of both convergent and divergent contours on the performance. Evaluation of these effects requires at least in part that investigation be carried out in two-dimensional or axisymmetric flow fields. This has been done by performing axisymmetric nonequilibrium and equilibrium nozzle performance calculations in selected optimum contours at high pressures (300 psia) and low pressures (60 psia). The optimum contours were selected from a family of nozzles designed for both shifting equilibrium and kinetic flow. In order to perform these investigations, both performance and design procedures treating two-dimensional flows in reactive gas mixtures were required. The procedures used were those developed under Contract NASw-366 and included analysis with two, two-dimensional/axisymmetric decks. These decks are described in Ref. 1. The first of these decks, the so-called "performance deck," has been used to determine the flow field associated with a given supersonic contour and prescribed conditions for the flow entering at the throat. The second deck, the so-called "design deck," has been used to determine a family of modified perfect nozzles from which optimum nozzle contours are selected by truncation.

The modified perfect nozzles selected for the current study are nozzles having axial exit flow but not necessarily uniform speed (in view of the different residence times for gases flowing along the various principal streamlines). The design of these nozzles involves in part the method of characteristics construction procedure used in much the same manner of conventional construction of perfect nozzles. The reaction kinetic equations are integrated forward along provisional principal streamlines to a provisional Mach line which is determined using frozen composition. The determination of the final Mach line, and final locations and directions for the principal streamlines is an iterative process. A full discussion of these techniques and modification of the conventional characteristics construction to include reaction kinetics is given in Ref. 1.

One-Dimensional Results for Different Convergent Contour Designs

Investigations performed under Contract NASw-366 and in the present work have indicated that significant departures from chemical equilibrium can occur in the convergent section of a nozzle for the H_2-O_2 propellant system at low chamber pressures (O/F = 5). Further studies with the Bray

criterion have indicated that a sizable portion of the resulting loss in specific impulse may be recovered by a relatively small displacement of the freezing point, if the freezing point occurs in the transonic region (see Fig. 15). The studies under Contract NASw-366 showed that appreciable changes in throat contour did not substantially alter the nozzle performance. It appeared, therefore, that a significant improvement in rocket nozzle performance might be achieved by a careful design of the subsonic section of the nozzle.

Two widely different convergent contours were selected with essentially the same divergent section (see Table 2 - Configurations 2 and 3) and the performance was calculated for each using the one-dimensional, kinetic-flow computer program. The results of these calculations are shown in Fig. 20 where the vacuum specific impulse is plotted against the area ratio. It is obvious from this figure that the difference in the specific impulse for the two nozzles is quite small, amounting to less than one-half percent, with the shallow convergence nozzle indicating only slightly better performance. The longer residence time achieved with this nozzle did result in some differences in thermodynamic properties and concentrations at the minimum area (see Table 6). As would be expected, the longer nozzle was closer to equilibrium as evidenced by the difference between γ and γ_P and by the reduced mass flow rate. The significance of this difference is discussed in Ref. 1. This, however, was not reflected in the vacuum specific impulse. It should also be noted that as a practical matter the increase in length would increase the friction losses and the net result could easily be a reduction in performance when compared to the shorter nozzle. Based on these results it was felt that for this propellant system the design of the convergent section should not be based on chemical kinetic considerations.

Axisymmetric Results for RL-10 and NASw-366 Nozzle Designs

Analytical studies to determine the effect of the gas model on nozzle performance for both high and low chamber pressure H_2-O_2 propellant systems were conducted using the RL-10 contour for the high pressure (P_c = 300 psia) investigation and the nozzle designed under Contract NASw-366 for the low pressure (60 psia) studies. The configurations of these nozzles are shown in Fig. 21. For both nozzles, three gas models were investigated: viz, kinetic flow with 100 percent combustion efficiency; kinetic flow with 90 percent combustion efficiency; and shifting equilibrium flow with frozen sound speed. The latter model, while known to be analytically inconsistent (the proper sound speed is the equilibrium sound speed), was considered initially to

approximate the extreme kinetic solution where the reaction rates are fast enough throughout the expansion to permit the thermodynamic properties to approach their equilibrium value while the sound speed remains frozen. If this were the case, this model could give a rapid method of calculating the maximum performance attainable with reacting gas flows. This, however, is not the case; the inconsistency in the model manifests itself in such a way that the continuity equation is not satisfied in the analytic model. As a result the performance calculated using the equilibrium composition with the frozen sound speed is considerably below that calculated kinetically for the low pressure nozzle (see Fig. 22) and is also below the equilibrium performance calculated for the high pressure nozzle (see Fig. 23). It can also be seen from the figures that the percentage difference in performance increases with increasing area ratio and as such the equilibrium composition-frozen sound speed model would be particularly poor for large area ratio nozzles.

The 90 percent combustion efficiency model was used in the axisymmetric, kinetic flow computer program for the NASw-366 nozzle and the flow field was calculated until the end of the circle body (X/R_o equals approximately 1). Here the flow field and the pressure and temperature distributions (see Fig. 24) were compared to those calculated for the 100 percent combustion efficiency model. While the temperature distribution and the species concentrations showed some small differences between the two models, the pressure distribution and flow field were very similar. Since the performance contribution of the supersonic portion of the nozzle is given by the $\int pdA$, it was felt that further calculation was unnecessary since the performance of both models would be effectively the same and the result would duplicate what had been found previously with one-dimensional calculations -- i.e., little or no performance difference due to a combustion inefficiency. Similar observations were made in the case of the high pressure RL-10 calculation, with the results of one-dimensional calculations up to a slightly supersonic Mach number showing only minor differences arising from use of the 90 percent and the 100 percent combustion efficiency models. Several axisymmetric Mach lines were calculated for both efficiencies, and their similarity supported the conclusion that no performance differences are observed between the results of the 90 percent and 100 percent combustion efficiency calculations. Since the nozzle flow was essentially in equilibrium for both calculations, an excessive amount of time would normally have been required to complete the kinetic axisymmetric integrations. In order to verify these conclusions an additional one-dimensional calculation was made using the 90 percent combustion efficiency model and an area variation that represents that

of the outer stream tube of the RL-10 nozzle. The performance from this stream tube calculation is compared to the equilibrium performance for the stream tube in Fig. 25. As is evident in Fig. 25, even for this stream tube which undergoes more rapid expansion than any other in the nozzle, the performance is close to equilibrium.

It should be pointed out here that the above results cannot be generalized. The H_2-O_2 propellant system is not a typical one since there is only about a 4 1/2 percent difference (about 20 sec at optimum O/F ratio at 300 psia) between the equilibrium and frozen performance (H_2-F_2 has a difference of about 11 1/2 percent or 55 sec for the same restrictions). The similarity between the 100 percent and 90 percent combustion efficiency results would probably not carry over to propellant combinations such as H_2-F_2 which exhibit large differences between equilibrium and frozen performance.

Axisymmetric Results for Different Assumed Gas Models

Two axisymmetric nozzles were designed for the same exit area ratio to be used with the H_2-O_2 propellant system at an O/F ratio of 5, and a chamber pressure of 60 psia. One of these nozzles was designed for an equilibrium gas model (i.e., equilibrium gas composition and equilibrium sound speed) while the other was designed for a frozen gas model (i.e., frozen gas composition and frozen sound speed). Figure 26 shows the contours of the two nozzles. The difference between the two contours results from the fact that flows with lower effective gammas (equilibrium) must turn through a greater expansion angle to achieve the same Mach number as achieved by flows with larger effective gammas (frozen). At the same time, for the same area ratio, the Mach number is lower for the lower gamma. While these two effects oppose each other, the net result is that the axisymmetric nozzle designed for a lower gamma (equilibrium) will have a greater initial expansion and will be shorter than an axisymmetric nozzle designed for a larger gamma (frozen) with the same area ratio.

The vacuum specific impulse calculated for these two nozzles is shown in Fig. 27. It is evident that the performance calculated for the equilibrium designed nozzle is quite different than that calculated for the frozen nozzle even though the difference in physical contours is small (see Fig. 26). However, if the performance using the reverse gas model in both nozzles (i.e., equilibrium flow in frozen design nozzle and frozen flow in the equilibrium design nozzle) is compared to the performance using the correct gas model, there is little effect due to the physical contour.

Task IV - Nozzle Scaling

Previous experience has indicated that performance of exact kinetic calculations for multireaction gas mixtures over a wide range of conditions and variables can involve excessive costs. This problem is a consequence of the relatively slow process of integrating the equations when near-equilibrium conditions exist in the flow. The problem is aggravated in large scale nozzles for which residence times are relatively long and near-equilibrium calculations prevail over a longer fraction of length.

Since it is desirable to establish the effect of chemical kinetics on the performance of geometrically scaled nozzles, the analytical techniques investigated and employed in Task II of this report were used in conjunction with the one-dimensional kinetic flow computer program.

The one-dimensional program was used to calculate the performance of a geometrically scaled RL-10 rocket nozzle for thrust levels of 150, 1500 and 15,000 pounds. These calculations were performed for H_2-O_2 at an O/F of 5 and a chamber pressure of 300 psia. Thrust levels of 150 and 15,000 lbs were investigated for a chamber pressure of 60 psia. The modified Bray analysis was also employed to investigate the performance for the same conditions and for additional thrust levels as high as 1,500,000 lbs and combustion pressures as high as 1000 psia.

The results for the 300 psia chamber pressure at thrust levels from 150 to 1,500,000 lbs of thrust are presented in Fig. 28. The curves shown include the results of calculations from both the kinetic-flow and composite-reaction sudden freezing analysis. The results indicate that performance improves as nozzle size is increased. Although the change in performance with scale from 150 to 15,000 lbs is slight, it is interesting to note that the sudden-freezing criterion not only correctly predicts this trend but also predicts the actual performance level obtained from the exact kinetic flow calculations. Also of interest is the fact that the performance results for 150,000 and 1,500,000 lbs thrust (from composite-reaction, sudden-freezing calculations) indicate no improvement in specific impulse above that for the 15,000 lbs thrust level. The extremely small variation in specific impulse with thrust is due to the high combustion pressure which is evidently sufficiently high to maintain the expansion near equilibrium.

Figure 29 presents the results of the kinetic and modified Bray calculations for a pressure of 60 psia at thrust levels of 150 and 15,000 lbs. As is evident in Fig. 29, the results of the modified Bray

analysis fall essentially along the corresponding curves calculated from the exact kinetic analysis. In contrast to the results at 300 psia, these low pressure results indicate a marked improvement in specific impulse as the thrust level (scale) is increased.

Additional results of modified Bray calculations for the 60 psia chamber pressure condition are shown in Fig. 30 for thrust levels extending up to 1,500,000 lbs. Again, in contrast to the high pressure results, continued improvement in performance is evidenced as thrust level is increased throughout the entire range of thrusts. A summary of the significant scaling (variation of kinetic flow performances in terms of specific impulse) results for this study utilizing the RL-10 nozzle geometry (H_2-O_2 propellant) for 150 to 1,500,000 lbs thrust and combustion pressures 60 to 1000 psia is presented in Fig. 31. The performance values are plotted as an energy recovery factor expressed in terms of specific impulse between the frozen and shifting equilibrium performance. The results for 1000 psia have been evaluated utilizing only the composite-reaction, sudden-freezing analysis. On the basis of the good agreement between the results of the exact and approximate analytical techniques throughout this report, it is felt that these 1000 psia results represent the kinetic solution.

It is apparent from Fig. 31 that, for geometrically-similar nozzles, a marked increase in the normalized specific impulse performance occurs with increased thrust levels, particularly for low combustion chamber pressure levels (60 psia). This is a consequence of shifting the freezing point from the throat region to a point downstream of the throat (see Fig. 32) and is a direct result of increased residence times. However, it follows that increases in thrust from levels which are already sufficiently high to establish the freezing point downstream of the throat region will not affect the specific impulse performance significantly (see Fig. 15). This is observed by correlating the performance results in Fig. 31 with the variation in freezing point location in Fig. 32. At the high pressures (1000 psia combustion pressure) the changes in specific impulse with thrust level are less significant than at the low pressures suggesting that the freezing point is downstream of the throat over the entire thrust range, i.e., near-equilibrium flow predominates.

These investigations suggest that the specific impulse performance of propellant systems may well be sensitive to a minimum critical thrust level for a given combustion pressure and that optimization of performance with respect to kinetics is related to gross thrust level.

Task V - Computer Program

A machine computational program developed by United Aircraft Corporation to treat the one-dimensional flow of reacting gas mixtures in variable area passages has been modified under this task to facilitate general use of the program on the NASA Lewis Research Center IBM 7094 Computer. A description of the equations, numerical techniques, general operating instructions, and flow charts have been published in a separate NASA Contractor's Topical Report CR-54042 entitled "Investigation of Nonequilibrium Flow Effects in High Expansion Ratio Nozzles, Computer Flow Manual". This report is available from NASA, Office of Technical Information and the machine program may be obtained by contracting the IBM Program Distribution Center.

General Description of Program

The exact nonequilibrium nozzle flow calculations require the simultaneous solution of mass, momentum, and energy conservation equations, state and mixture enthalpy equations, kinetic differential equations for the finite rate of production of molecular species, and atomic continuity equations for all atoms present. These equations have been solved for one-dimensional, inviscid, adiabatic flow, with negligible diffusion. Solution on a digital computer by numerical means is required, since $n + 6$ equations are involved in the complete solution, where n is the total number of species present. By this method, a reaction is never dropped in the computational procedure because of "sudden freezing" as predicted by the Bray criterion, and in addition it is possible to treat all reactions that are known to occur, regardless of their speed or exothermicity.

The machine procedure developed for analysis of one-dimensional chemically reacting flows is quite flexible and may be operated in either of two modes; (1) combustion chamber, or (2) nozzle. The equation system and numerical techniques are basically the same in both modes but there are differences in the controls and input information necessary for each mode.

Modes of Operation

Combustion Chamber

In a combustion chamber it is assumed that the oxidizer and fuel are individually in equilibrium and are then instantaneously mixed at

an arbitrarily selected temperature. The resulting mixture is homogeneous but not in chemical equilibrium. The numerical integration proceeds from this point of mixing. The combustion chamber contour can be of the general form $A = ax + b$ where A is the cross-section area at any axial location x, b is the initial area and a is the slope. The flow in the chamber may be either subsonic or supersonic. Starting from given conditions of temperature, pressure, velocity and composition, the numerical integration continues until one of three criteria is met. In subsonic combustion if the length of the chamber exceeds the maximum desired length or the temperature gradient falls below a prescribed tolerance, the calculation will stop, while in supersonic flow in addition to these, the calculation will be terminated when the difference between the Mach number and unity is less than a prescribed amount.

Exhaust Nozzle

A nozzle contour may be prescribed by any area distribution which is input in tabular form and subsequently spline-fitted. The starting point of the calculation may be anywhere in the nozzle where the temperature, pressure, velocity and composition are known. The numerical integration proceeds using the given area distribution until the transonic region is reached or until either a preselected Mach number or nozzle length is exceeded.

Two major difficulties exist in the integrating the system of equations through a convergent-divergent nozzle that is flowing choked. These arise from (a) the necessity of integrating the equation through a sonic location, and (b) the significant figure loss when the flow is near equilibrium. The Computer Program Manual, therefore, includes a set of equations transformed to facilitate calculations near equilibrium and in the transonic region of convergent-divergent nozzles. In addition, a description of the numerical techniques and the integration routines is presented along with a discussion of round-off-error control.

Flow Charts and Formats

Extensive flow charts indicating the detailed steps employed in the main computer program and various subroutines are included in the manual. These should permit a computer specialist to alter the machine program and tailor the numerical techniques for specialized systems if such alterations are desirable.

Information such as input and output formats, general instructions for the use of the program involving various combustion chamber and nozzle combainations, and preselected nozzle throat contours are included. Input instructions and output format are illustrated for the recombination of the combustion products of H_2-O_2 in a convergent-divergent nozzle involving a multireaction system.

REFERENCES

1. Investigation of Nonequilibrium Flow Effects in High Expansion Nozzles, Final Report under Contract NASw-366. United Aircraft Corporation Research Laboratories Report B910056-12, September 20, 1963.

2. Zupnik, T. F., E. N. Nilson and V. J. Sarli: Investigation of Nonequilibrium Flow Effects in High Expansion Ratio Nozzles, Computer Program Manual, NASA Contract No. NAS3-2572, Report No. NASA CR-54042, September 15, 1964. United Aircraft Corporation Research Laboratories Report C910096-11.

3. Sarli, V. J., A. W. Blackman, and R. F. Buswell: Kinetics of Hydrogen Air Flows. II. Calculations of Nozzle Flows for Ramjets. Ninth International Symposium on Combustion, Academic Press, New York, 1963.

4. Montchiloff, I. N., E. D. Taback, and R. F. Buswell: Kinetics of Hydrogen Air Flow Systems I. Calculation of Ignition Delays for Hypersonic Ramjets. Ninth International Symposium on Combustion, Academic Press, New York, 1963.

5. Westenberg, A. A. and S. Favin: Complex Chemical Kinetics in Supersonic Nozzle Flow, Ninth Symposium (International on Combustion, Academic Press, New York, 1963, pp. 785-798.

6. Westenberg, A. A., And R. N. Fristrom: Journal of Physical Chemistry, Vol. 65, 1961, p. 591.

7. Fenimore, C. P., and C. W. Jones: Journal of Physical Chemistry, Vol. 62, 1958, p. 1578.

8. Penner, S. S.: Introduction to the Study of Chemical Reactions in Flow Systems. Butterworths Scientific Publications, London, 1955.

9. Bray, K. N. C.: Journal of Fluid Mechanics, Vol. 6, No. 1, 1959.

10. Heims, S. P.: Effect of Oxygen Recombination on One-Dimensional Flow at High Mach Numbers, NACA TN 4144, January 1958.

11. Boyer, D. W., A. Q. Eschenroeder, and A. L. Russo: Approximate Solutions for Nonequilibrium Airflow in Hypersonic Nozzles. Cornell Aeronautical Laboratories, Inc., Report No. A.D.-1345-W3, August 1960.

12. Wegener, P. P.: Experiments in the Departure from Chemical Equilibrium on a Supersonic Flow. ARS Journal, Vol. 30, No. 4, April 1960, p. 322.

13. Zupnik, T. F., E. N. Nilson, F. Landis, J. R. Keilbach, and D. Ables: Application of the Method of Characteristics Including Reaction Kinetics to Nozzle Flow. AIAA Aerospace Science Meeting, January 20-22, 1964, New York.

14. Eschenroeder, A. W. and J. A. Lordi: Catalysis of Recombination in Nonequilibrium Flows, Ninth Symposium (International) on Combustion, Academic Press, New York, 1963. pp. 741-756.

15. Penner, S. S.: Chemistry Problems in Jet Propulsion. Pergamon Press Books, The Macmillan Co., New York, 1957.

16. Brinkley, S. R., Jr.: Journal of Chemical Physics, Vol. 15, No. 2, February 1947.

17. McMahon, D. G. and R. Roback: Kinetics, Equilibria and Performance of High Temperature Systems. Proceedings of 1st Conference, Western States Section, Butterworths Scientific Publications, London, 1960.

18. Duff, R. E.: Journal of Chemical Physics, Vol. 28, No. 6, June 1958.

19. Lordi, J. A.: Comparison of Exact and Approximate Solutions for Nonequilibrium Nozzle Flows. ARS Journal, Vol. 32, August 1962.

20. Stollery, J. L., and J. E. Smith: A Note on the Variation of Vibrational Temperature Along a Nozzle. Journal of Fluid Mechanics, Vol. 13, 1962, p. 226.

21. Musgrove, P. J. and J.P. Appleton: On Molecular Vibrational Relaxation in Flow of Chemical Reacting Gas. University of Southampton, Department of Aeronautics and Astronautics, June 1961 (AD267761).

22. Millikan, R. C. and D. R. White: Systematics of Vibrational Relaxation, Journal of Chemical Physics. Vol. 39, No. 12, 1963, p. 3209.

LIST OF SYMBOLS

a	Constant
a	Forward rate Parameter (Eq. (8))
A^*	Nozzle cross-sectional area
b	Constant
c	Constant
d	Constant
ΔH_R	Heat of reaction
I_{sp}	Vacuum specific impulse
J	Arbitrary species
k_f, k_b	Specific reaction rate constant, forward and reverse reactions
M	Symbol representing any species
M	Mach number
$\dot{m}$	Mass flow rate
N	Number of reactions
n	Number of species
P	Pressure
R	Universal gas constant
R_o	Throat radius
r_f	Forward rate parameter
T	Temperature
t	Time

V	Velocity
W_i	Molecular weight of species i
$\bar{W}$	Mean molecular weight
x	Axial distance
x	Change in reaction rate constant
x_i	Mole fraction of species i
y	Concentration Ratio defined by (Eq. (8))
y	Change in reaction rate constant
y	Radial distance
z	Change in reaction rate constant
a'_{ij}, a''_{ij}	The stoichiometric coefficients of the ith species in the jth reaction, reactants and products, respectively
γ	Ratio of specific heat
γ_p	Defined as $\frac{d \log p}{d \log \rho}$
ρ	Density

Subscripts

c	Refers to combustion chamber
i, k	Refers to species i or k
j	Refers to reaction j

APPENDIX I

DISTRIBUTION LIST

No. of Copies	Recipient
	NASA Lewis Research Center, 21000 Brookpark Road Cleveland, Ohio 44135
6	Mr. P. N. Herr Project Manager
4	Mr. Donald L. Nored Liquid Rocket Technology Branch
2	Mr. J. A. Durica Contracting Officer
1	Mr. Norman T. Musial Patent Counsel
2	Captain J. O. Tinius AFSC Liaison Officer
2	Lewis Library
1	Report Control Office Technical Information Division
	National Aeronautics and Space Administration Headquarters Washington, D. C. 20546
4	Mr. Henry Burlage, Jr. Chief, Liquid Propulsion Technology, RPL
1	Contracting Officer Code BCA
1	Patent Office Code AGP
25	Scientific and Technical Information Facility NASA Representative, Code CRT P. O. Box 5700 Bethesda, Maryland 20014

No. of Copies	Recipient
2	Ames Research Center Attn: Harold Hornby, Mission Analysis Division Moffett Field, California 94035
2	Goddard Space Flight Center Attn: Merland L. Moseson, Code 623 Greenbelt, Maryland 20771
2	Jet Propulsion Laboratory Attn: R. F. Rose, Propulsion Division, 38 California Institute of Technology 4800 Oak Grove Drive Pasadena, California 91103
2	Langley Research Center Langley Station Attn: Floyd L. Thompson, Director Hampton, Virginia 23365
2	Marshall Space Flight Center Attn: Hermann K. Weidner, Code M-P&VED Huntsville, Alabama 35812
2	Manned Spacecraft Center Attn: Robert R. Gilruth, Director (Code D) Houston, Texas 77001
2	Western Operations Office Attention: R. W. Kamm 150 Pico Blvd. Santa Monica, California 90406
1	Aeronautical Systems Division Air Force Systems Command Wright-Patterson Air Force Base Dayton, Ohio Attn: D. L. Schmidt, Code ASRCNC-2

No. of Copies	Recipient
1	Air Force Missile Development Center Attn: Maj. R. E. Bracken, Code MDGRT Holloman Air Force Base, New Mexico
1	Air Force Missile Test Center Attn: L. J. Ullian Patrick Air Force Base, Florida
1	Air Force Systems Command, Dyna-Soar Attn: Col. Clark, Technical Data Center Air Force Unit Post Office Los Angeles 45, California
1	Arnold Engineering Development Center Arnold Air Force Station Attn: Dr. H. K. Doetsch Tullahoma, Tennessee
1	Bureau of Naval Weapons Attn: J. Kay, Code TRMS-41 Department of the Navy Washington 25, D. C.
1	Defense Documentation Center Headquarters Cameron Station, Building 5 5010 Duke Street Alexandria, Virginia 22314 Attention: TISIA
1	Headquarters, U. S. Air Force Attn: Col. C. K. Stambaugh, Code AFRST Washington 25, D. C.
1	Picatinny Arsenal Dover, New Jersey 07801 Attention: I. Forsten, Chief Liquid Propulsion Laboratory
1	Rocket Research Laboratories Attn: Col. J. Silk Edwards Air Force Base Edwards, California 93523

No. of Copies	Recipient
1	U. S. Atomic Energy Commission Technical Information Services Attention: A. P. Huber, Code ORGDP Box 62 Oak Ridge, Tennessee
1	U. S. Army Missile Command Attn: Dr. Walter Wharton Redstone Arsenal, Alabama 35809
1	U. S. Naval Ordnance Test Station China Lake, California 93557 Attention: W. F. Thorn, Code 4562 Chief, Missile Propulsion Division
1	Chemical Propulsion Information Agency Johns Hopkins University Applied Physics Laboratory 8621 Georgia Avenue Silver Spring, Maryland Attention: Neil Safeer
1	Aerojet-General Corporation Attn: L. F. Kohrs P. O. Box 296 Azusa, California
1	Aerojet-General Corporation Attn: R. Stiff P. O. Box 1947 Technical Library, Bldg. 2015, Dept. 2410 Sacramento 9, California
1	Aeronutronic A Division of Ford Motor Company Attn: D. A. Carrison Ford Road Newport Beach, California

No. of Copies	Recipient
1	Aerospace Corporation 2400 East El Segundo Boulevard P. O. Box 95085 Los Angeles, California 90045 Attention: J. G. Wilder, MS-2293 Propulsion Department
1	Arthur D. Little, Inc. Attn: A. C. Tobey Acorn Park Cambridge 40, Massachusetts
1	Astropower, Inc., Subsidiary of Douglas Aircraft Company Attn: Dr. George Moc, Director, Research 2968 Randolph Avenue Costa Mesa, California
1	Astrosystems, Inc. Attn: A. Mendenhall 1275 Bloomfield Avenue Caldwell Township, New Jersey
1	Atlantic Research Corporation Attn: A. Scurlock Edsall Road and Shirley Highway Alexandria, Virginia
1	Beech Aircraft Corporation Boulder Facility Attn: J. H. Rodgers Box 631 Boulder, Colorado
1	Bell Aerosystems Company Attn: W. M. Smith P. O. Box 1 Buffalo 5, New York

No. of Copies	Recipient
1	Bendix Systems Division Bendix Corporation Attn: John M. Brueger Ann Arbor, Michigan
1	Boeing Company Attn: J. D. Alexander P. O. Box 3707 Seattle 24, Washington
1	Chrysler Corporation Missile Division Attn: John Gates Warren, Michigan
1	Curtiss-Wright Corporation Wright Aeronautic Division Attn: G. Kelley Woodridge, New Jersey
1	Douglas Aircraft Company, Inc. Missile and Space Systems Division 3000 Ocean Park Boulevard Santa Monica, California 90406 Attention: R. W. Hallet, Chief Engineer Advanced Space Technology
1	Fairchild Stratos Corporation Aircraft Missiles Division Attn: J. S. Kerr Hagerstown, Maryland
1	General Dynamics/Astronautics Library & Information Services (128-00) Attn: Frank Dore P. O. Box 1128 San Diego, California 92212

C910096-13

No. of Copies	Recipient
1	General Electric Company Missile and Space Vehicle Department Attn: F. E. Schultz 3198 Chestnut Street, Box 8555 Philadelphia 1, Pennsylvania
1	General Electric Company Flight Propulsion Lab Department Attn: D. Suichu Cincinnati 14, Ohio
1	Grumman Aircraft Engineering Corporation Attn: Joseph Gavin Bethpage, Long Island, New York
1	Kidde Aero-Space Division Walter Kidde and Company, Inc. 675 Main Street Belleville 9, New Jersey Attention: R. J. Hanville Director of Research Engineering
1	Lockheed California Company Attn: G. D. Brewer 10445 Glen Oaks Boulevard Pacoima, California
1	Lockheed Missiles and Space Company Technical Information Center Attn: Y. C. Lee, Power Systems R&D P. O. Box 504 Sunnyvale, California
1	Lockheed Propulsion Company Attn: H. L. Thackwell P. O. Box 111 Redlands, California

No. of Copies	Recipient
1	The Marquardt Corporation Attn: W. P. Boardman, Jr. 16555 Saticoy Street Box 2013 - South Annex Van Nuys, California 91409
1	Martin Division Martin Marietta Corporation Attn: John Calathes (3214) Baltimore 3, Maryland
1	Martin Denver Division Martin Marietta Corporation Denver, Colorado Attention: J. D. Goodlette Mail A-241
1	McDonnell Aircraft Corporation Attn: R. A. Herzmark P. O. Box 6101 Lambert Field, Missouri
1	North American Aviation, Inc. Space & Information Systems Division Attn: H. Storms Downey, California
1	Northrop Space Laboratories Attn: Dr. Wm. Howard 1001 East Broadway Hawthorne, California
1	Pratt & Whitney Aircraft Corporation Florida Research & Development Center Attn: R. J. Coar P. O. Box 2691 West Palm Beach, Florida 33402

C910096-13

No. of Copies	Recipient
1	Radio Corporation of America Astro-Electronics Division Defense Electronic Products Princeton, New Jersey Attention: S. Fairweather
1	Reaction Motors Division Thiokol Chemical Corporation Attn: Arthur Sherman Denville, New Jersey 07832
1	Republic Aviation Corporation Attn: Dr. William O'Donnell Farmingdale Long Island, New York
1	Rocketdyne (Library Dept. 586-306) Division of North American Aviation Attn: E. B. Monteath 6633 Canoga Avenue Canoga Park, California 91304
1	Space General Corporation Attn: C. E. Roth 9200 Flair Avenue El Monte, California
1	Space Technology Laboratories Subsidiary of Thompson-Ramo-Wooldridge Attn: G. W. Elverum One Space Park Redondo Beach, California
1	Stanford Research Institute Attn: Thor Smith 333 Ravenswood Avenue Menlo Park, California

No. of Copies	Recipient
1	TAPCO Division, Thompson-Ramo-Wooldridge, Inc. Attn: P. T. Angell 23555 Euclid Avenue Cleveland 17, Ohio
1	Thiokol Chemical Corporation Redstone Division Attn: J. Goodloe Huntsville, Alabama
1	United Aircraft Corporation Research Laboratories Attn: Erle Martin 400 Main Street East Hartford 8, Connecticut 06108
1	United Technology Center Attn: B. Abelman 587 Methilda Avenue P. O. Box 358 Sunnyvale, California
1	Vought Astronautics Attn: Warren C. Trent Box 5907 Dallas 22, Texas

TABLE I

REACTION MECHANISM AND RATE DATA FOR HYDROGEN-OXYGEN AND N_2O_4 - 50% N_2H_4 /50% UDMH SYSTEM

	REACTION MECHANISM	REACTION RATE *
1.	$H_2 + OH \underset{k_b^1}{\overset{k_f^1}{\rightleftharpoons}} H_2O + H$	$k_f^1 = 4.2 \times 10^9 \times T^{0.5} \exp(-10/RT)$
2.	$H + O_2 \underset{k_b^2}{\overset{k_f^2}{\rightleftharpoons}} OH + O$	$k_f^2 = 5.64 \times 10^{10} \exp(-15.1/RT)$
3.	$H_2 + O \underset{k_b^3}{\overset{k_f^3}{\rightleftharpoons}} OH + H$	$k_f^3 = 1.2 \times 10^{10} \exp(-9.2/RT)$
4.	$H + H + M \underset{k_b^4}{\overset{k_f^4}{\rightleftharpoons}} H_2 + M$	$k_b^4 = 10^{18} \times T^{-1.5} \exp(-103.2/RT)$
5.	$H + OH + M \underset{k_b^5}{\overset{k_f^5}{\rightleftharpoons}} H_2O + M$	$k_b^5 = 2 \times 10^{19} \times T^{-1.5} \exp(-114.7/RT)$
6.	$O + O + M \underset{k_b^6}{\overset{k_f^6}{\rightleftharpoons}} O_2 + M$	$k_f^6 = 18.5 \times 10^{10} \times T^{-0.5}$
7.	$CO + OH \underset{k_b^7}{\overset{k_f^7}{\rightleftharpoons}} CO_2 + H$	$k_f^7 = 10^{10} \exp(-10/RT)$
8.	$N_2 + O \underset{k_b^8}{\overset{k_f^8}{\rightleftharpoons}} NO + N$	$k_f^8 = 6.71 \times 10^{10} (4500/T)^{-0.5} \exp(-38.0/T)$
9.	$O_2 + N \underset{k_b^9}{\overset{k_f^9}{\rightleftharpoons}} NO + O$	$k_f^9 = 6.8 \times 10^9 (4500/T)^{-0.5} \exp(-3.12/T)$
10.	$NO + M \underset{k_b^{10}}{\overset{k_f^{10}}{\rightleftharpoons}} N + O + M$	$k_f^{10} = 1.43 \times 10^9 (T/4500)^{-1.5}$
11.	$O_2 + N_2 \underset{k_b^{11}}{\overset{k_f^{11}}{\rightleftharpoons}} 2NO$	$k_f^{11} = 2.7 \times 10^{10} \exp(-53.8/T)$

NOTE: UNITS FOR REACTION RATE DATA ARE LITER, GM-MOLE, SEC, AND °K. ACTIVATION ENERGY TERMS ARE GIVEN IN KCAL.

* REACTION RATES SAME AS IN REF. 1

TABLE 2

NOZZLE GEOMETRIES EMPLOYED IN KINETIC ANALYSES

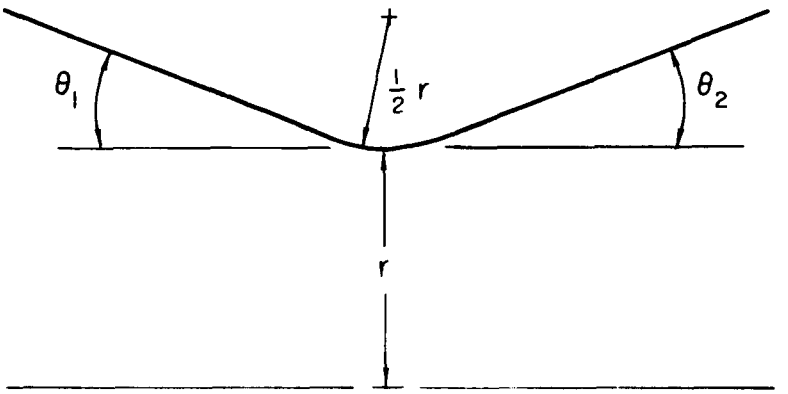

NOZZLE CONFIGURATION	r FT	θ_1 DEG	θ_2 DEG
1	0.054014	30	20
2	0.054242	14.5	20
3	0.054035	45	20

TABLE 3

VARIATION IN PERFORMANCE WITH REACTION RATE

Propellant: N_2O_4-50% N_2H_4/50% UDMH

Oxidizer-fuel ratio: O/F = 1.75

Chamber pressure: P_c = 60 psia

Reaction	I_{sp} (vac) @ throat
1 2 3*	
H H H**	216.37
L L H	216.37
H L L	215.17
L H L	216.17
Standard kinetic rates	215.00
Frozen	212.05
Equilibrium	216.37

* 1 $H + H + M \rightleftharpoons H_2 + M$
2 $CO + OH \rightleftharpoons CO_2 + H$
3 $H + OH + M \rightleftharpoons H_2O + M$

** The designation H means that the standard reaction rate is multiplied by 10^3
The designation L means that the standard reaction rate is multiplied by 10^{-3}

TABLE 4

FLOW VARIABLES EMPLOYED IN
SIMULATION OF COMBUSTION INEFFICIENCY
FOR N_2O_4-50% N_2H_4/50% UDMH

P_c = 60 psia

		Equilibrium Stream 1	Equilibrium Stream 2	Non-equilibrium Mixture Stream
O/F		1.25	4.00	1.75
Mass fraction (stream)		0.667	0.333	1.00
P, psia		54.545	54.545	54.545
T, ^oR		4929.2	4950.3	4940
V, ft/sec		1581	1344	1502
ρ, lbs/ft^3		0.01933	0.02681	0.02124
Mass fraction:	H	8.921×10^{-4}	1.125×10^{-4}	6.325×10^{-4}
	O_2	1.952×10^{-4}	2.246×10^{-1}	7.492×10^{-2}
	O	1.994×10^{-4}	6.010×10^{-3}	2.134×10^{-3}
	OH	4.974×10^{-3}	2.421×10^{-2}	1.138×10^{-2}
	NO	8.279×10^{-4}	2.529×10^{-2}	8.973×10^{-3}
	CO_2	4.946×10^{-2}	1.277×10^{-1}	7.552×10^{-2}
	H_2	2.548×10^{-2}	5.238×10^{-4}	1.717×10^{-2}
	H_2O	2.754×10^{-1}	2.138×10^{-1}	2.549×10^{-1}
	N_2	4.666×10^{-1}	3.658×10^{-1}	4.330×10^{-1}
	CO	1.756×10^{-1}	1.192×10^{-2}	1.211×10^{-1}

TABLE 5

FLOW VARIABLES EMPLOYED IN
SIMULATION OF COMBUSTION EFFICIENCY
FOR H_2-O_2

P_c = 60 psia

		Equilibrium Stream 1	Equilibrium Stream 2	Equilibrium Mixture Stream
O/F		3.824	20.34	5.00
Mass Fraction (stream)		0.747	0.253	1.000
P, psia		56.000	56.000	56.000
T, ^{o}R		4965.3	4986.7	4970.0
V, ft/sec		1888.6	1209.3	1716.8
ρ, lbs/ft^3		0.010052	0.024522	0.01182
Mass Fraction:	H_2O	8.793×10^{-1}	3.881×10^{-1}	7.550×10^{-1}
	H_2	1.055×10^{-1}	6.822×10^{-4}	7.899×10^{-2}
	OH	1.188×10^{-2}	4.399×10^{-2}	2.001×10^{-2}
	O_2	2.661×10^{-4}	5.564×10^{-1}	1.410×10^{-1}
	H	2.683×10^{-3}	1.439×10^{-4}	2.040×10^{-3}
	O	3.490×10^{-4}	1.070×10^{-2}	2.967×10^{-3}

C910096-13

Comparison of Flow Properties at Nozzle Throat for Different Converging Section Contours

Table 6

		Long Nozzle	Short Nozzle
V	ft/sec	5063	5122
P	lbf/ft^2	4936	4863
T	R	5150	5079
M	nondimensional	0.978	0.994
I_{sp}	$\frac{lbf - sec}{lbm}$	292.6	291.5
ρ	lbm/ft^3	0.00721	0.00718
γ_p	nondimensional	1.164	1.202
γ	nondimensional	1.217	1.218
$\dot{m}$	lbm/sec	0.335	0.340
A_{min}	ft^2	0.00917	0.00994
H	$mole/lb_{m_{mix}}$	0.00406	0.00440
OH	"	0.00207	0.00217
H_2O	"	0.0496	0.0495

COMPARISON OF ROCKET NOZZLE SPECIFIC IMPULSE CALCULATED FOR VARIOUS COMBINATIONS OF KINETIC RATE DATA

N_2O_4 - 50% N_2H_4/50% UDMH

O/F = 2.25

CHAMBER PRESSURE = 60 PSIA

THRUST = 150 LBS

NOZZLE CONFIGURATION 1 OF TABLE 2

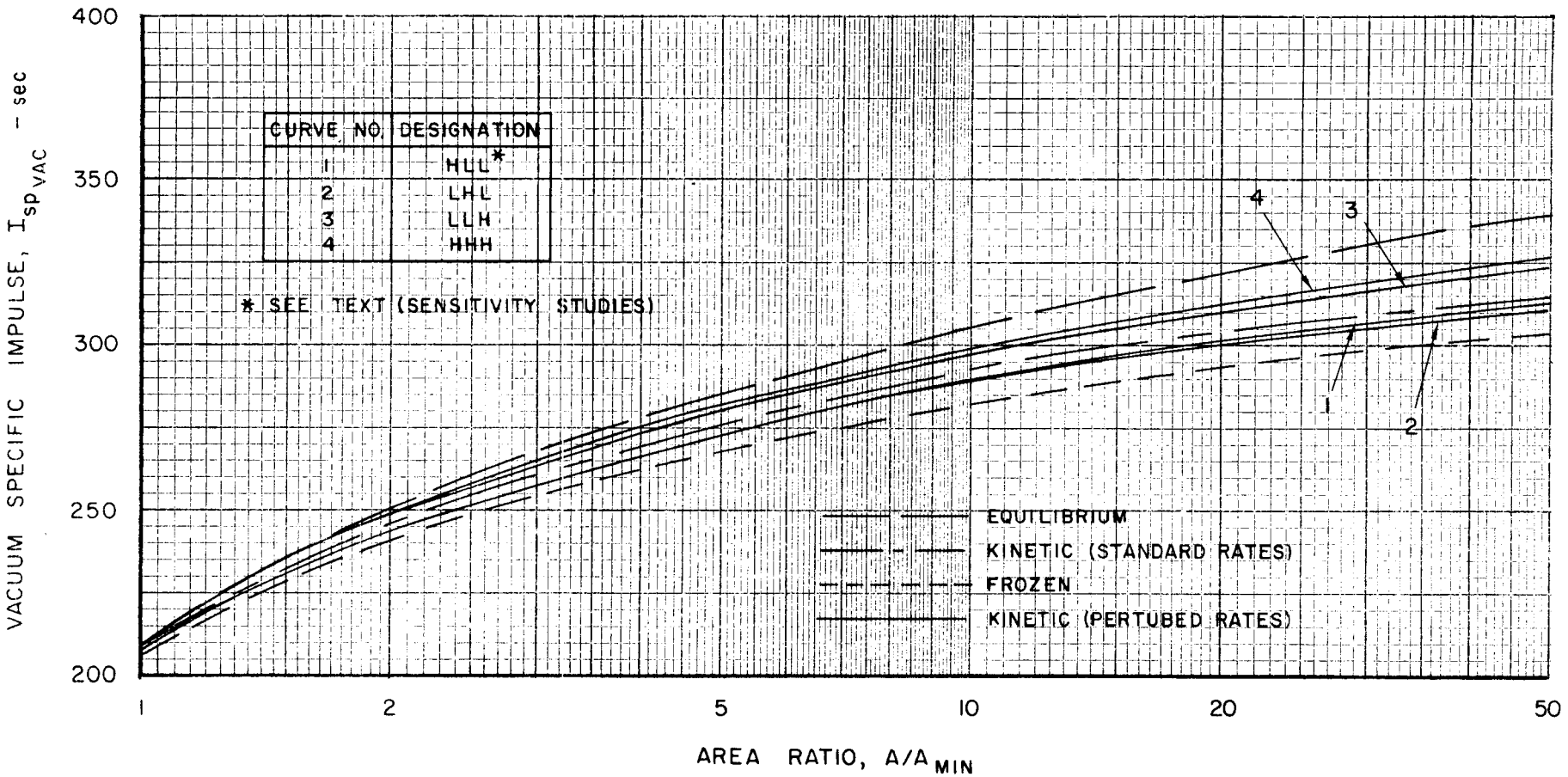

FIG. 1

C91096-13

COMPARISON OF ROCKET NOZZLE SPECIFIC IMPULSE CALCULATED FOR VARIOUS COMBINATIONS OF KINETIC RATE DATA

N_2O_4 – 50% N_2H_4 / 50% UDMH

O/F = 1.75
CHAMBER PRESSURE = 60 PSIA
THRUST = 150 LBS
NOZZLE CONFIGURATION 1 OF TABLE 2

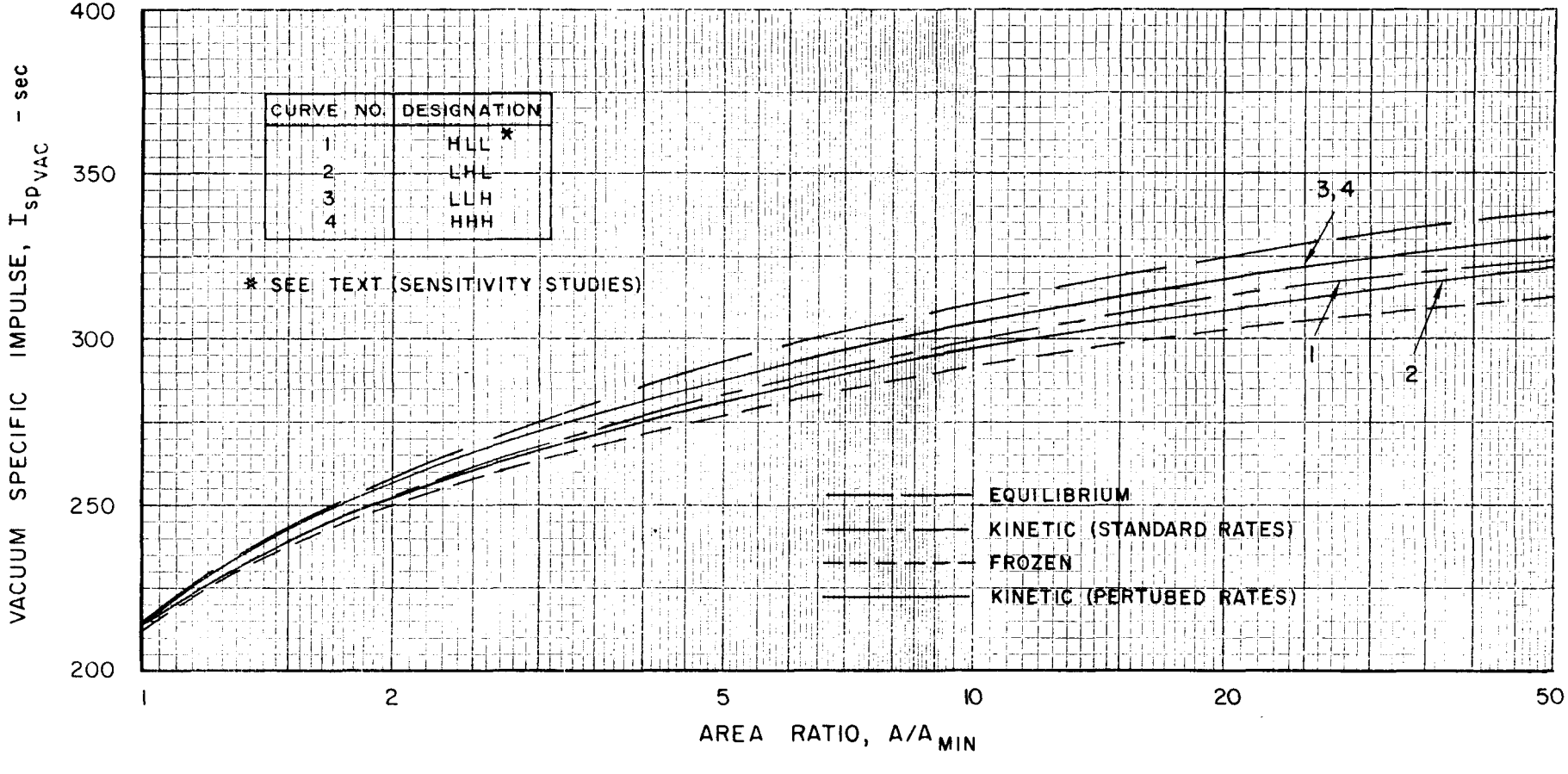

FIG. 2

PERFORMANCE SENSITIVITY TO VARIATIONS IN THE H_2-O_2 THREE-BODY RECOMBINATION RATE CONSTANTS

O/F = 8

P_C = 60 PSIA

$(A/A_{MIN})_{EXIT}$ = 40

NOZZLE CONFIGURATION 1 OF TABLE 2

NOTE : $k_{f_1}°$ AND $k_{f_2}°$ ARE RATES SPECIFIED IN TABLE 1

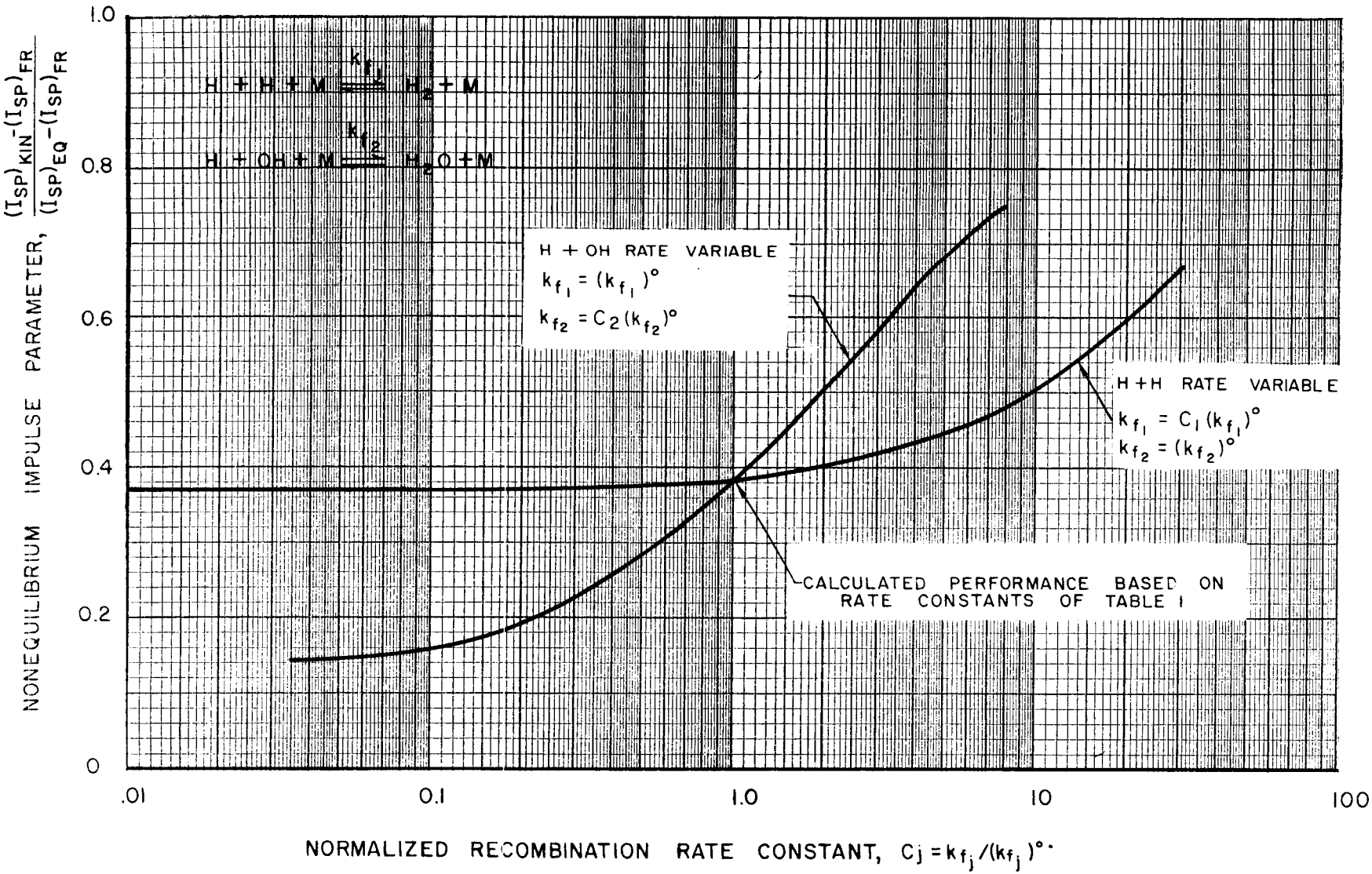

C910096-13

FIG. 3

FIG. 4

COMPARISON OF NOZZLE NONEQUILIBRIUM SPECIFIC IMPULSE PROFILES FOR COMBUSTION EFFICIENCIES OF 90 AND 100 PERCENT

$H_2 - O_2$

O/F = 5.0, CHAMBER PRESSURE = 60 PSIA

NOZZLE CONFIGURATION 1 OF TABLE 2

NOTE: COMBUSTION CHAMBER EXIT FLOW PROPERTIES FOR 90% EFFICIENCY ARE GIVEN IN TABLE 5

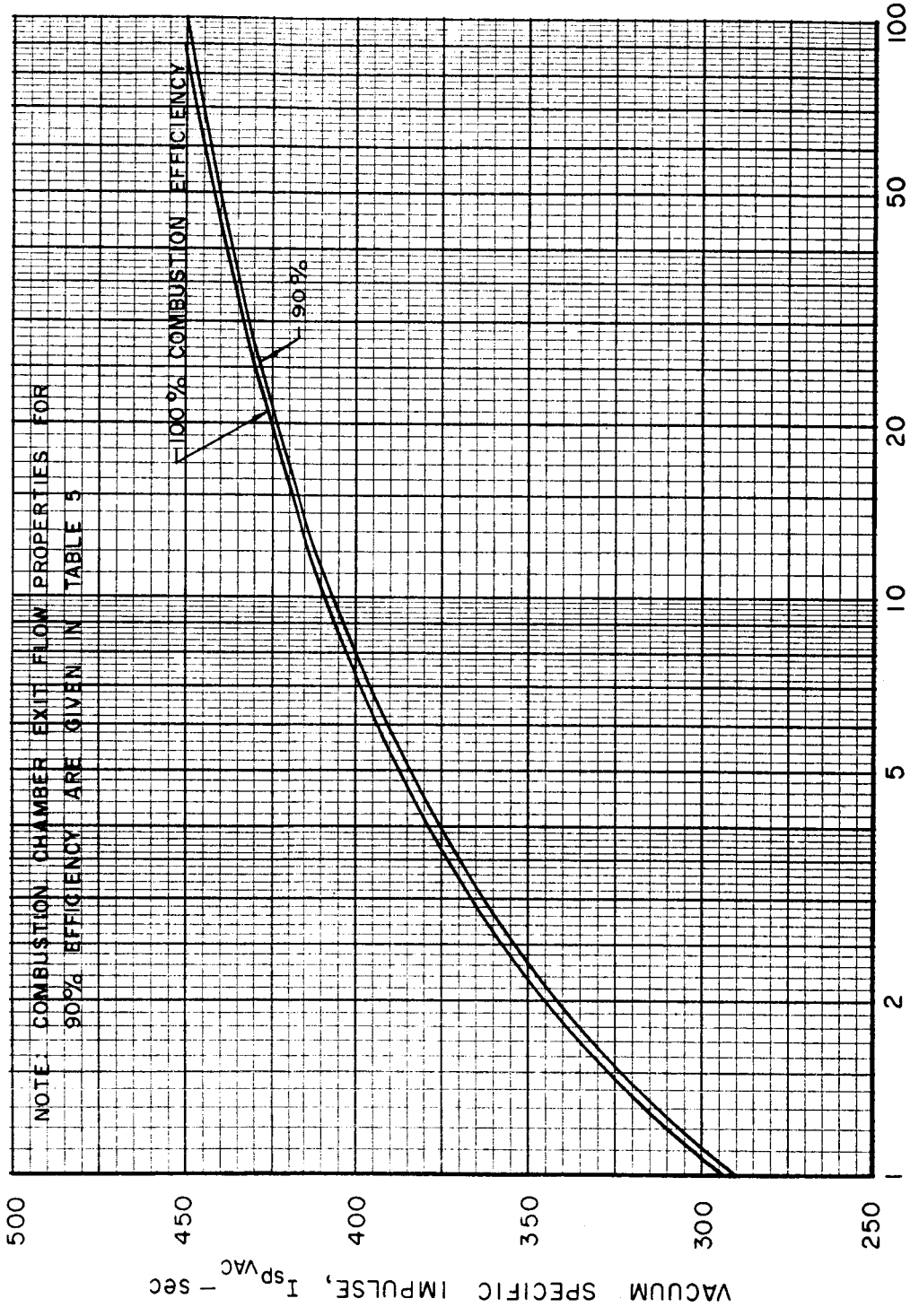

FIG. 5

VARIATION OF EQUILIBRIUM AND KINETIC HYDROGEN CONCENTRATION GRADIENTS WITH AREA RATIO FOR H_2-O_2 PROPELLANT SYSTEM

O/F = 8.0, CHAMBER PRESSURE = 60 PSIA
NOZZLE CONFIGURATION 1 OF TABLE 2

$$\left(\frac{\partial [H]_1}{\partial t}\right)_{\rho,KIN} = -2k_{f_1}[H]^2[M] \qquad \left(\frac{\partial [H]_2}{\partial t}\right)_{\rho,KIN} = -k_{f_2}[H][OH][M]$$

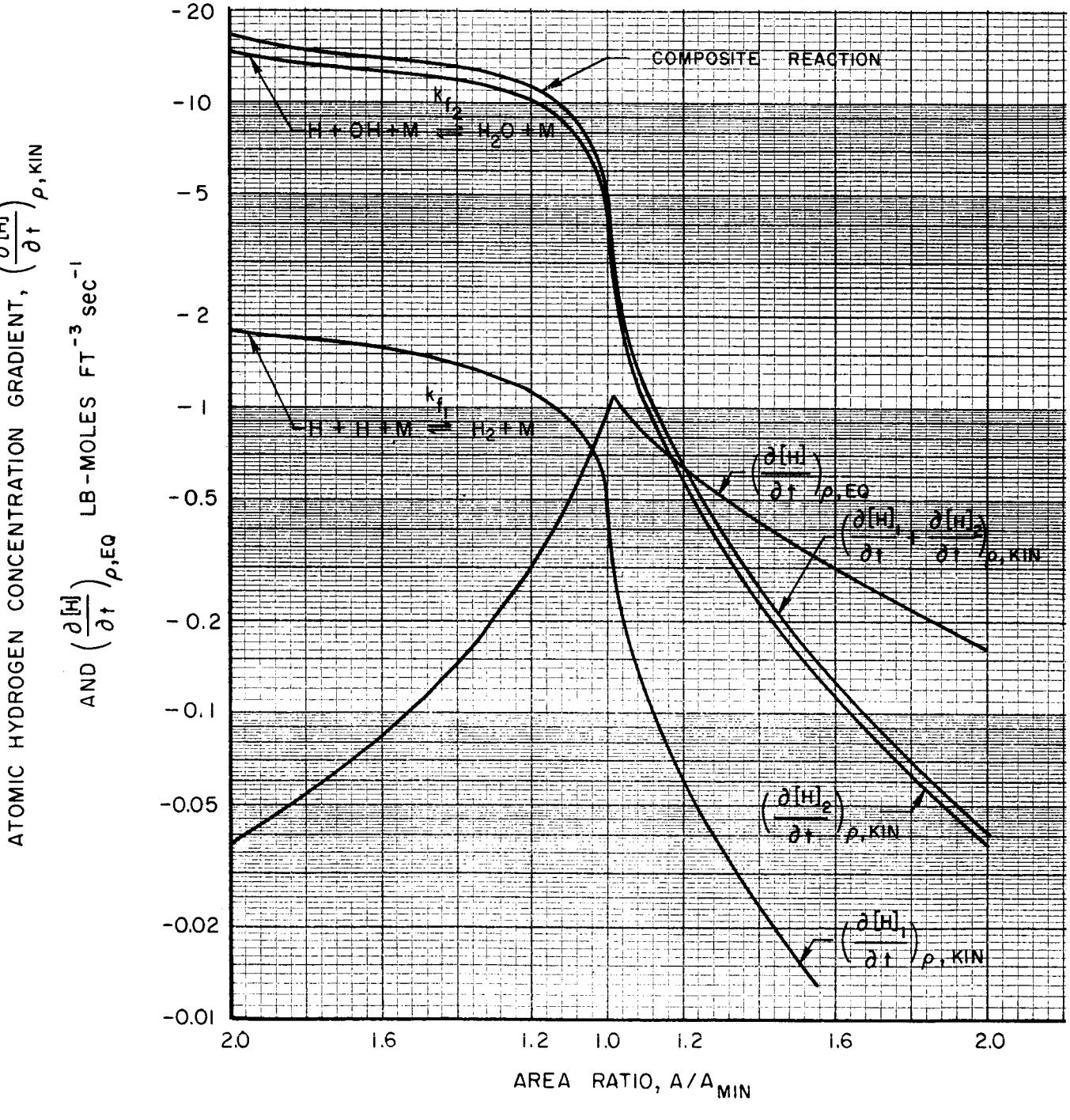

COMPARISON OF ROCKET NOZZLE SPECIFIC IMPULSE DATA CALCULATED FROM KINETIC AND BRAY ANALYSES

$H_2 - O_2$

O/F = 5.0

CHAMBER PRESSURE = 60 PSIA

THRUST = 150 LBS

NOZZLE CONFIGURATION 1 OF TABLE 2

CURVE NO	REACTION	SPECIES	FREEZING A/A_{MIN}
1	$H+H+M \rightleftharpoons H_2+M$	H	1.17 (SUB)
2	$H+OH+M \rightleftharpoons H_2O+M$	OH	1.01 (SUB)
3	$H+OH+M \rightleftharpoons H_2O+M$	H	1.01 (SUB)
4	COMPOSITE	H	1.00

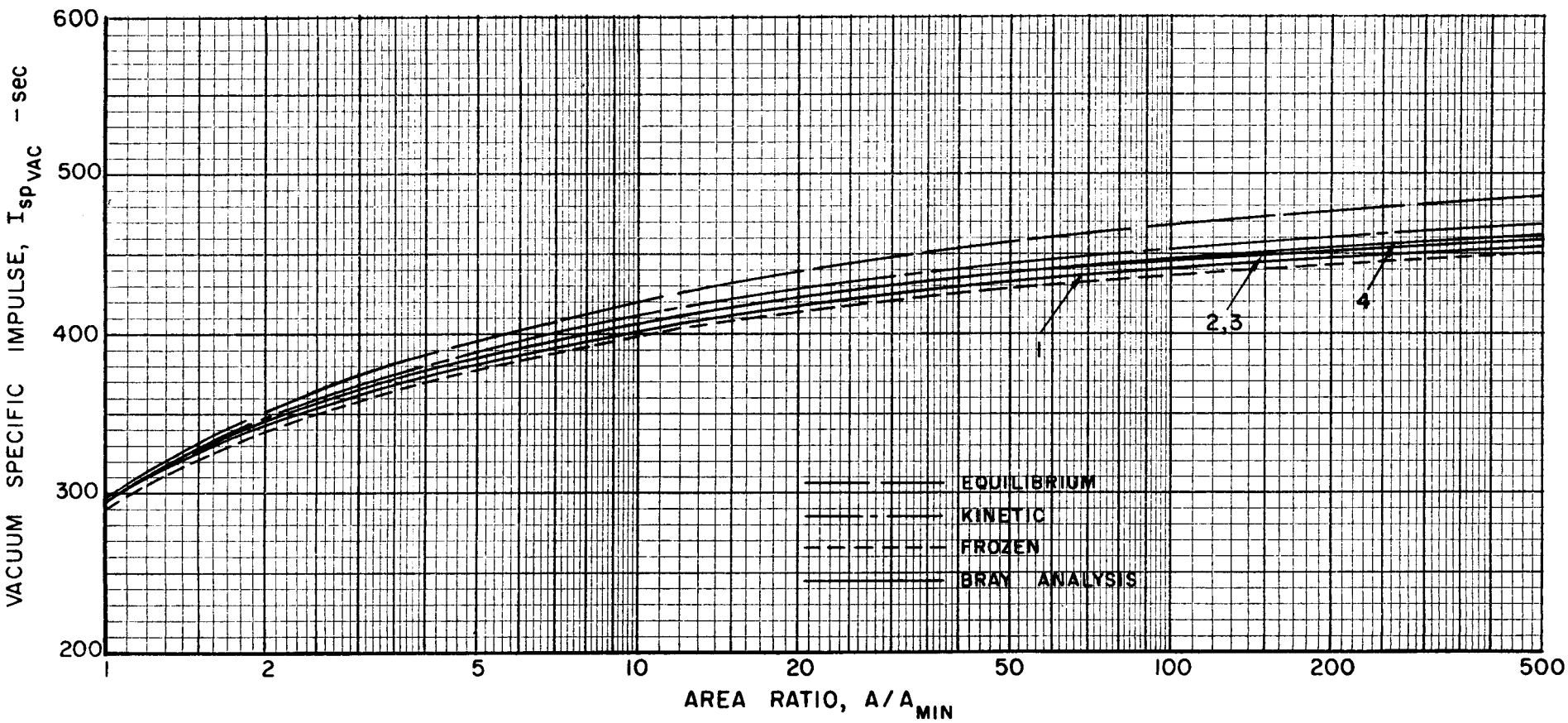

C910096-13

FIG. 6

COMPARISON OF ROCKET NOZZLE SPECIFIC IMPULSE DATA CALCULATED FROM KINETIC AND BRAY ANALYSES

$H_2 - O_2$

O/F = 8.0

CHAMBER PRESSURE = 60 PSIA

THRUST = 150 LBS

NOZZLE CONFIGURATION 1 OF TABLE 2

CURVE NO	REACTION	SPECIES	FREEZING A/A_{MIN}
1	$H+H+M \rightleftharpoons H_2+M$	H	1.04 (SUB)
2	$H+OH+M \rightleftharpoons H_2O+M$	H	1.17
3	$H+OH+M \rightleftharpoons H_2O+M$	OH	1.06
4	COMPOSITE	H	1.22

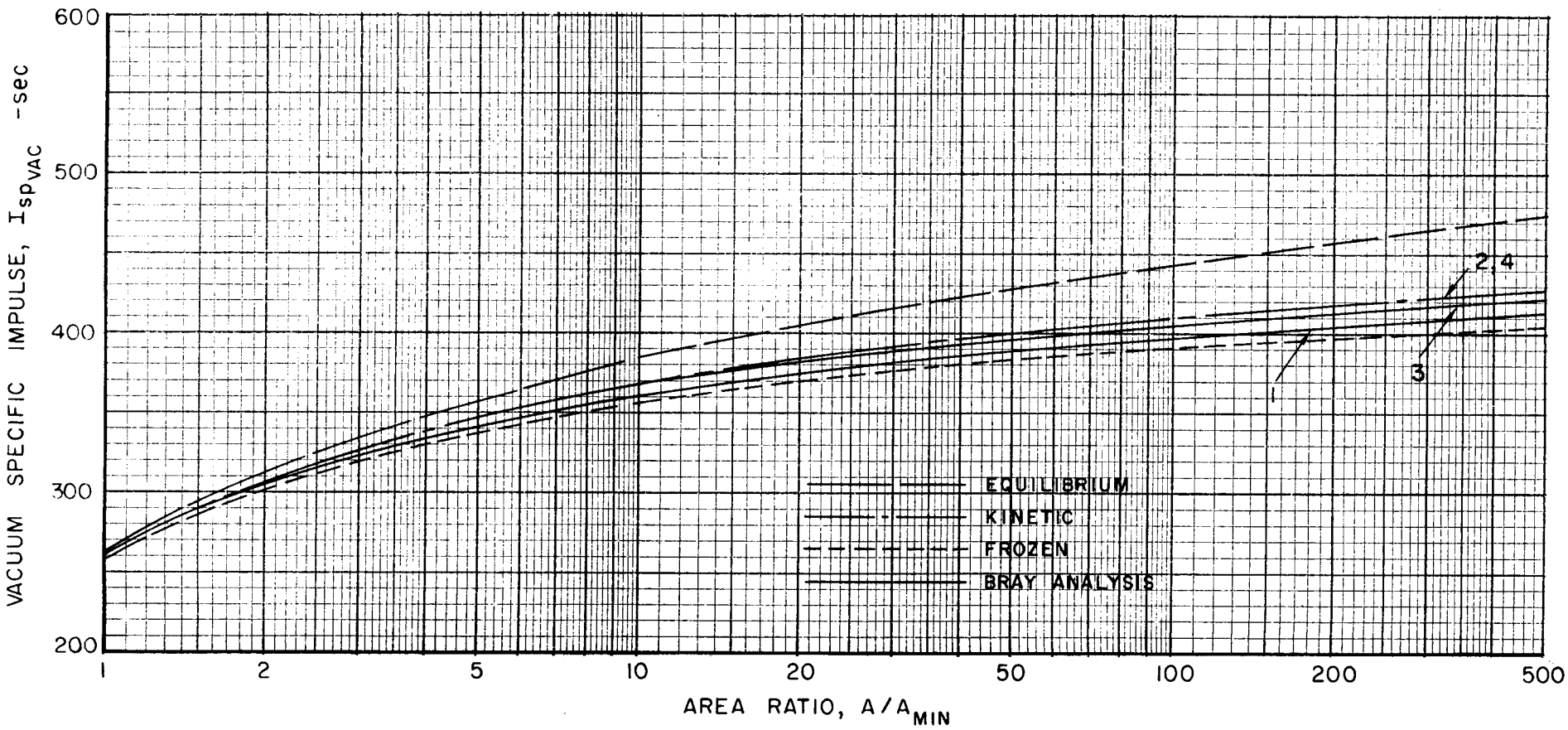

C910096-13

FIG 7

COMPARISON OF ROCKET NOZZLE SPECIFIC IMPULSE DATA CALCULATED FROM KINETIC AND BRAY ANALYSES

$H_2 - O_2$

O/F = 5.0

CHAMBER PRESSURE = 1000 PSIA

THRUST = 150 LBS

NOZZLE CONFIGURATION 1 OF TABLE 2

CURVE NO	REACTION	SPECIES	FREEZING A/A_{MIN}
1	$H+H+M \rightleftharpoons H_2+M$	H	1.26
2	$H+OH+M \rightleftharpoons H_2O+M$	H	1.65
3	$H+OH+M \rightleftharpoons H_2O+M$	OH	1.93
4	COMPOSITE	H	1.73

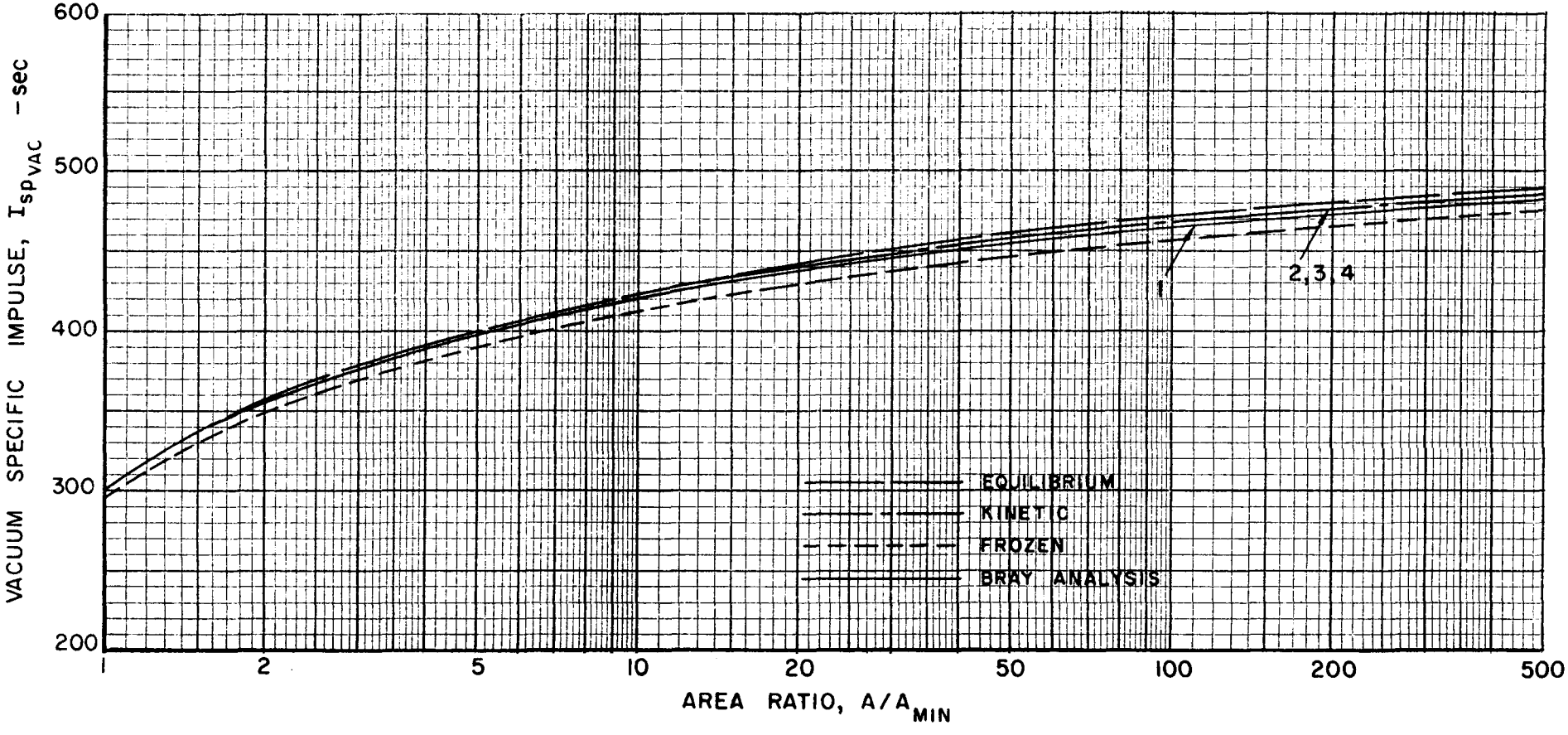

C910096-13

FIG. 8

COMPARISON OF ROCKET NOZZLE SPECIFIC IMPULSE DATA CALCULATED FROM KINETIC AND BRAY ANALYSES

$H_2 - O_2$

O/F = 8.0

CHAMBER PRESSURE = 1000 PSIA

THRUST = 150 LBS

NOZZLE CONFIGURATION 1 OF TABLE 2

CURVE NO	REACTION	SPECIES	FREEZING A/A_{MIN}
1	$H+H+M \rightleftharpoons H_2+M$	H	1.80
2	$H+OH+M \rightleftharpoons H_2O+M$	H	6.29
3	$H+OH+M \rightleftharpoons H_2O+M$	OH	4.25
4	COMPOSITE	H	6.30

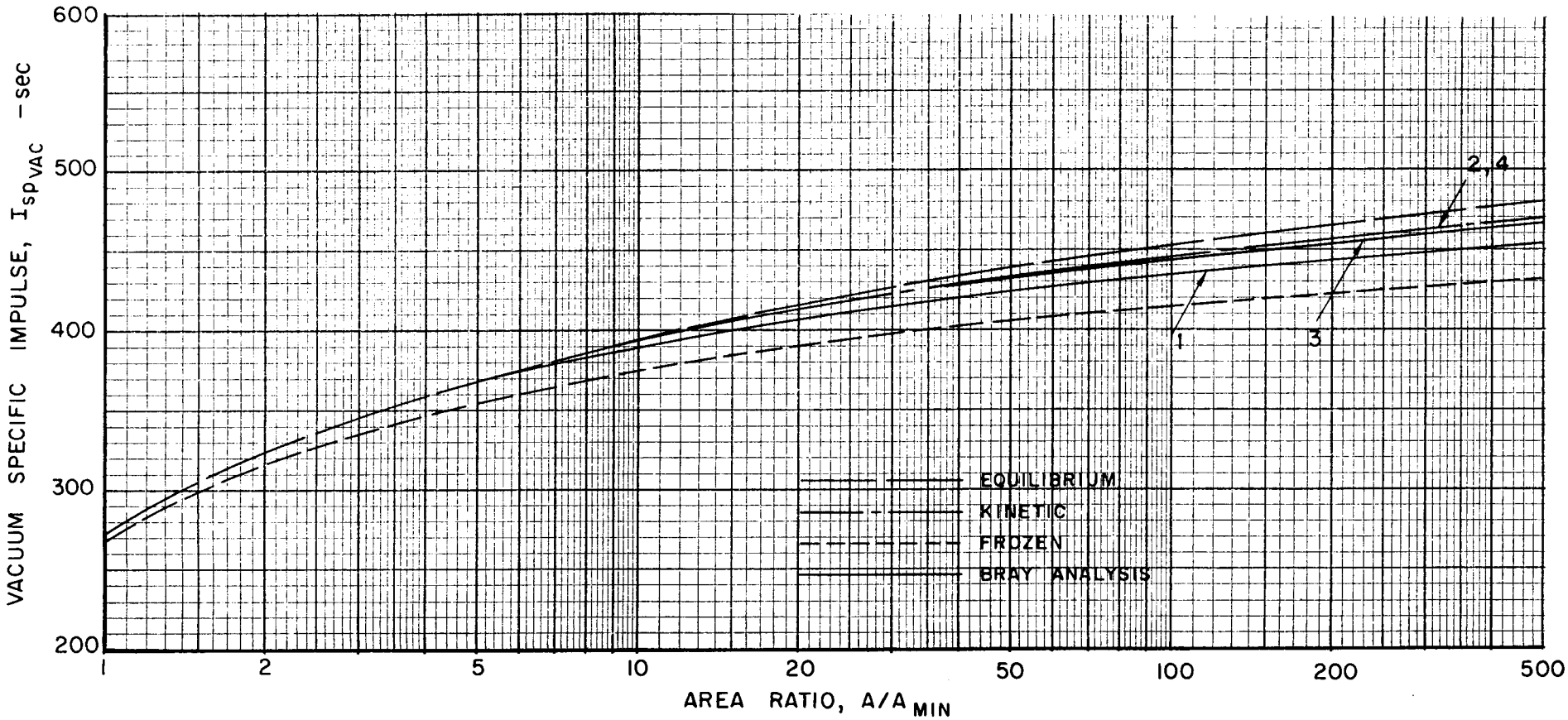

C910096-13

FIG. 9

COMPARISON OF ROCKET NOZZLE SPECIFIC IMPULSE DATA CALCULATED FROM KINETIC AND BRAY ANALYSES

N_2O_4 – 50% N_2H_4 / 50% UDMH

O/F = 1.75

CHAMBER PRESSURE = 60 PSIA

THRUST = 150 LBS NOZZLE CONFIGURATION 1 OF TABLE 2

CURVE NO	REACTION	SPECIES	FREEZING A/A_{MIN}
1	$H+H+M \rightleftharpoons H_2+M$	H	1.25 (SUB)
2	$H+OH+M \rightleftharpoons H_2O+M$	OH	1.00
3	$H+OH+M \rightleftharpoons H_2O+M$	H	1.00
4	$CO+OH \rightleftharpoons CO_2+H$	CO	2.92
5	$CO+OH \rightleftharpoons CO_2+H$	OH	2.72
6	COMPOSITE	H	1.00

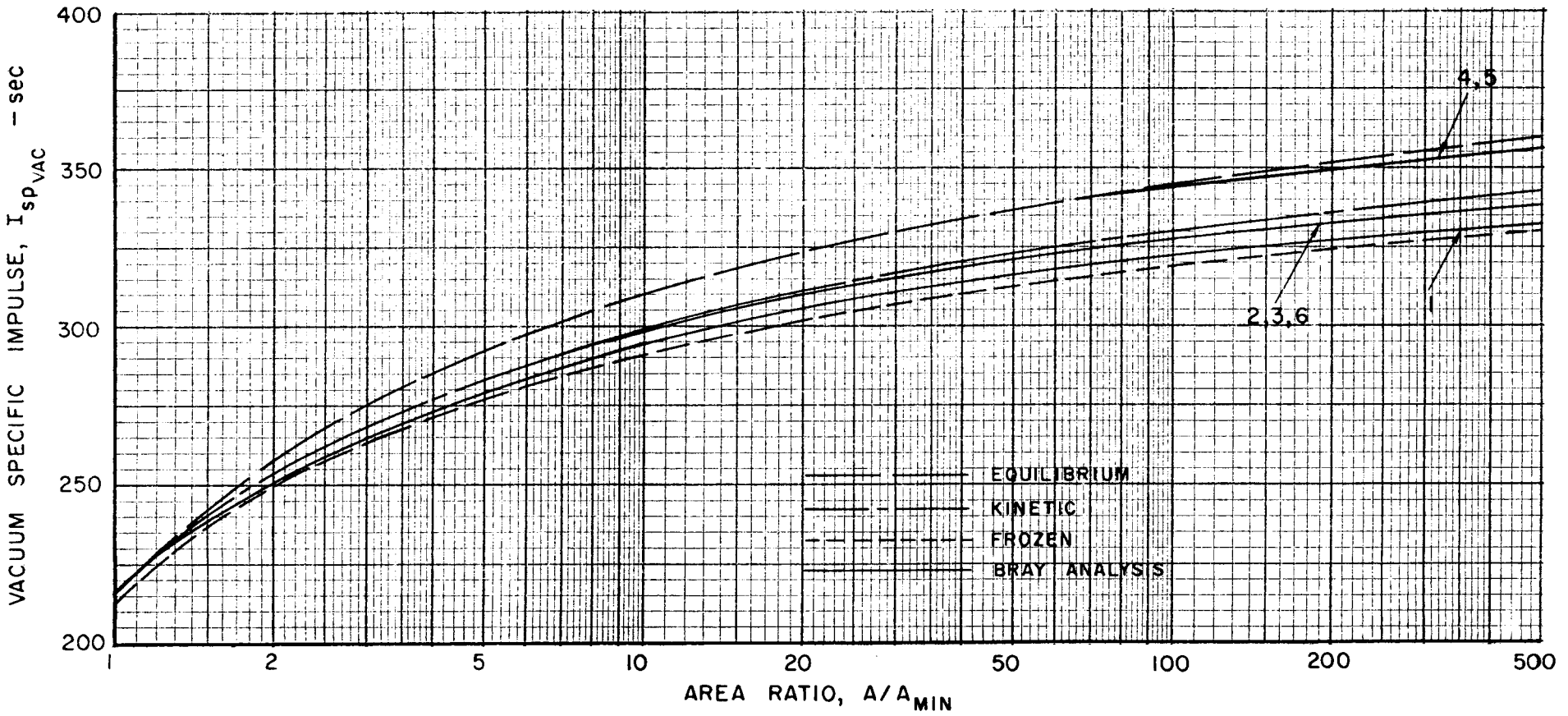

C910096-13

FIG. 10

COMPARISON OF ROCKET NOZZLE SPECIFIC IMPULSE DATA CALCULATED FROM KINETIC AND BRAY ANALYSES

N_2O_4 - 50% N_2H_4/ 50% UDMH

O/F = 2.25

CHAMBER PRESSURE = 60 PSIA

THRUST = 150 LBS NOZZLE CONFIGURATION 1 OF TABLE 2

CURVE NO	REACTION	SPECIES	FREEZING A/A_{MIN}
1	$H+H+M \rightleftharpoons H_2+M$	H	1.27 (SUB)
2	$H+OH+M \rightleftharpoons H_2O+M$	OH	1.00
3	$H+OH+M \rightleftharpoons H_2O+M$	H	1.02
4	$CO+OH \rightleftharpoons CO_2+H$	CO	3.20
5	$CO+OH \rightleftharpoons CO_2+H$	OH	3.50
6	COMPOSITE	H	1.02

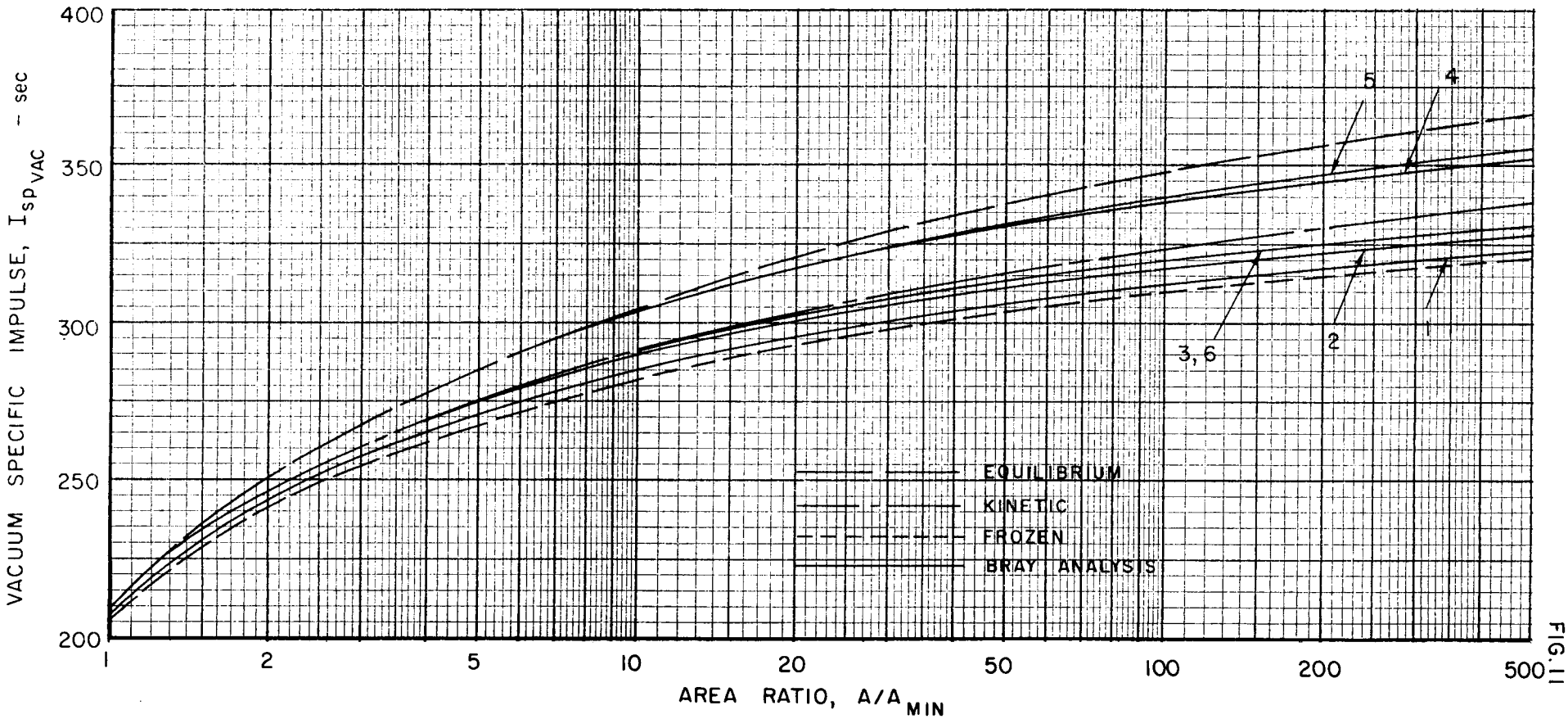

FIG. 11

C910096-13

COMPARISON OF ROCKET NOZZLE SPECIFIC IMPULSE DATA CALCULATED FROM KINETIC AND BRAY ANALYSES

N_2O_4 – 50% N_2H_4/ 50% UDMH

O/F = 1.75

CHAMBER PRESSURE = 1000 PSIA

THRUST = 150 LBS NOZZLE CONFIGURATION 1 OF TABLE 2

CURVE NO	REACTION	SPECIES	FREEZING A/A_{MIN}
1	$H+H+M \rightleftharpoons H_2+M$	H	1.15 (SUB)
2	$H+OH+M \rightleftharpoons H_2O+M$	OH	1.71
3	$H+OH+M \rightleftharpoons H_2O+M$	H	1.83
4	$CO+OH \rightleftharpoons CO_2+H$	CO	3.52
5	$CO+OH \rightleftharpoons CO_2+H$	OH	9.02
6	COMPOSITE	H	1.86

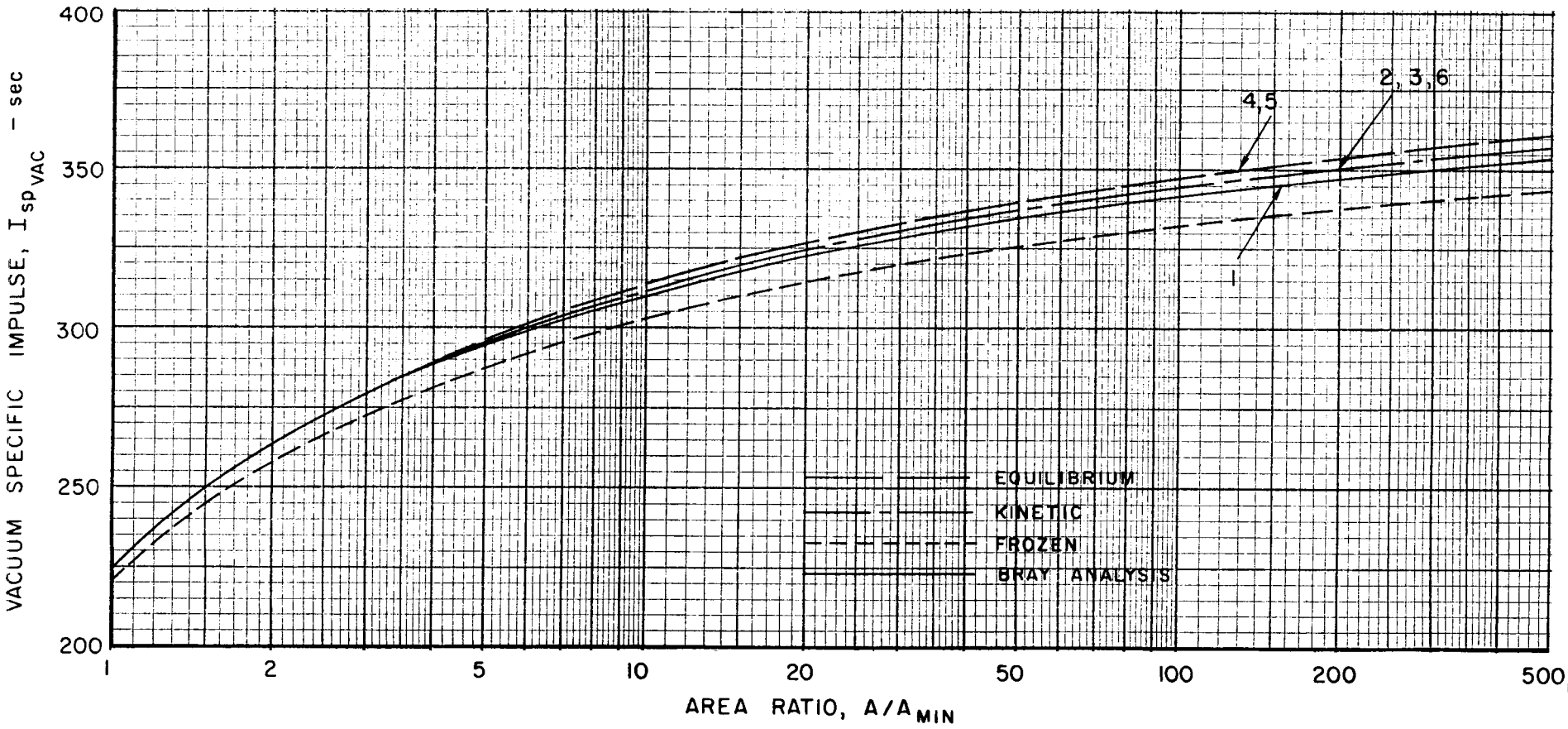

C910096-13

FIG. 12

COMPARISON OF ROCKET NOZZLE SPECIFIC IMPULSE DATA CALCULATED FROM KINETIC AND BRAY ANALYSES

N_2O_4 – 50% N_2H_4 / 50% UDMH

O/F = 2.25

CHAMBER PRESSURE = 1000 PSIA

THRUST = 150 LBS NOZZLE CONFIGURATION 1 OF TABLE 2

CURVE NO	REACTION	SPECIES	FREEZING A/A_{MIN}
1	$H+H+M \rightleftharpoons H_2+M$	H	1.16 (SUB)
2	$H+OH+M \rightleftharpoons H_2O+M$	OH	2.28
3	$H+OH+M \rightleftharpoons H_2O+M$	H	3.64
4	$CO+OH \rightleftharpoons CO_2+H$	CO	12.52
5	$CO+OH \rightleftharpoons CO_2+H$	OH	14.73
6	COMPOSITE	H	3.65

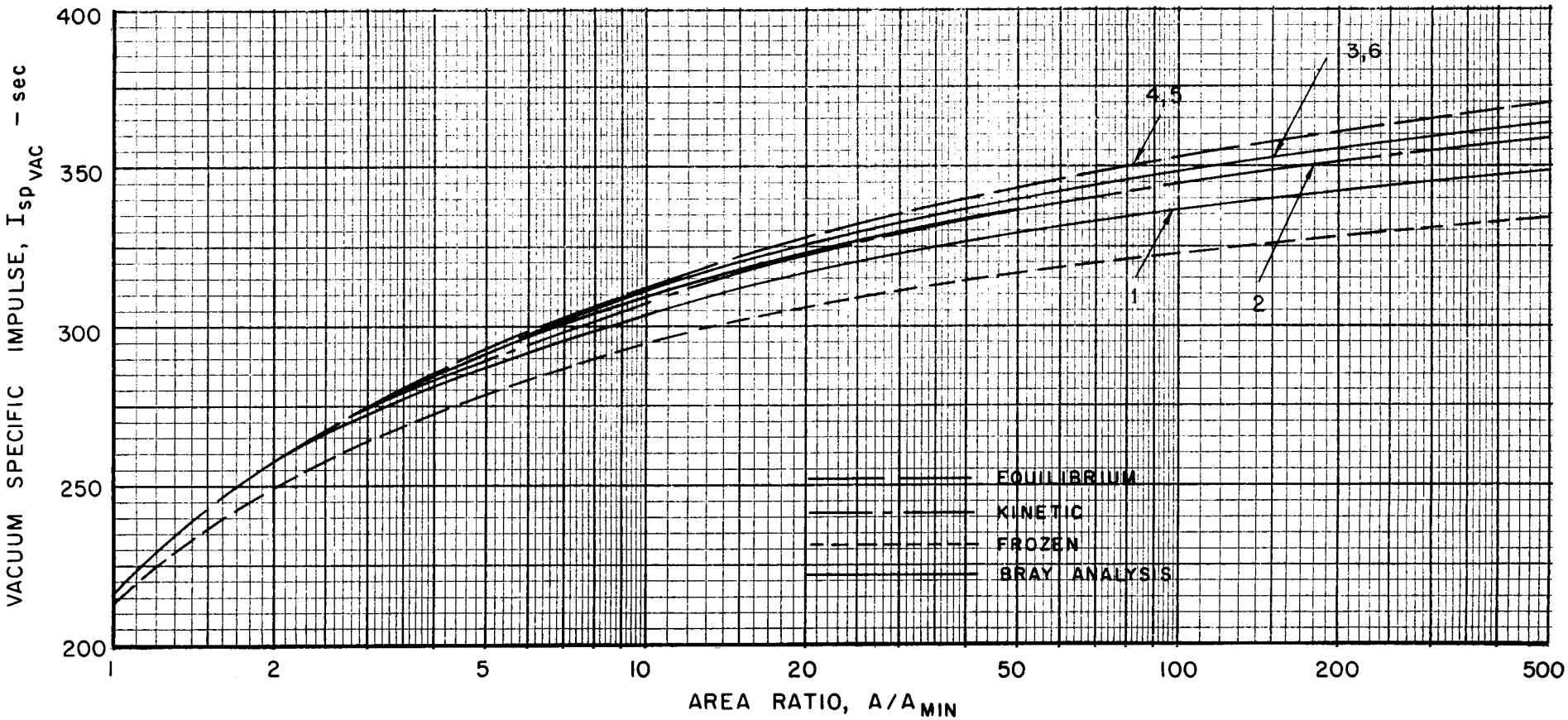

C910096-13

FIG. 13

FIG. 14

EFFECT OF FREEZING AREA RATIO ON NONEQUILIBRIUM PERFORMANCE FOR N_2O_4 — 50 % N_2H_4 / 50 % UDMH PROPELLANT SYSTEM

NOZZLE CONFIGURATION I OF TABLE 2 $(A/A_{MIN})_{EXIT} = 50$

CURVE	O/F	P_C PSIA	$(I_{SP})_{EQ}$	$(I_{SP})_{FR}$
———	1.75	60	337	312.5
– – –	2.25	60	337.5	303
- - - - -	1.75	1000	340	325
———	2.25	1000	343	316

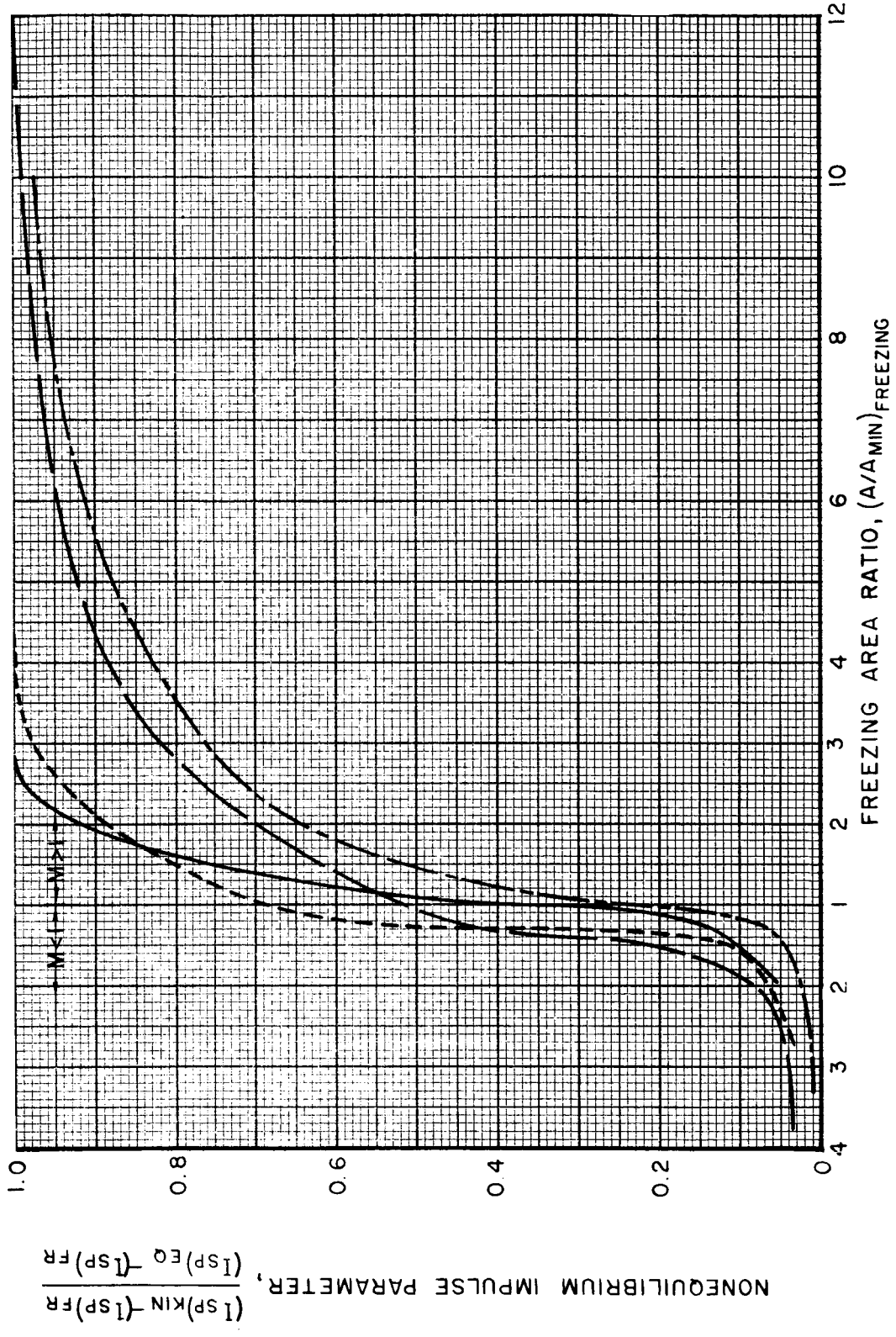

FIG. 15

EFFECT OF FREEZING AREA RATIO ON NONEQUILIBRIUM PERFORMANCE FOR HYDROGEN-OXYGEN PROPELLANT SYSTEM

NOZZLE CONFIGURATION I OF TABLE 2 $(A/A_{MIN})_{EXIT} = 40$

CURVE	O/F	P_C PSIA	$(I_{SP})_{EQ}$	$(I_{SP})_{FR}$
———	5	60	454	426
— — —	8	60	422	380
- - - - -	5	1000	457	442
— — —	8	1000	434	402

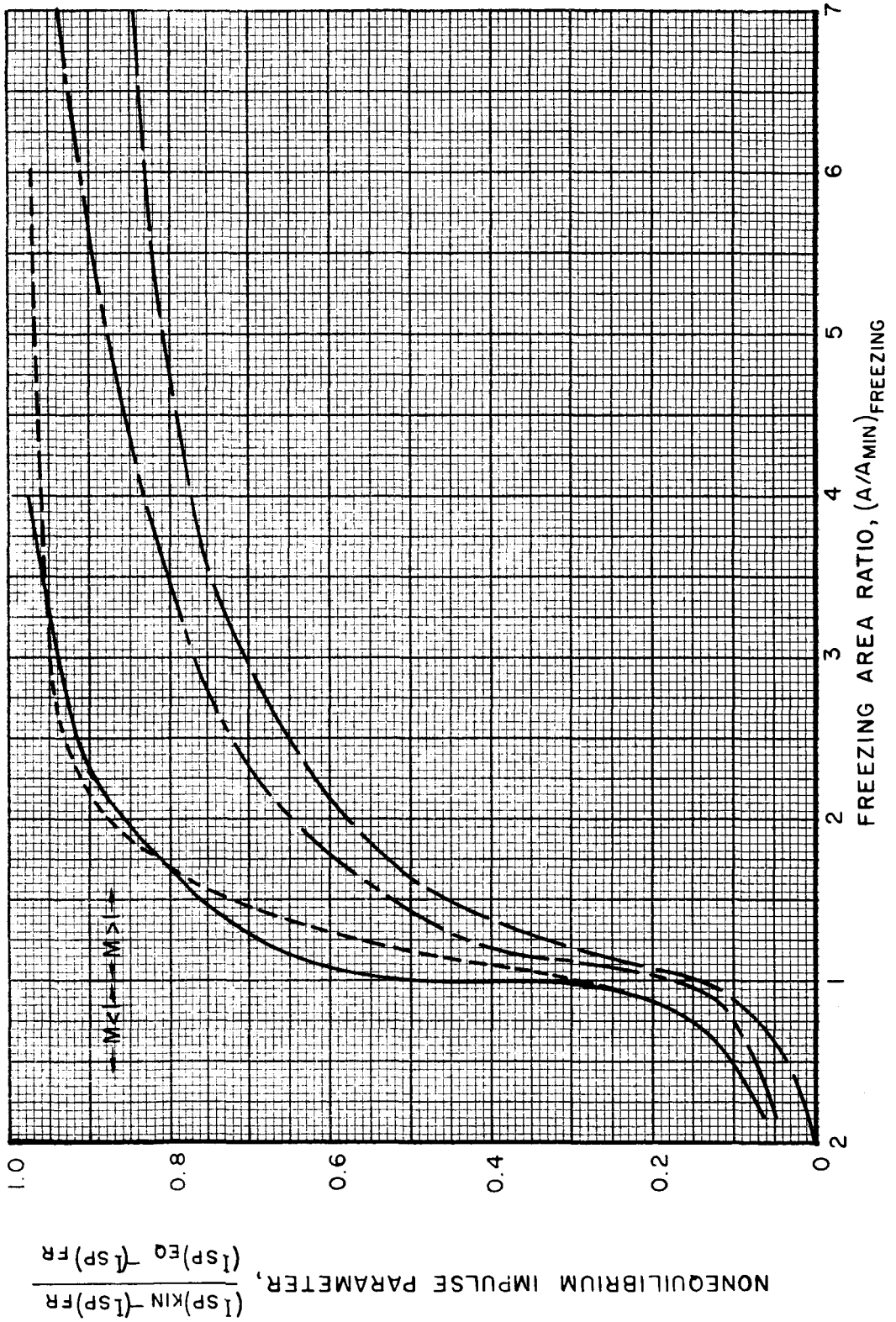

C910096-13

COMPARISON OF TEMPERATURE PROFILES BASED ON SUDDEN FREEZING AND EXACT NONEQUILIBRIUM CALCULATIONS

N_2O_4 – 50% N_2H_4/50% UDMH

O/F = 2.25 P_c = 60 PSIA

$(A/A_{MIN})_{FREEZING}$ = 1.014

NOZZLE CONFIGURATION I OF TABLE 2

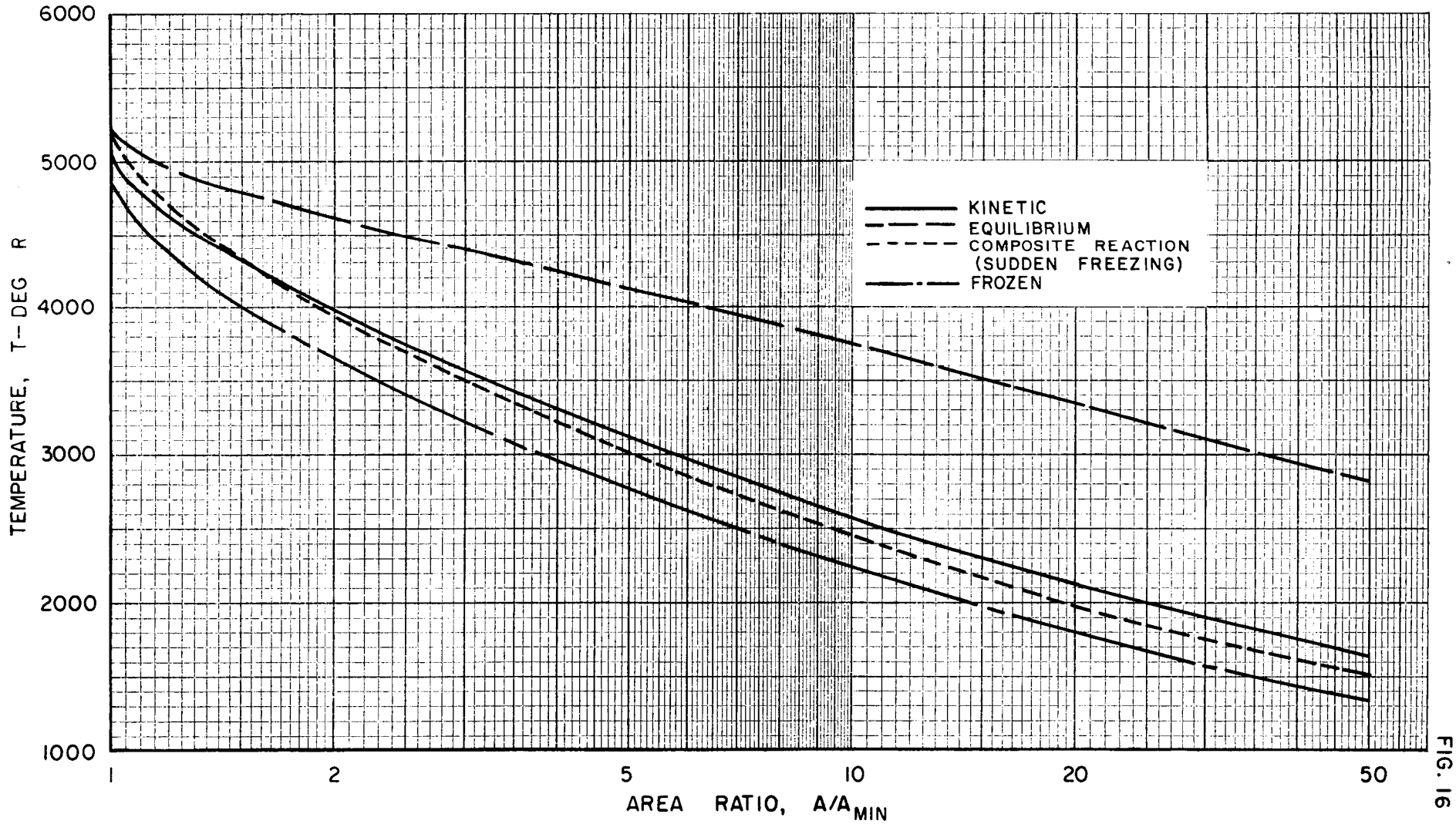

FIG. 16

FIG. 17

COMPARISON OF PRESSURE PROFILES BASED ON SUDDEN FREEZING AND EXACT NONEQUILIBRIUM CALCULATIONS

N_2O_4 - 50% N_2H_4/50% UDMH

O/F = 2.25 P_c = 60 PSIA

$(A/A_{MIN})_{FREEZING}$ = 1.014

NOZZLE CONFIGURATION I OF TABLE 2

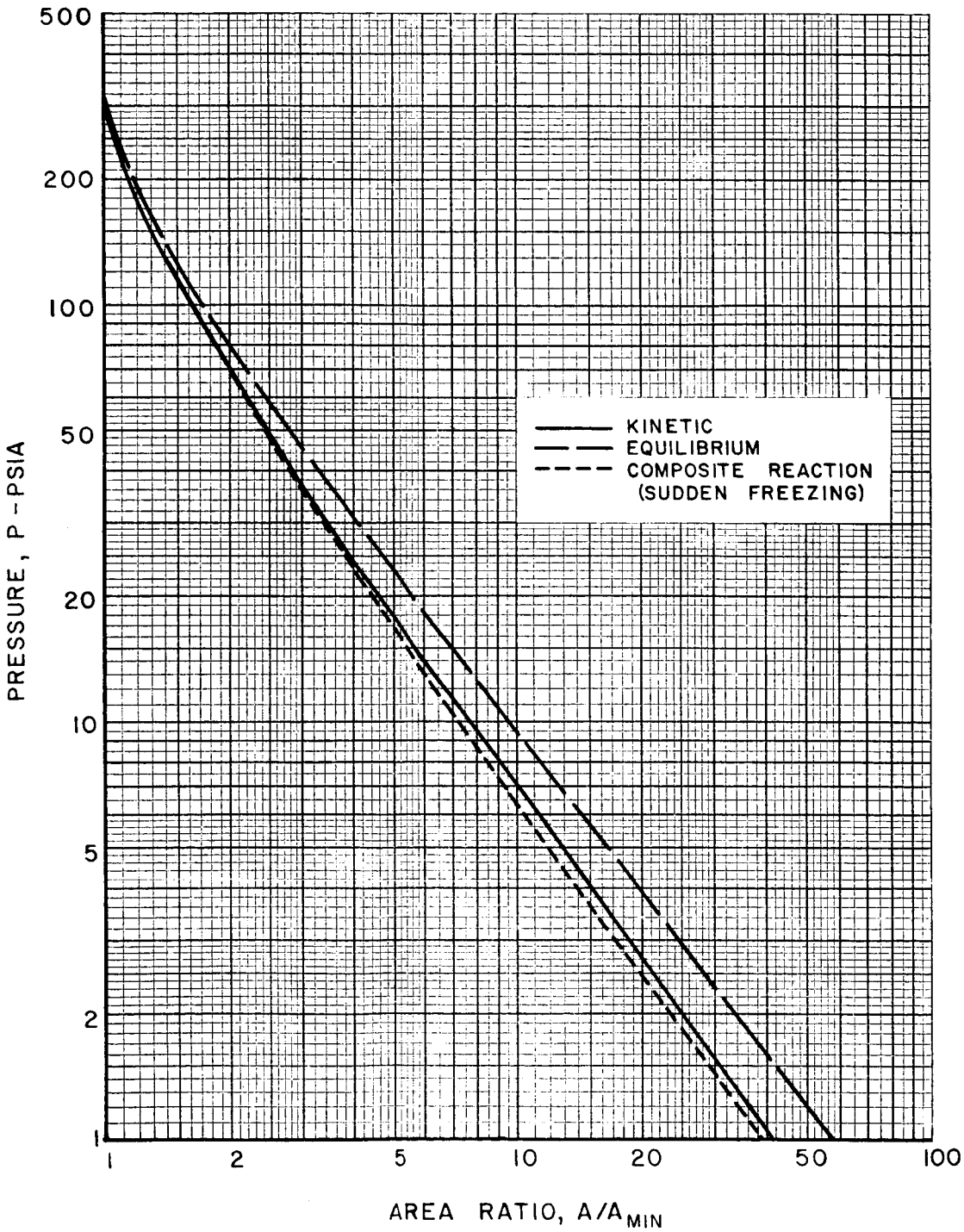

FIG. 18

COMPARISON OF ATOM AND MOLECULE CONCENTRATION PROFILES BASED ON SUDDEN FREEZING AND EXACT NONEQUILIBRIUM CALCULATIONS

N_2O_4 - 50 % N_2H_4 / 50 % UDMH

O/F = 2.25 P_c = 60 PSIA

$(A/A_{MIN})_{FREEZING}$ = 1.014

NOZZLE CONFIGURATION I OF TABLE 2

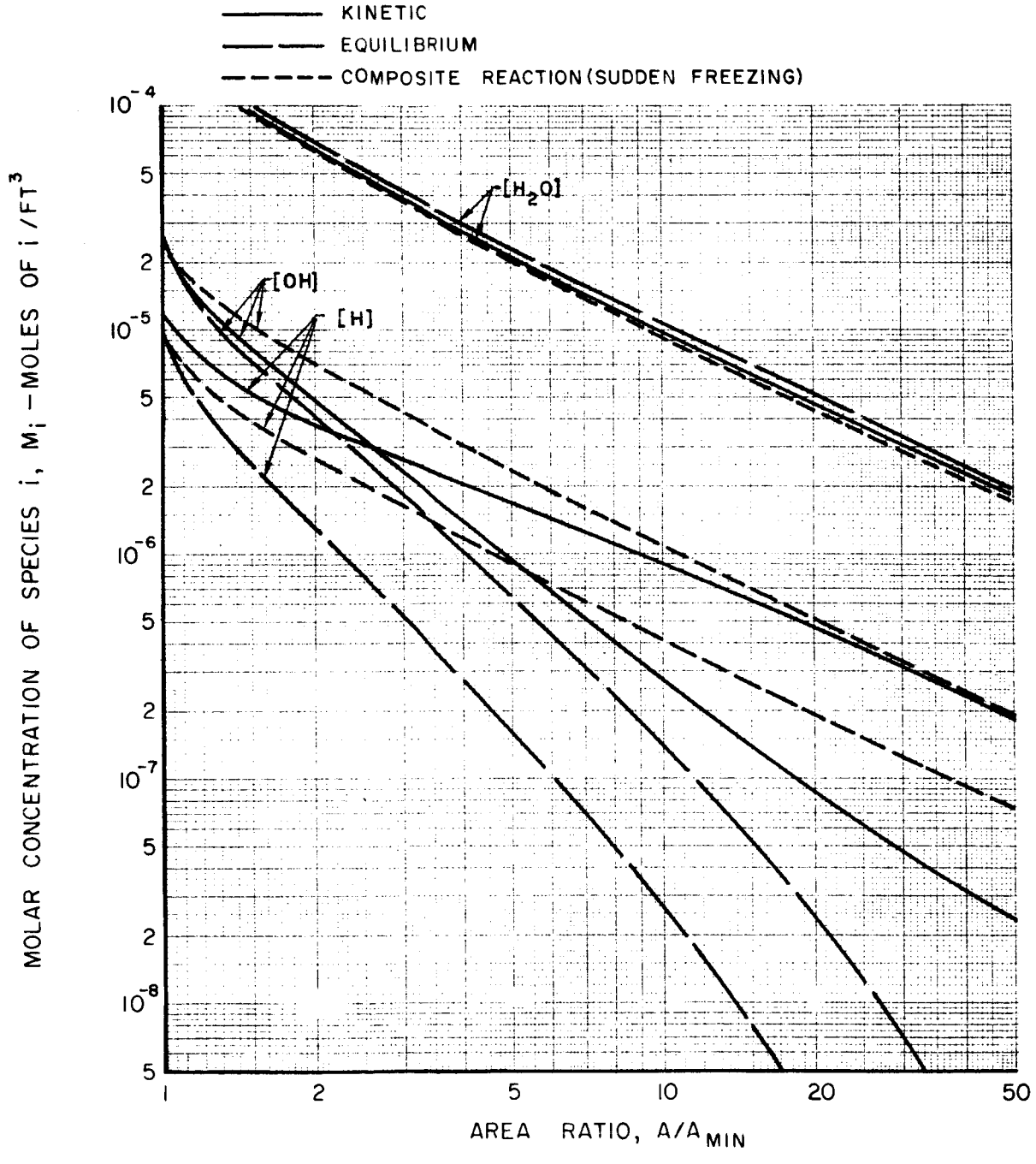

C910096-13

FIG. 19

COMPARISON OF ATOM AND MOLECULE CONCENTRATION PROFILES BASED ON SUDDEN FREEZING AND EXACT NONEQUILIBRIUM CALCULATIONS

N_2O_4–50%N_2H_4/50% UDMH

O/F = 2.25 P_c = 60 PSIA

$(A/A_{MIN})_{FREEZING}$ = 1.014

NOZZLE CONFIGURATION I OF TABLE 2

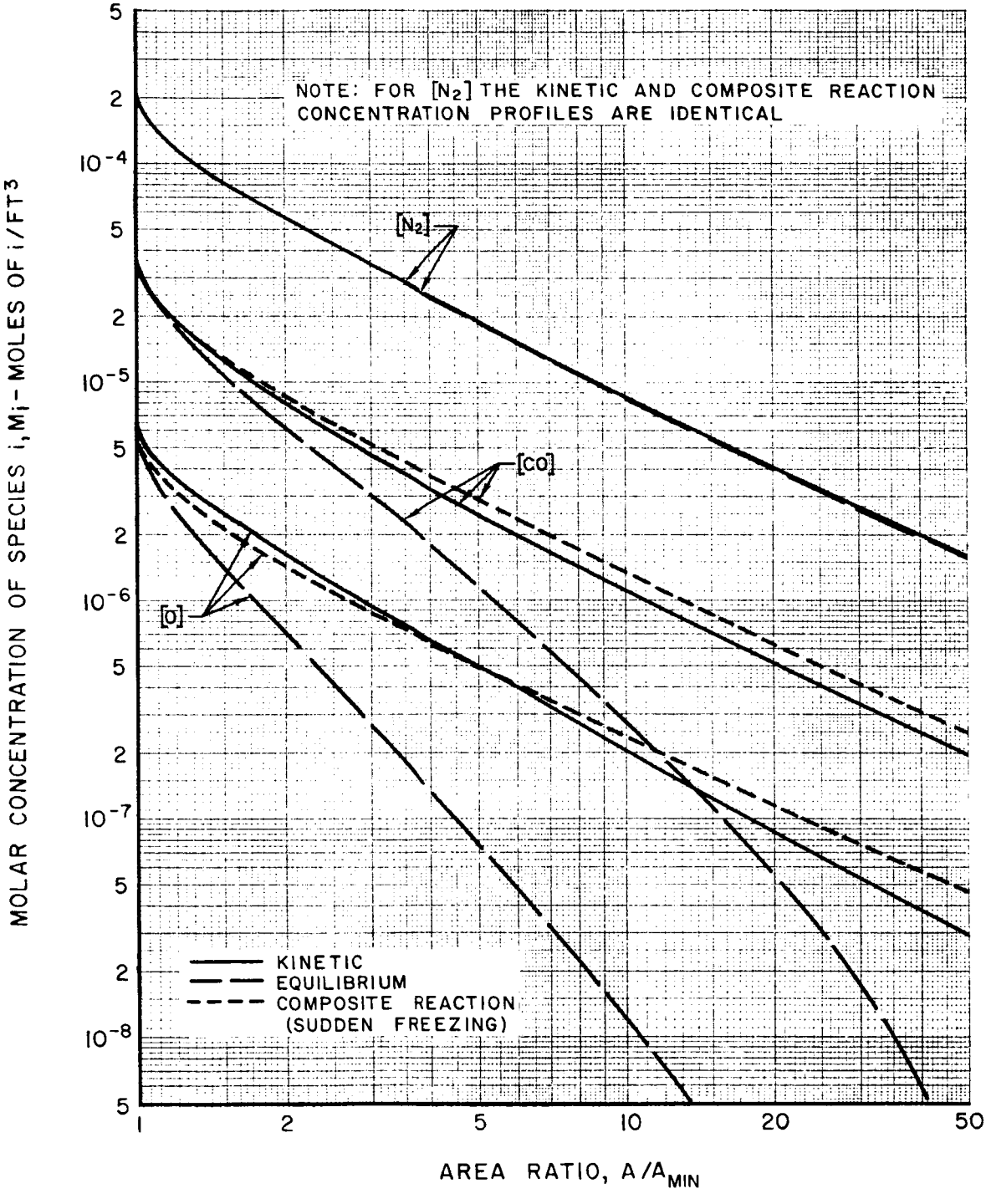

FIG. 20

COMPARISON OF NOZZLE NONEQUILIBRIUM SPECIFIC IMPULSE PROFILES FOR DIFFERENT CONVERGENT SECTION CONTOURS

H_2-O_2

O/F = 5.0, CHAMBER PRESSURE = 60 PSIA

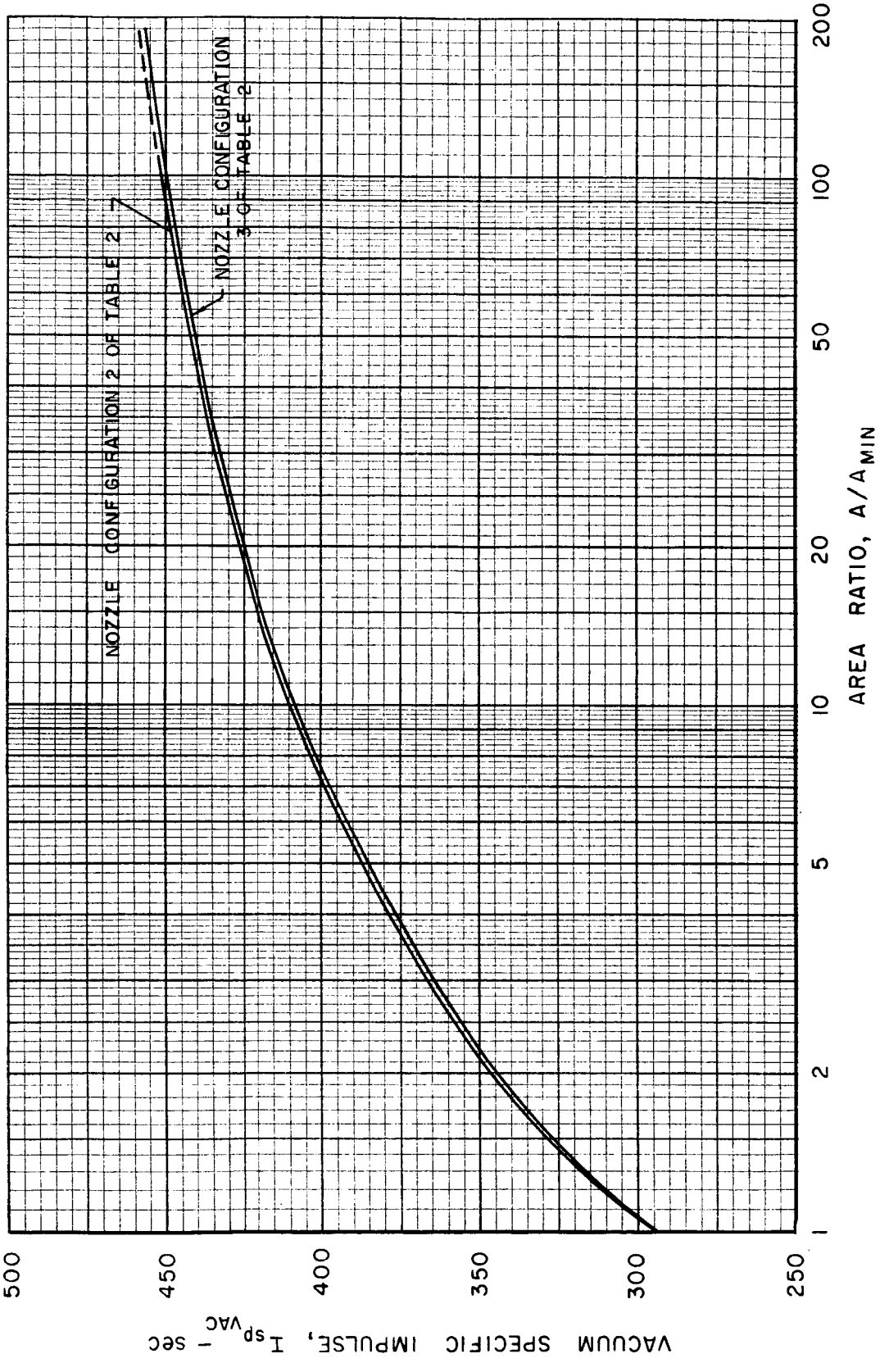

FIG. 21

RL-10 AND NASw-366 DESIGN NOZZLE CONTOURS

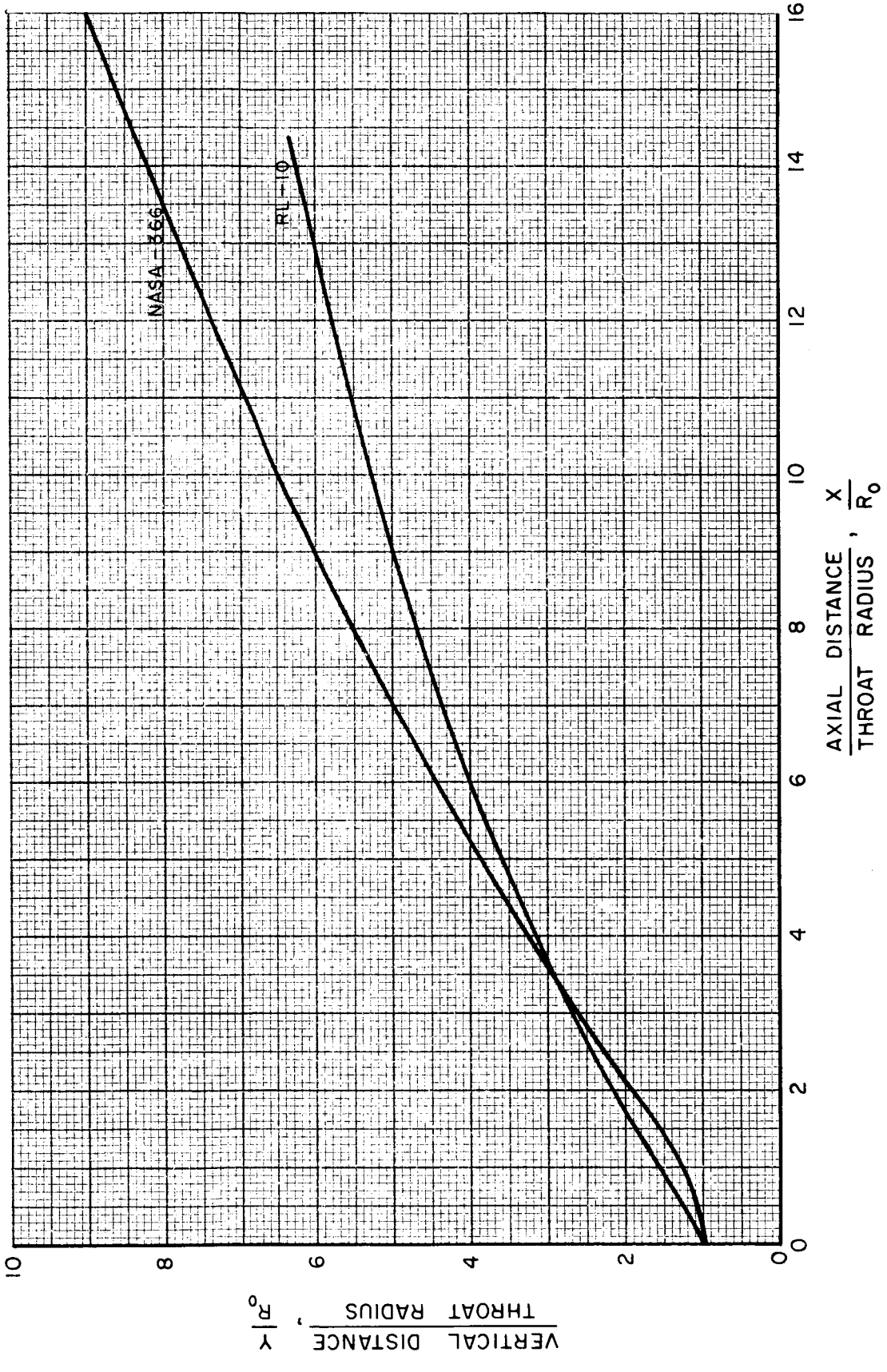

FIG. 22

COMPARISON OF NASw-366 NOZZLE PERFORMANCE RESULTS CALCULATED FOR KINETIC AND EQUILIBRIUM FLOW WITH FROZEN SOUND SPEED

$H_2 - O_2$

O/F = 5.0, CHAMBER PRESSURE = 60 PSIA

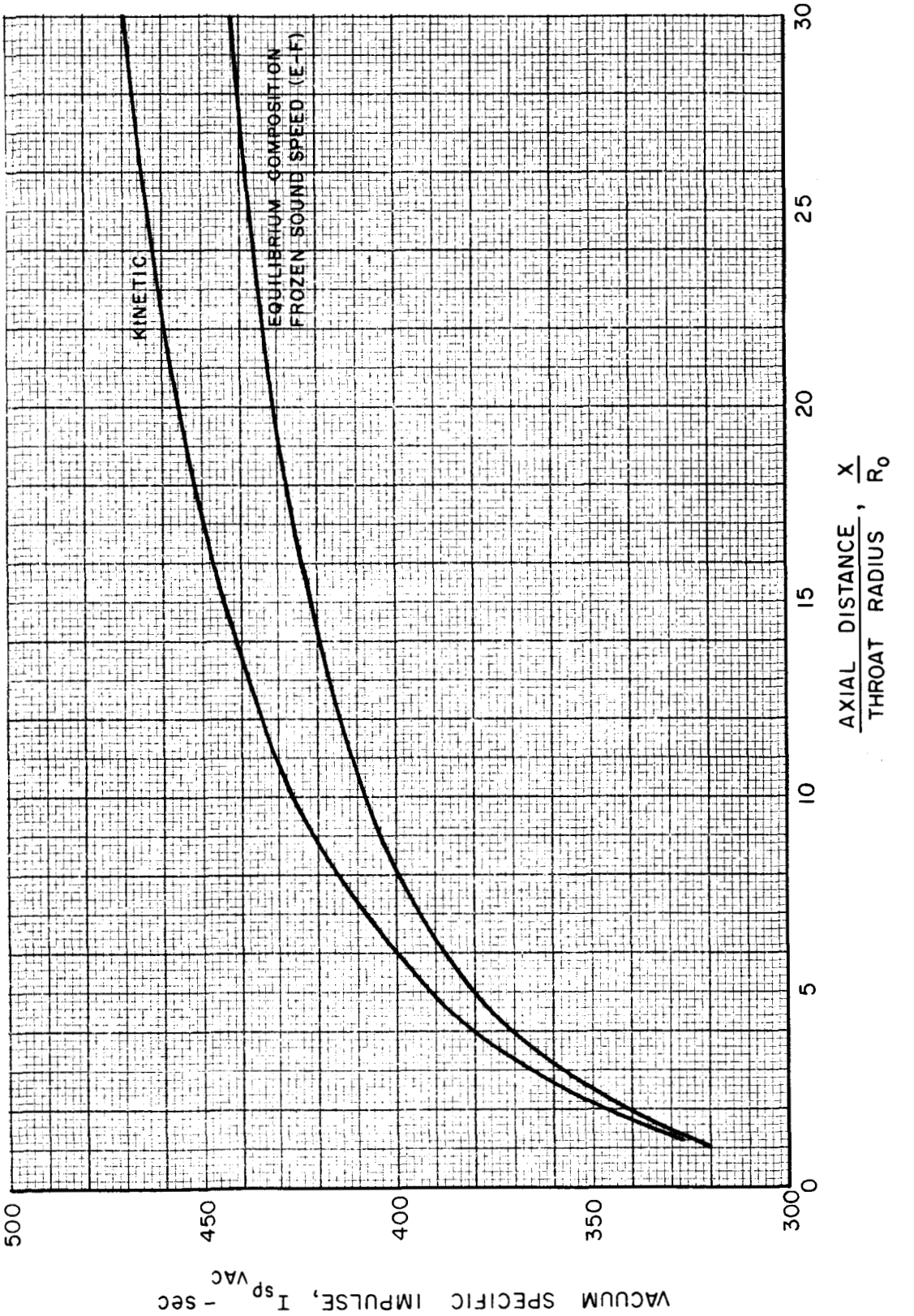

FIG. 23

COMPARISON OF RL-10 NOZZLE PERFORMANCE CALCULATED FOR EQUILIBRIUM FLOW WITH EQUILIBRIUM SOUND SPEED AND EQUILIBRIUM FLOW WITH FROZEN SOUND SPEED

$H_2 - O_2$

O/F = 5.0, CHAMBER PRESSURE = 300 PSIA

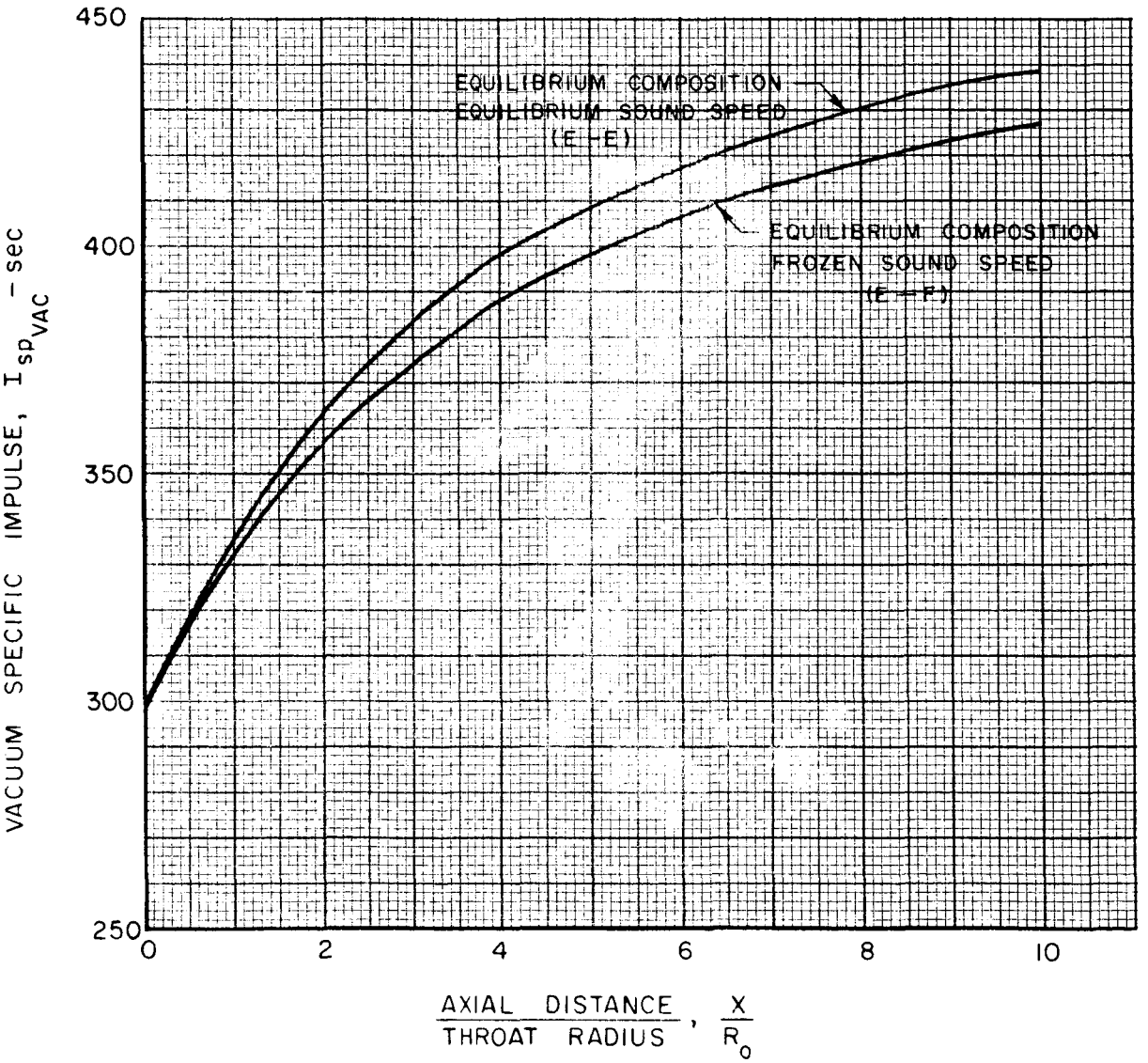

FIG. 24

PRESSURE AND TEMPERATURE PROFILES IN NASW-366 DESIGN NOZZLE FOR 100% AND 90% COMBUSTION EFFICIENCY

$H_2 - O_2$, O/F = 5.0, CHAMBER PRESSURE = 60 PSIA

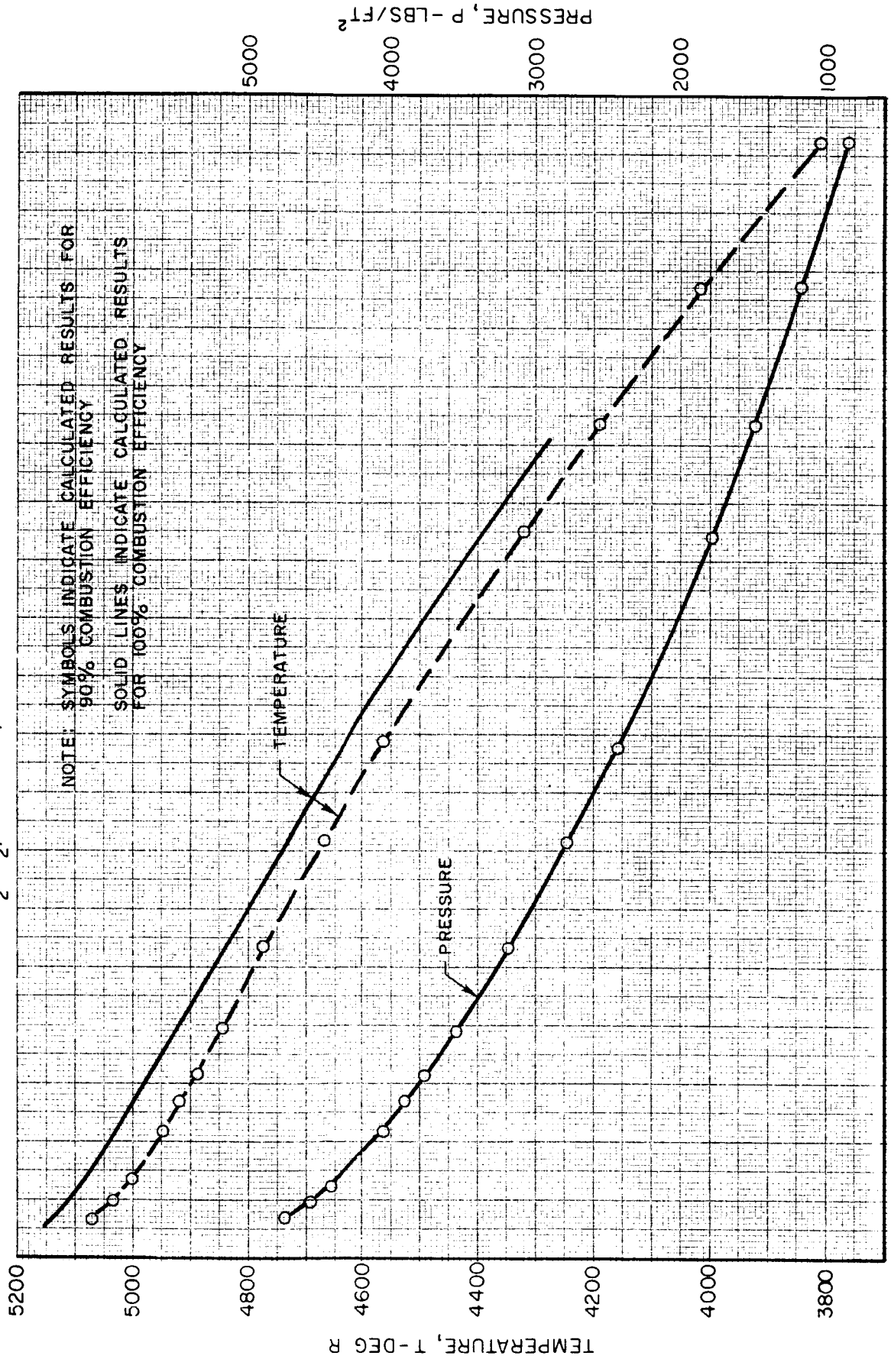

FIG. 25

COMPARISON OF PERFORMANCE IN THE OUTER STREAMTUBE OF RL-10 NOZZLE

$H_2 - O_2$

O/F = 5.0, CHAMBER PRESSURE = 60 PSIA

COMBUSTION EFFICIENCY = 90%

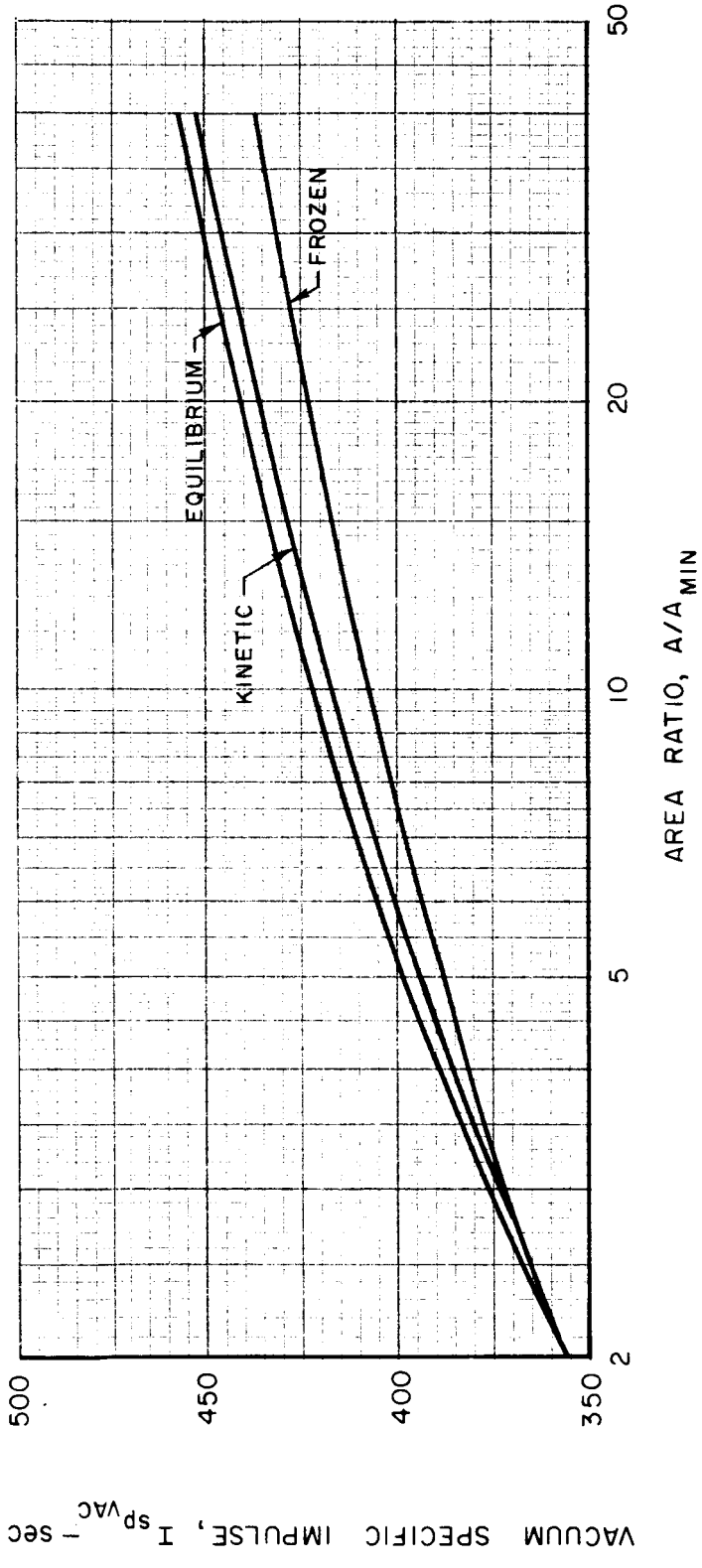

COMPARISON OF PERFECT NOZZLE CONTOURS DESIGNED FOR EQUILIBRIUM FLOW – EQUILIBRIUM SOUND SPEED AND FROZEN COMPOSITION – FROZEN SOUND SPEED

H_2-O_2, O/F = 5, CHAMBER PRESSURE = 60 PSIA, $(A/A_{MIN})_{EXIT}$ = 53.44

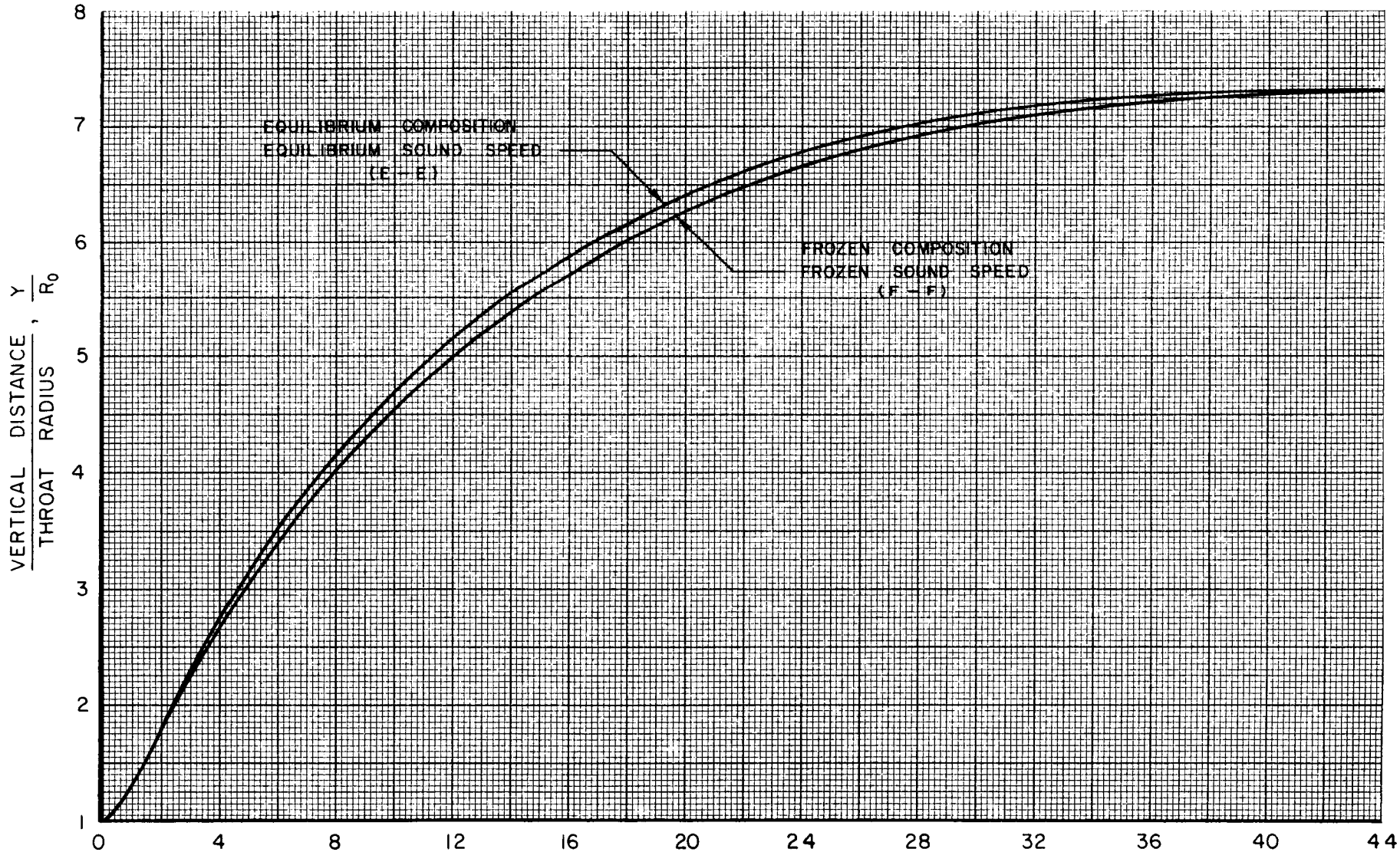

C91096-13

FIG. 26

COMPARISON OF PERFORMANCE FOR EQUILIBRIUM AND FROZEN COMPOSITION GAS MODELS IN EQUILIBRIUM AND FROZEN DESIGN NOZZLES

H_2-O_2, O/F = 5.0, CHAMBER PRESSURE = 60 PSIA

SYMBOL	NOZZLE DESIGN GAS MODEL	PERFORMANCE EVALUATION GAS MODEL
----	E - E	E - E
O	E - E	F - F
———	F - F	F - F
□	F - F	E - E

NOTE: E - E INDICATES EQUILIBRIUM COMPOSITION, EQUILIBRIUM SOUND SPEED
F - F INDICATES FROZEN COMPOSITION, FROZEN SOUND SPEED

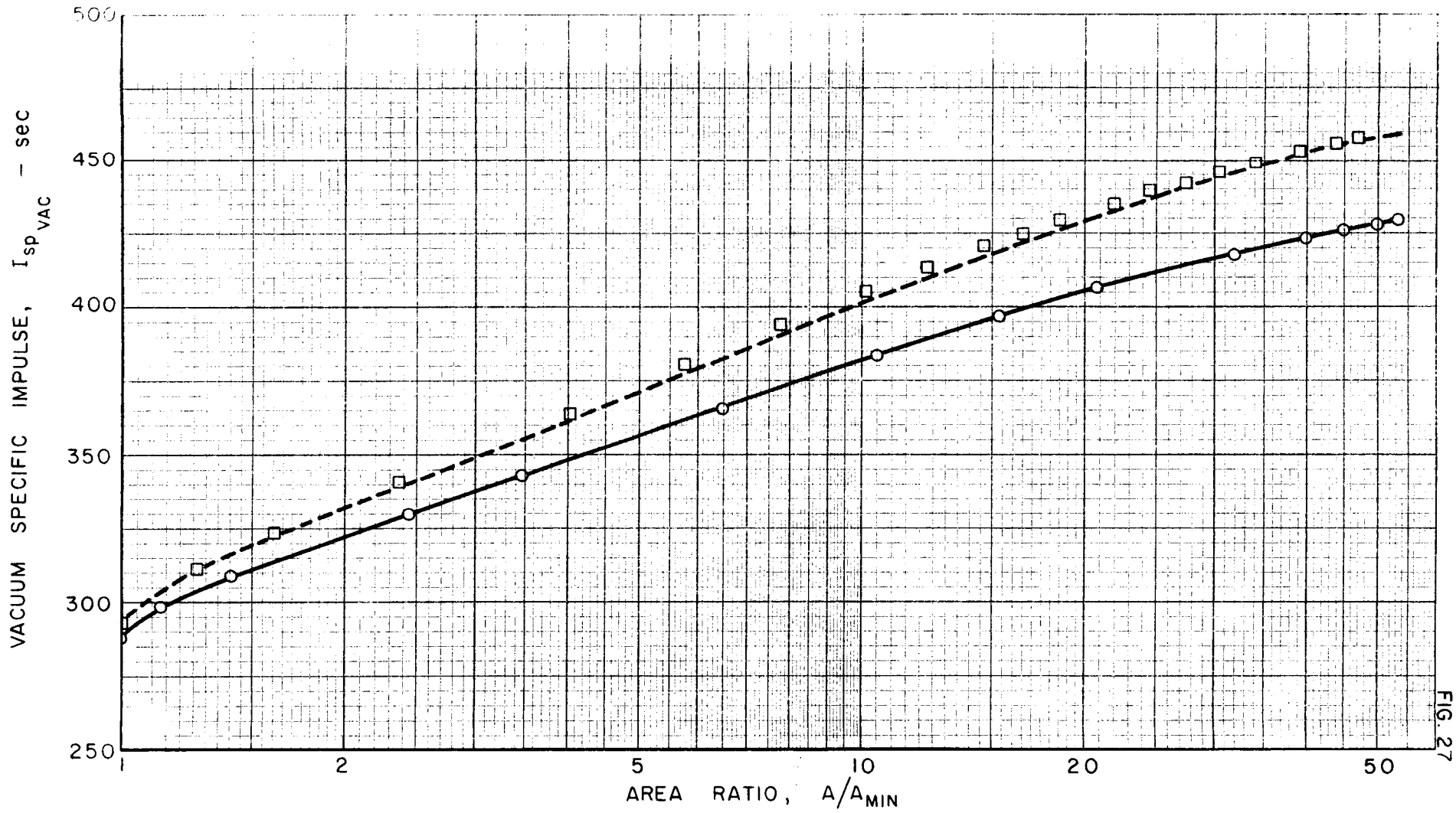

C910096-13

FIG. 27

FIG. 28

COMPARISON OF SPECIFIC IMPULSE DATA FOR SCALED RL-10 ROCKET NOZZLES CALCULATED FROM KINETIC AND MODIFIED BRAY ANALYSES

$H_2 - O_2$

O/F = 5.0, CHAMBER PRESSURE = 300 PSIA

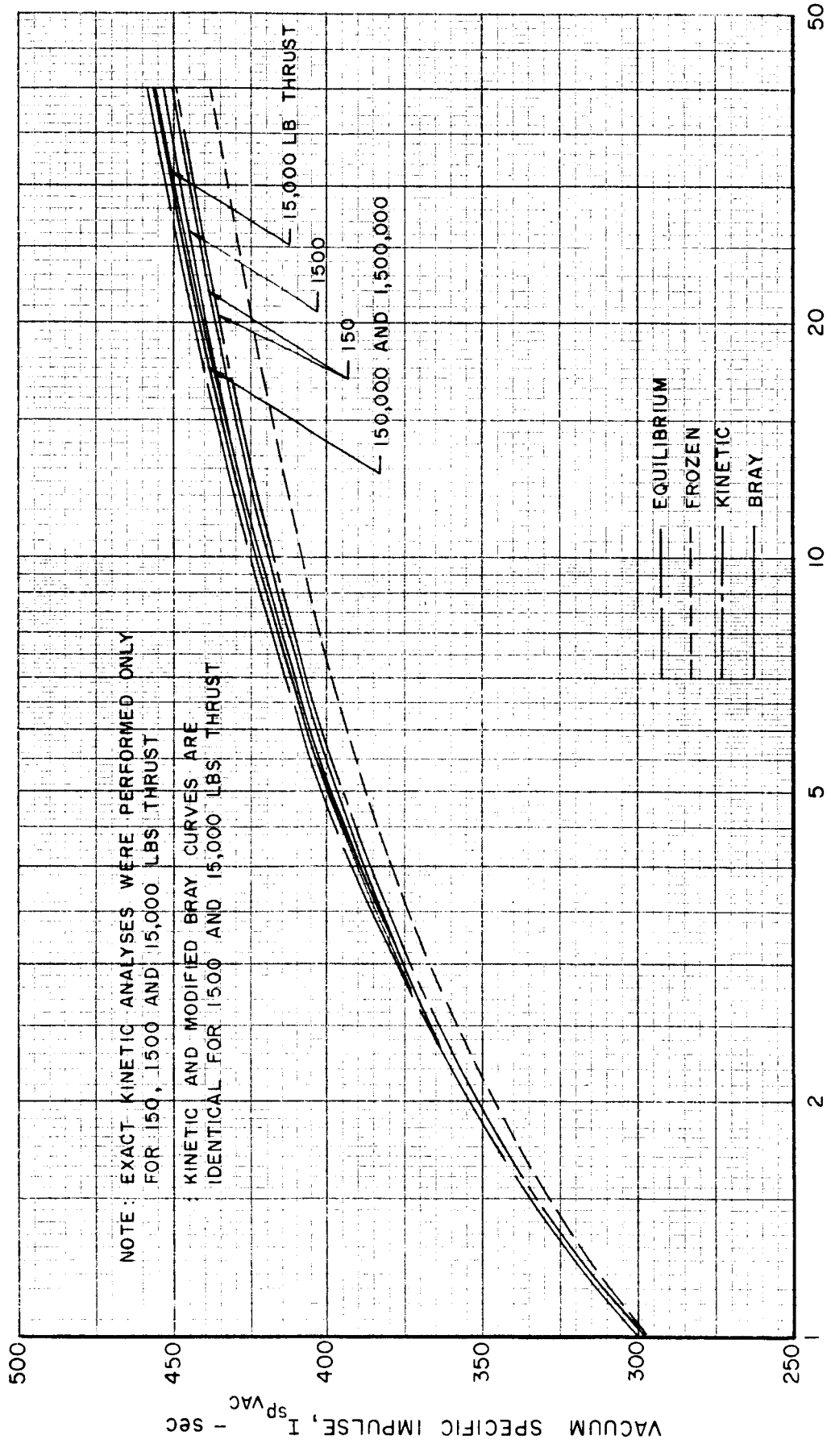

FIG. 29

COMPARISON OF SPECIFIC IMPULSE DATA FOR SCALED RL-10 ROCKET NOZZLES CALCULATED FROM KINETIC AND MODIFIED BRAY ANALYSES

H_2-O_2

O/F = 5.0, CHAMBER PRESSURE = 60 PSIA

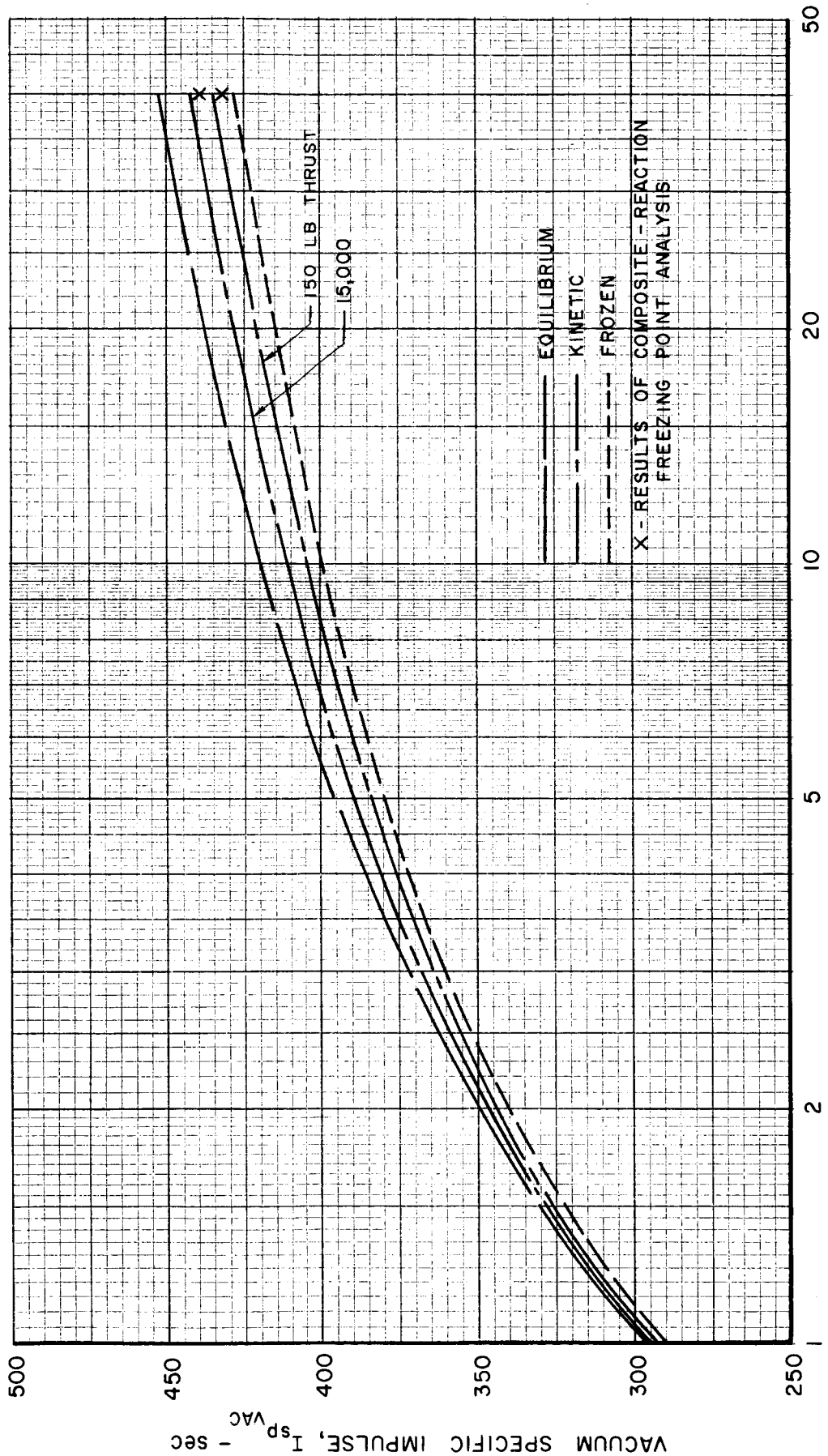

FIG. 30

COMPARISON OF SPECIFIC IMPULSE DATA FOR SCALED RL-10 ROCKET NOZZLES CALCULATED FROM MODIFIED BRAY ANALYSES

$H_2 - O_2$

O/F = 5.0, CHAMBER PRESSURE = 60 PSIA

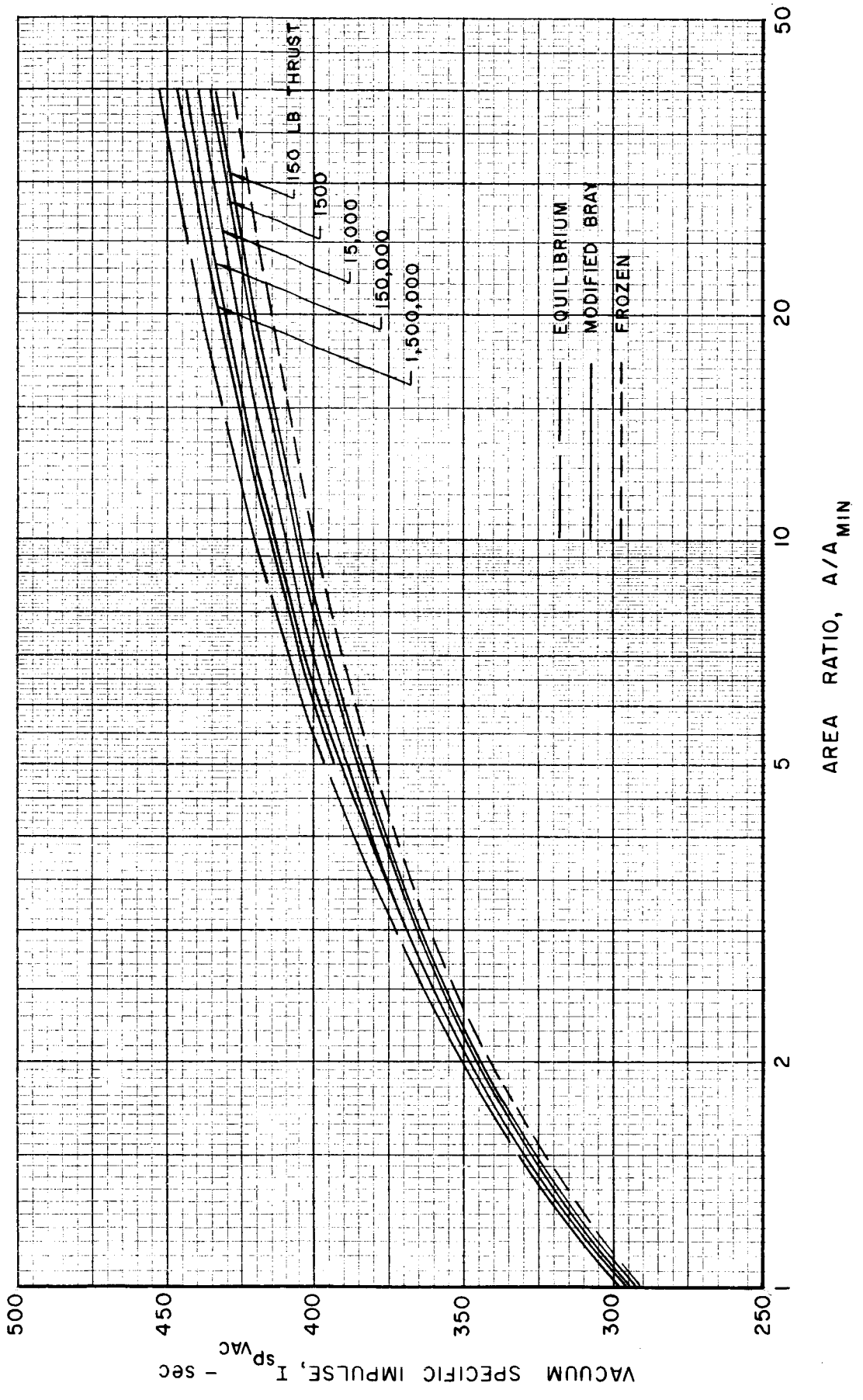

FIG. 31

EFFECT OF THRUST LEVEL ON NONEQUILIBRIUM PERFORMANCE IN RL-10 NOZZLE FOR VARIOUS CHAMBER PRESSURES

$H_2 - O_2$

O/F = 5.0

A/A_{MIN} = 40

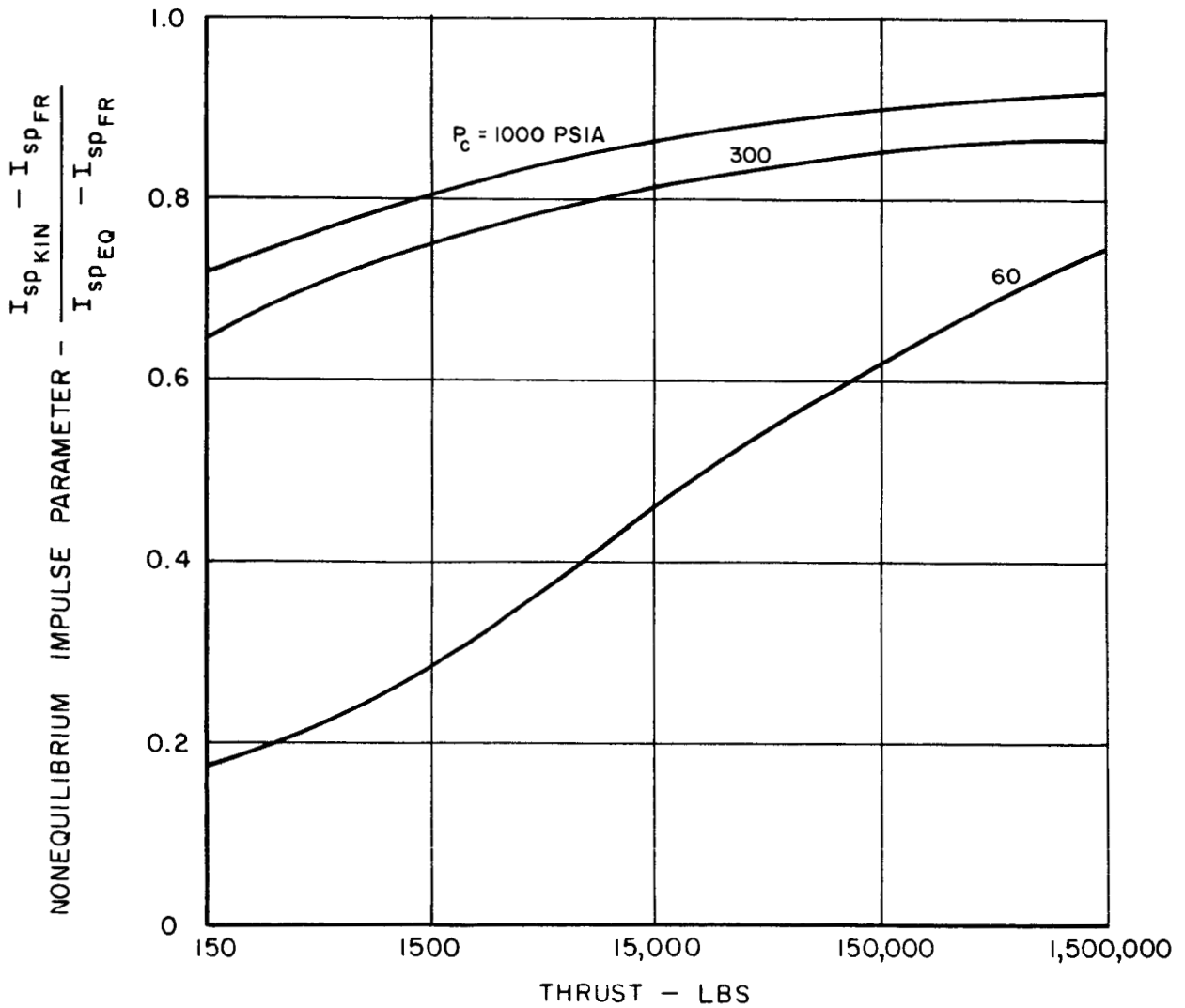

FIG. 32

EFFECT OF THRUST LEVEL ON FREEZING POINT IN RL-10 NOZZLE FOR VARIOUS CHAMBER PRESSURES

$H_2 - O_2$

O/F = 5